EXPERIMENTAL STUDIES OF STEAM AND STEAM-PROPANE INJECTION USING A NOVEL SMART HORIZONTAL PRODUCER TO ENHANCE OIL PRODUCTION IN THE SAN ARDO FIELD

A Dissertation

by

JOSE ANTONIO RIVERO DIAZ

Submitted to the Office of Graduate Studies of
Texas A&M University
in partial fulfillment of the requirements for the degree of

DOCTOR OF PHILOSOPHY

May 2007

Major Subject: Petroleum Engineering

EXPERIMENTAL STUDIES OF STEAM AND STEAM-PROPANE INJECTION USING A NOVEL SMART HORIZONTAL PRODUCER TO ENHANCE OIL PRODUCTION IN THE SAN ARDO FIELD

A Dissertation

by

JOSE ANTONIO RIVERO DIAZ

Submitted to the Office of Graduate Studies of
Texas A&M University
in partial fulfillment of the requirements for the degree of

DOCTOR OF PHILOSOPHY

Approved by:

Chair of Committee,	Daulat Mamora
Committee Members,	Thomas Blasingame
	Akhil Datta-Gupta
	Luc Ikelle
Head of Department,	Steve Holditch

May 2007

Major Subject: Petroleum Engineering

ABSTRACT

Experimental Studies of Steam and Steam-Propane Injection Using a Novel Smart Horizontal Producer to Enhance Oil Production in the San Ardo Field. (May 2007).
Jose Antonio Rivero Diaz, B.S., Universidad Central de Venezuela;
M.S., Texas A&M University
Chair of Advisory Committee: Dr. Daulat Mamora

A 16×16×5.6 in. scaled, three-dimensional, physical model of a quarter of a 9-spot pattern was constructed to study the application of two processes designed to improve the efficiency of steam injection. The first process to be tested is the use of propane as a steam additive with the purpose of increasing recovery and accelerating oil production. The second process involves the use of a novel production configuration that makes use of a vertical injector and a smart horizontal producer in an attempt to mitigate the effects of steam override.

The experimental model was scaled using the conditions in the San Ardo field in California and crude oil from the same field was used for the tests. Superheated steam at 190 – 200ºC was injected at 48 cm^3/min (cold water equivalent) while maintaining the flowing pressures in the production wells at 50 psig. Liquid samples from each producer in the model were collected and treated to break emulsion and analyzed to determine water and oil volumes.

Two different production configurations were tested: (1) a vertical well system with a vertical injector and three vertical producers and (2) a vertical injector-smart horizontal well system that consisted of a vertical injector and a smart horizontal producer divided into three sections. Runs were conducted using pure steam injection and steam-propane injection in the two well configurations.

Experimental results indicated the following. First, for the vertical configuration, the addition of propane accelerated oil production by 53% and increased ultimate recovery

by an additional 7% of the original oil in place when compared to pure steam injection. Second, the implementation of the smart horizontal system increased ultimate oil recovery when compared to the recovery obtained by employing the conventional vertical well system (49% versus 42% of the OOIP).

To

My father, José Antonio "Totón" Rivero Alvarez for being the example I have always followed

and

My daughter, Victoria Isabel for being the biggest joy in my life

ACKNOWLEDGMENTS

I would like to thank my wife, Meiling, who gave me the greatest gift of my life, my daughter, Victoria Isabel. Meiling has stood by my side from day one, selflessly supporting my aspirations and, sometimes, giving up her own, so I could follow my goals. She has tolerated the sacrifices brought by the life of a graduate student, enduring at first the long hours of study during my coursework, and later, the continued separation imposed by my work in the laboratory. Without her support, I would have not been able to complete my research. This work is hers as much as it is mine.

I also wish to express my gratitude for the support and love of my mother, Mercedes, who has always encouraged me to follow my aspirations, and whose exemplary life has been a model for all of those who know her. My family in Venezuela deserves my recognition for the continued support they have given me. I really appreciate the encouragement that my sisters, María, Mayra and Mariela and my nephews and nieces have always offered me. I feel humbled for the confidence they have always deposited in my person.

I would like to express my sincere appreciation to my advisor, Dr. Daulat Mamora, who guided me not only through this research, but also through my years at Texas A&M. I owe to Dr. Mamora the interest in thermal recovery that he sparked in me and all the knowledge and experience that I acquired while I was under his guidance. After seven years of working with Dr. Mamora I hope to take with me his work ethic, passion and dedication to his labor.

The contributions of my committee members, Dr. Thomas A. Blasingame, Dr. Akhil Datta-Gupta, and Dr. Luc Ikelle are also greatly appreciated. I want to thank also Dr. Ben Welch and Dr. Jerome Schubert for serving as substitutes in my preliminary and final examinations respectively.

I wish to express my appreciation to the faculty and staff of the Department of Petroleum Engineering at Texas A&M. I want to especially recognize Dr. Thomas Blasingame for his guidance and words of encouragement.

My friends at Texas A&M made my time in College Station a very rewarding experience. I want to recognize the help and friendship of my fellow Venezuelans at A&M, whose names would form such a long list that it would impossible to put them all in here. I will always especially remember the time shared with Angel and Delmira and also the special friendship with Alonso and Marjorie, who have been by our side all these years. I am confident that they will continue to do so in the years to come. I wanted to also thank my friend Nolys Javier who came with me to Texas A&M and with whom I have shared a friendship of almost 15 years. Nolys helped me a lot during my graduate studies and also encouraged me during my research. My appreciation also goes to Rajivmenon Madhavan and Namit Jaiswal, who provided invaluable support during the realization of my experiments. Freddy Alvarado, my friend and brother-in-law, also deserves my recognition for his continued encouragement during my graduate studies.

This research was made possible by the sponsorship of the Ramey Laboratory Research Program and the Crisman Institute of the Department of Petroleum Engineering at Texas A&M University. The Ramey Laboratory Program was supported by Chevron, ConocoPhillips and Total. Funding for the Crisman Institute was provided by Anadarko, Baker Hughes, BP, Chevron, ConocoPhillips, El Paso, ExxonMobil, Halliburton, IHS, Nexen, Newfield, Saudi Aramco, Schlumberger and Total.

TABLE OF CONTENTS

Page

Page

LIST OF FIGURES

Page

Page

Page

Page

Page

Page

Page

Page

Page

Page

CHAPTER I

INTRODUCTION

As the ever-growing world energy demand strains the supply of conventional oil and gas, the role of unconventional resources becomes increasingly more prominent. Heavy oil, extra-heavy oil and bitumen constitute a large portion of the so-called unconventional resources, which include tight gas, coalbed methane and gas hydrates. Moreover, about 70% of the world's total oil resources is made up of heavy oil and bitumen.[1]

Most of the world's heavy and extra-heavy oil reserves are located in Canada and Venezuela, which some estimates point to a combined total of about 3 to 4.5 trillion barrels original oil-in-place.[1] In the United States, heavy oil reserves are estimated to be around 200 million barrels, mostly located in California and Alaska.

The San Ardo field is located in Monterey County, California. The original oil-in-place is estimated to be in excess of 1 billion STB of heavy oil with gravity ranging from 11 to 12ºAPI.[2-4] San Ardo produces from the Monterey formation, specifically from the Lombardi and Aurignac sands. The shallower Lombardi sand lies at a depth of about 2100 ft with an average net pay thickness of 115 ft in the Main Area and 40 ft in the North Area. Oil from Lombardi has a gravity of 11ºAPI and in-situ oil viscosity of 3000 cp. The deeper Aurignac sand lies at about 2350 ft with an average net pay thickness of 100 ft, oil gravity of 12ºAPI and in-situ oil viscosity of 300 cp.

Given its high viscosities, heavy oils like San Ardo are produced using thermal recovery methods, such as steam injection. Steamflooding operations have been in place in San Ardo since 1968. Several mechanisms operate in steam injection, mainly oil viscosity reduction and steam distillation of the oil.

This dissertation follows the style and format of the *SPE Journal*.

When steam is injected into a reservoir, the resulting phase distribution forms five distinct zones. Each zone has different characteristics with respect to the distance from the injection well (**Fig. 1.1**). The first zone – nearest to the injector – coresponds to the steam zone, where water in liquid and vapor phase and mainly residual oil are present. The light fractions of the oil are distilled off and condense ahead of the steam front creating a solvent bank, which comprises the second zone. The solvent bank is miscible with the oil, thereby reducing its interfacial tension and viscosity. The third zone consists of the hot water zone where steam and volatile oil condense upon contact with the cold matrix. As a result of oil viscosity reduction and displacement in the first three zones, an oil bank (fourth zone) is formed. The fifth zone (farthest away from the injector) is composed of original oil.[5]

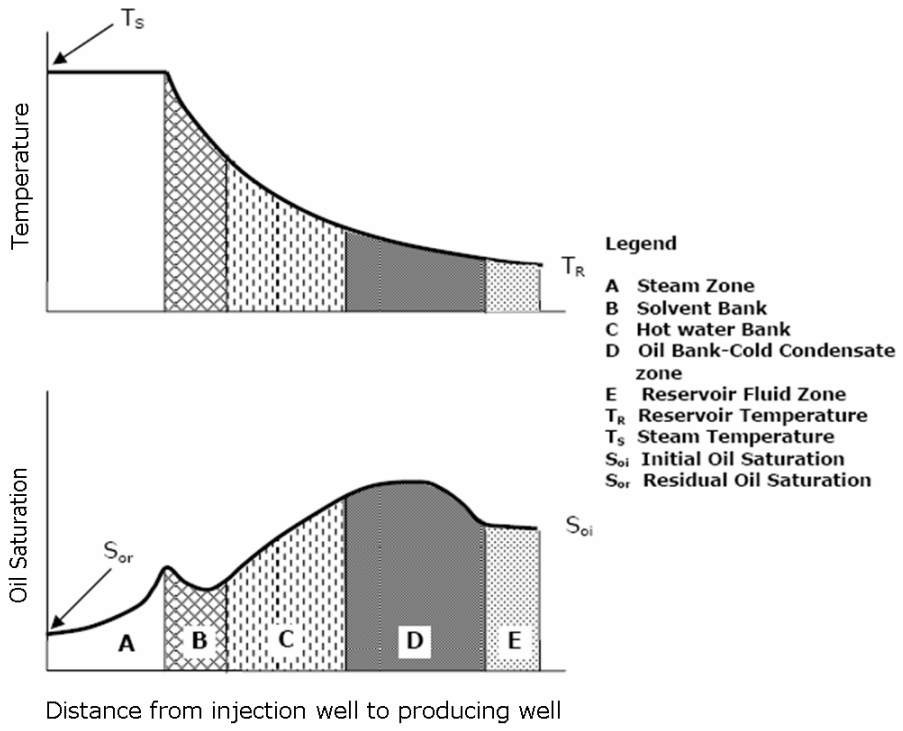

Fig. 1.1- Temperature and saturation profiles during steamflooding (after K.C. Hong[5]).

The efficiency of steam injection is typically reduced by gravitational forces. Given the large density difference between steam and oil, steam tends to rise to the top of the reservoir causing a series of drawbacks in the steamflooding process. First, the steam

creates a path of preferential flow at the top of the reservoir which in turn accelerates steam breakthrough in the production well. This establishes a preferential path for the steam to be recirculated from the injector to the producer (**Fig. 1.2**). This situation reduces the amount of contacted oil in the reservoir, only heating its upper portion and the oil directly below it. Lastly, due to the accumulation of steam in the top of the reservoir, heat losses to the overburden by conduction are exacerbated.

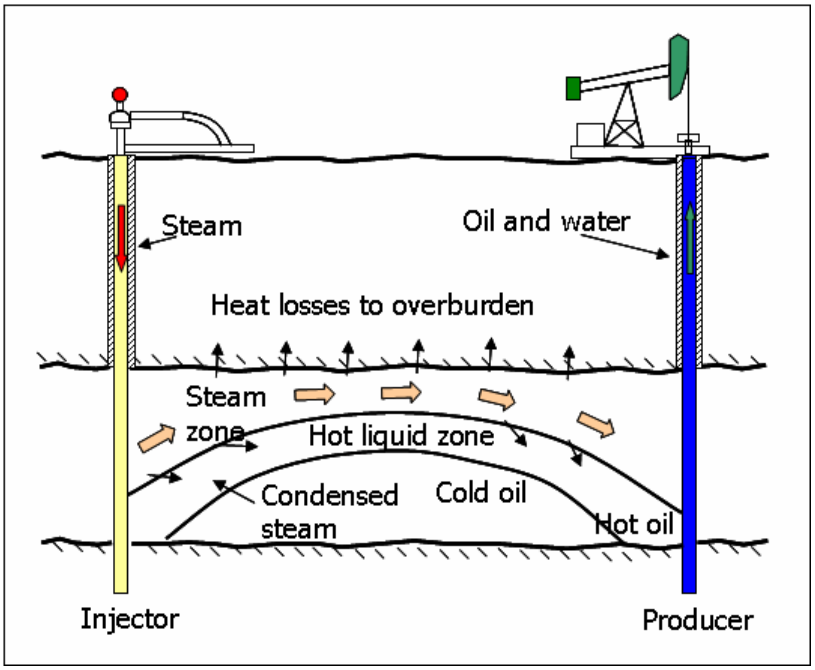

Fig. 1.2- Steamflood cross section showing gravity override (after K.C. Hong[5]).

To mitigate the problem of steam override and early steam breakthrough, numerous alternatives have been proposed, most prominently, the use of foams[6-8]. An alternative method was proposed by Sandoval and Mamora[9-10] in which the producing vertical wells in a nine-spot pattern (as San Ardo field) are replaced by a smart horizontal well. They conducted a series of numerical simulation studies and showed that increased recovery was obtained with the use of the vertical injector-smart horizontal well system compared to the conventional vertical well system.[10]

Since it was first implemented, the principles of steamflooding have remained basically unchanged. In order to improve the process, investigations have been made to determine

the viability of injecting steam along with other additives with the purpose of enhancing recovery. Additives like carbon dioxide and light hydrocarbons have been tested and showed to improve the recovery of heavy oils in the laboratory. However, the combined injection of steam and hydrocarbon additives (solvent) is often too costly and economically unattractive due to the solvent's costs. Therefore, the need exists to better understand the oil recovery mechanisms associated with steam-hydrocarbon injection (e.g. steam-propane) in order to evaluate the technical and economical feasibility of these processes.

A series of experimental studies[11-21] have been carried out in the Ramey Laboratory of the Petroleum Engineering Department at Texas A&M University to investigate the effects of the combined injection of steam and propane on heavy oil recovery. These experiments have shown encouraging results, which among others include accelerated oil recovery and improved injectivity when compared to pure steam injection. All of these previous tests are linear experiments that have shown the potential of the steam-propane process. However, no three-dimensional experiments have been conducted so far.

The main goal of this research is to test different approaches to improve the efficiency of the steam injection process as a method of enhanced oil recovery. The first approach to be investigated is to attempt to accelerate and increase oil recovery by using propane as an additive to steam. The motivation for considering this approach comes from the encouraging results obtained at Texas A&M University with steam-propane injection.[11-21]

The second approach involves studying a method to tackle the problem of steam override by utilizing a smart horizontal well as the one proposed by Sandoval and Mamora.[9-10] To achieve these objectives, a three-dimensional scaled model of a quarter of a 9-spot will be constructed. The field conditions from the San Ardo field in California will be used as a prototype to scale the experimental model. Crude oil from San Ardo will be employed in the experimental runs to test both, the use of steam-propane injection, and the smart horizontal well. Additional experiments will be performed to test the feasibility of applying both approaches simultaneously.

1.1 Research objectives

This research has two main objectives:

1. Conduct experimental studies using a three-dimensional scaled model of a conventional 9-spot pattern of the San Ardo heavy oil reservoir to evaluate oil recovery under steam-propane injection.

2. Using the 3D scaled model, evaluate the performance of a novel vertical injector-smart horizontal producer system under steam and steam-propane injection for the San Ardo heavy oil field.

The experimental runs are conducted using a 3D scaled model of a quarter of a 10-acre, inverted 9-spot pattern, which corresponds to a typical well pattern configuration used in the San Ardo field.

The first objective of this research is aimed at obtaining a better understanding of the production mechanisms involved in steam-propane injection. So far, experiments using only a one-dimensional cell have been carried out in the Ramey Laboratory.[11-21] Although these experiments have provided invaluable information about the potential benefits of steam-propane injection, they do not accurately represent all the mechanisms involved in a three-dimensional flood. The linear experiments are almost piston-like and they do not describe the sweep efficiency found in three-dimensional experiments. Moreover, steam override cannot be modeled in a 1D displacement experiment. Therefore, the natural progression in the investigation of steam-propane injection is to conduct scaled three-dimensional experiments capable of representing all the phenomena inherent to steamflooding, such as steam override.

One of the motivations to conduct 3D experiments with steam-propane injection is that we expect that this kind of tests solve some of the questions that the previous 1D experiments have been unable to answer. For instance, all the linear experiments have shown that ultimate recovery is not increased by the use of propane as an additive to steam. This result is unexpected and numerical reservoir simulation of steam-propane

injection in the Hamaca[16,17] field have indeed shown an increase in the recovery factor when propane is used along with steam.

An important aspect of this research is the construction of the 3D experimental apparatus used to conduct the tests. This experimental setup will allow the Ramey Laboratory in the Department of Petroleum Engineering at Texas A&M University to expand its testing capabilities to include three-dimensional modeling of thermal processes.

CHAPTER II

LITERATURE REVIEW

2.1 Use of steam additives

The use of liquid and gaseous additives in steam injection has been tested extensively. Redford (1982)[22] conducted experiments to study the effect of adding carbon dioxide, ethane and/or naphtha in combination with steam. His results showed that the addition of carbon dioxide or ethane improved the recovery. Higher recovery was reached when naphtha was added.

Harding et al. (1983)[23] presented both experimental and simulation results suggesting that the co-injection of carbon dioxide or flue gas with steam yielded higher recoveries when compared to pure steam injection.

Stone and Malcolm (1985)[24] performed several tests to study the benefits of injecting carbon dioxide along with steam. Higher production rates were obtained for the case of steam-carbon dioxide injection. Good agreement was found when comparing the experimental results with a numerical simulation also conducted in the study.

Stone and Ivory (1987)[25] carried out further investigations using the model from Stone and Malcolm.[5] This time, experiments with CO_2 presoak and CO_2 co-injection with a solvent were conducted. They found that under certain conditions, carbon dioxide pre-soaking increased recovery above the conventional CO_2-steam injection.

Nasr *et al*. (1987)[26] presented results of experiments conducted to test the effects of injecting CO_2, N_2 and flue gas with steam. Both continuous and cyclic injections were tested. The addition of gasses increased bitumen recovery. The use of CO_2 resulted in higher recoveries when compared to N_2 and flue gas.

Frauenfeld *et al*. (1988)[27] presented results showing that for oils without an initial gas content, co-injection of CO_2 with steam was capable of improving oil recovery over that obtained with pure steam. On the other hand, when an initial non-zero gas saturation was present, co-injection of CO_2 was not beneficial.

Metwally (1990)[28] employed cores from the Lindbergh Field to investigate the effects of carbon dioxide and methane on the performance of steam processes. The experiments were carried out to determine the differences in performance of simultaneous injection of steam and a gaseous additive and an injection of a gas slug prior to steam injection. The results showed that injecting a CO_2 slug prior to the steam improved injectivity. However, the presence of a non-condensible gas with steam did not improve steam drive recovery and resulted in higher residual oil saturation compared to steam injection alone.

Gumrah and Okandan (1992)[29] performed linear and 3-D displacement experiments to evaluate the performance of CO_2 addition to steam on the recovery of 24 ºAPI, 12 ºAPI and 10.6 ºAPI oils. The 1D tests indicated that oil recovery increased with increasing CO_2/steam ratios until an optimum value was reached. The addition of CO_2 did not produce a significant increase in the recovery of the lighter oil. However, for the heavier oils, the oil production rate was increased considerably.

Bagci and Gumrah (1998)[30] performed experiments with both linear and 3D models to investigate the effects of injecting methane and carbon dioxide along with steam in a 12.4 ºAPI heavy oil. The results showed that the use of CO_2 or CH_4 combined with steam yielded a higher incremental oil recovery than of steam only tests.

Butler and Mokrys (1991)[31] described a new recovery concept related to the steam-assisted gravity drainage (SAGD) process. The process was intended to be used in thin reservoirs, where the application of SAGD alone was uneconomical due to the high heat losses to the formations above and below the reservoir. The process, called VAPEX, used a solvent, such as propane, which could form a vapor-filled chamber within the reservoir. Vapor dissolves in the oil around the chamber and the resulting solution drains, driven by gravity, to a horizontal production well placed low in the formation. A well, located at the top of the reservoir, is used to inject hot water and the solvent.

Additional work by Butler and Mokrys[32-34] presented results of further investigations conducted on the VAPEX process. Their results showed that the process could be applied economically for heavy oil recovery. Additional advantages derived from VAPEX are a partial in situ deasphalting and a reduction of the content of heavy metals. The resulting oil can be lighter, of a higher quality and better suited for direct refining.

Goite (1999)[11] conducted several experiments to determine the influence of injecting propane as a gaseous additive to steam injection in the Morichal field, Venezuela. Results showed that the optimal concentration of propane lies somewhere in the region of 5%.

Ferguson (2000)[12] continued Goite's experiments using a constant steam injection rate. Several test were performed to determine the optimum propane:steam mass ratio. Acceleration of production was found in the steam-propane runs when compared to pure steam. The optimum propane:steam mass ratio was found to be around 5:100. The acceleration in oil production was thought to be due to the dry distillation process in which the lighter oil fractions are distilled off and carried by propane. On contact with the colder part of the reservoir, the light fractions condense and are miscible with the oil, thus lowering the interfacial tension and decreasing the viscosity of the oil.

Tinns (2001)[13] carried out steam-propane experiments using 5:100 propane:steam mass ratio on 21ºAPI Kulin oil from Indonesia. The same effect of production acceleration was observed in these experiments. Viscosity and density measurements indicated an increase in API gravity and a reduction of viscosity in the produced oil. Furthermore, injectivity was improved with the addition of propane to the steam. A reduction in the maximum injection pressure from 85 psig to 78 psig was observed in the experiments.

Rivero (2002)[14-15] performed steam-propane injection experiments using extra-heavy oil (9ºAPI) from the Hamaca field in the Orinoco Belt, Venezuela. The use of propane was found to accelerate oil production by about 20% in time when compared to pure steam injection. Additionally, steam injectivity increased by a factor of three when propane was added to the steam.

Venturini (2002)[16] used a thermal-compositional reservoir simulator to history-match the experiments performed by Rivero.[15] He then extended the history-matched model to field scale and predicted an increase in ultimate oil recovery with the use of steam-propane compared to steam alone.

Hendroyono (2003)[17] conducted steam-propane experiments using 20ºAPI Duri oil from Indonesia. Acceleration in oil production and steam injectivity increase were also observed.

Plazas (2002)[18] carried out a series of experiments of steam distillation and steam-propane distillation on a light crude oil (34ºAPI) and an intermediate crude oil (25ºAPI) from Venezuela. The results showed that for the intermediate crude oil, the yield obtained by steam-propane distillation is higher than that obtained by pure steam distillation. On the contrary, the yields for the light oil are very similar for both steam and steam-propane distillation.

Ramirez (2004)[19] conducted steam-propane distillation experiments on synthetic oil samples and found that the use of propane effectively reduced the boiling point of the hydrocarbon components being distilled. Higher distillation yields were obtained with steam-propane distillation compared to those obtained with pure steam distillation.

Nesse (2004)[20] carried out experiments to test hot water injection combined with propane in San Ardo oil from California. The use of hot water along with propane did not yield the same oil production acceleration observed with steam-propane injection. The considerable lower amount of heat injected with the hot water did not lower the oil viscosity as much as that with steam injection.

Simangunsong (2005)[21] tested propane and liquid petroleum distillates as additives to steam. Oil production acceleration was observed with both propane and petroleum distillate addition (30% and 38%, respectively). Steam injectivity was also, improved. However, ultimate oil recovery was the same with pure steam and steam plus additives.

Using a compositional-thermal numerical simulator, Deng (2005)[35] modeled a typical Athabasca SAGD pattern under pure steam injection and steam-propane injection. Three

propane:steam ratios were tested: 265:1, 44:1 and 22:1. Results showed that oil recovery was accelerated by using propane as an additive, irrespective of the amount of propane used. Ultimate oil recovery was, however, dependent on the amount of propane injected. When the lowest propane:steam molar ratio was used (22:1), ultimate oil recovery was the same as the base case (pure steam). Lower recoveries were obtained when higher concentrations of propane were injected. An economic analysis was performed and the author pointed out that the cost of propane was a very small fraction of the total costs to run the pattern. Therefore, he concluded that both schemes (pure steam and steam-propane injection) had very similar cost structures.

Imperial Oil of Canada has investigated extensively the use of liquid additives in cyclic steam injection processes. Leaute[36] reports the results of physical model experiments conducted with Cold Lake bitumen and numerical simulation. Results showed that the addition of diluent can increase significantly the recovery of bitumen. With the encouraging results from the physical experiments, a pilot test was proposed and initiated in August 2002 with 8 wells in the H22 pad in Cold Lake.[37] Improved bitumen recovery was observed in the pilot with the addition of diluent. Additionally, diluent recovery was very high, improving the economics of the project.

2.2 Vertical injector–smart horizontal well system

Sandoval and Mamora[10] proposed a method to mitigate the problem of steam override in steamflooding operations (see **Fig. 1.2**). In this method, the producing vertical wells in a nine-spot pattern (such as San Ardo's) are replaced by a horizontal well (**Fig. 2.1**).

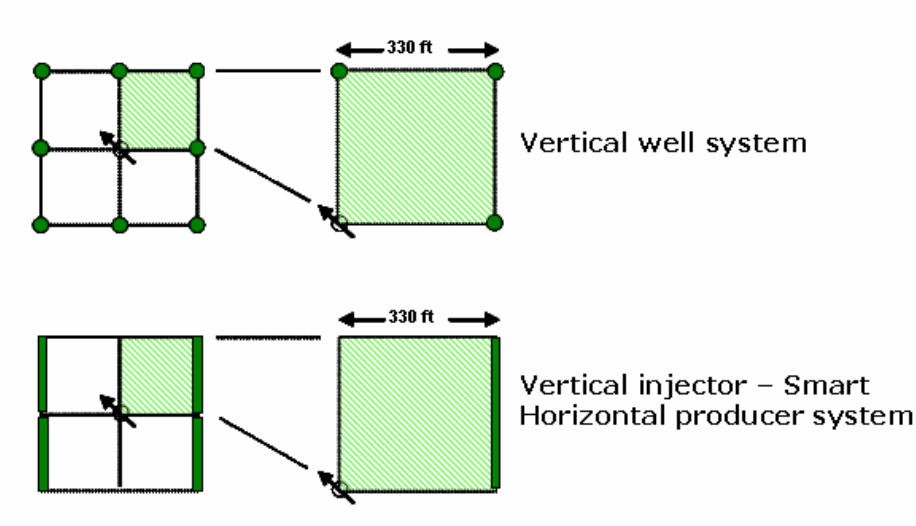

Fig. 2.1- Schematic diagrams comparing a vertical well system (10-acre, inverted 9-spot pattern) and a vertical injector-smart horizontal producer system.[10]

The proposed smart horizontal well is divided into sections that can be selectively opened and closed. The main idea of this system is to initially produce only through the section closest to the injector and close it when steam breaks through. At the same time, the next section is opened and the process is successively repeated for all the sections in the smart horizontal well (**Fig. 2.2**).

Sandoval[10] conducted a series of numerical simulation studies to test the performance of the smart horizontal well system. Results showed that the use of the smart horizontal well system yielded higher recoveries (an additional 10% of OOIP) than the corresponding vertical well system. He tested a range of configurations varying several parameters such as: (1) the number of sections in which the horizontal well is divided; (2) production time after breakthrough and (3) injection rate. It was determined that the optimum configuration for the smart horizontal well requires only three sections. The highest oil recovery was found when all the horizontal sections are opened from the beginning of the injection and nine months after breakthrough, only the section in the heel end of the well remains open.

Simulations were carried out to investigate the effect of combining the smart horizontal well system with steam-propane injection. In these tests, oil recovery was found to be

heavily dependent on the steam injection rate. High steam injection rates (100 - 150 BCWE/D) combined with propane yielded lower recoveries when compared to pure steam runs conducted with the same injection rates.

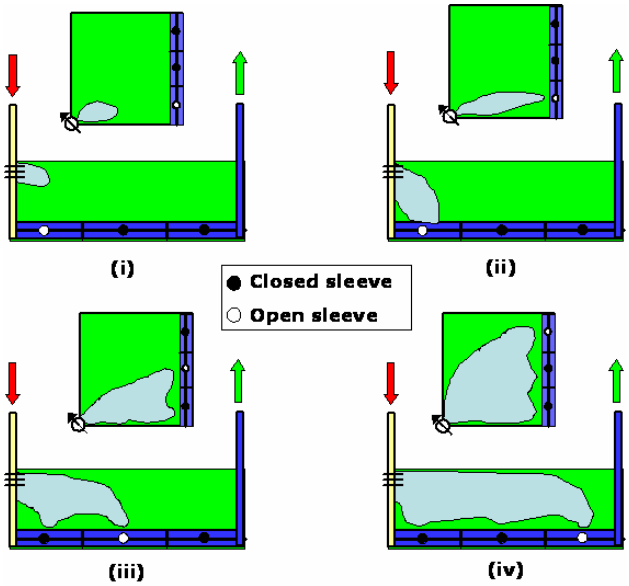

Fig. 2.2- Vertical injector–smart horizontal producer (view from above at the top, cross-sectional view at bottom of each set of figures). (i) Toe-end sleeve open, start of steam injection, (ii) steam breakthrough in first sleeve, (iii) steam breakthrough in second sleeve, and (iv) steam breakthrough in heel-end sleeve.[10]

2.3 Scaling of steam injection experiments

Several techniques have been proposed to scale steamflooding experiments.[38-43] Basically, these approaches can be divided into two distinct groups: (1) Low-pressure models, and (2) High-pressure models.

The technique proposed by Stegemeier *et al*.[38] is a low-pressure model that uses vacuum and lower-than-ambient temperatures to scale steam injection. This technique requires scaling of the fluid viscosities; therefore, a synthetic oil with the scaled viscosity has to be used.

High pressure models such as the ones presented by Pujol and Boberg[39] and Kimber and Farouq Ali[40-43] use field pressures and temperatures and scale the geometry allowing the use of reservoir fluids. These characteristics make this type of scaling ideal for testing processes in which additives such as propane are involved. Fluid properties, emulsification, steam-distillation, gas solubility and compressibility are better scaled using high-pressure models; therefore for this study, it was decided to use a high-pressure scaling approach, specifically Kimber's method.

CHAPTER III

SCALING OF THE PHYSICAL MODEL

The physical model is designed to scale down a quarter of a 10-acre, inverted 9-spot injection pattern, typically used in the San Ardo field. The average thickness of the area to be scaled is about 115 ft. Current San Ardo field conditions will be used in the scaling, except when it is operationally impossible to represent them in the laboratory with our experimental setup.

Kimber[40-43] proposes several approaches to scale steam injection experiments. Each approach is designed to properly scale the most important phenomena in the particular recovery process studied. For instance, if a process like SAGD –where gravitational force plays a significant role – is going to be modeled, the approach should scale these forces appropriately. The approach recommended by Kimber to model processes that involve steam injection plus additives is used to scale the physical model built for this research.

The maximum allowable size of the physical model was constrained by the available hardware in the laboratory, specifically by the oven used to provide reservoir temperature. Considering the oven size, the maximum diameter for the confining pressure jacket was found to be 24 inches. Based on this diameter, it was determined that the three-dimensional cell had to be no bigger than 18 in. by 18 in. In order to account for the thickness of the material used to construct the cell, the size of the physical model was set to be 16 in. by 16 in. (**Fig. 3.1**). The geometric scaling factor is given by:

$$a = \frac{\text{Prototype well spacing}}{\text{Model well spacing}} = \frac{330\ \text{ft}}{1.333\ \text{ft}} = 247.5 \qquad (3.1)$$

The cell thickness is then given by:

$$\text{Model thickness} = \frac{\text{Prototype thickness}}{a} = \frac{112\ \text{ft}}{247.5} = 0.4646\ \text{ft} = 5.58\ \text{in} \qquad (3.2)$$

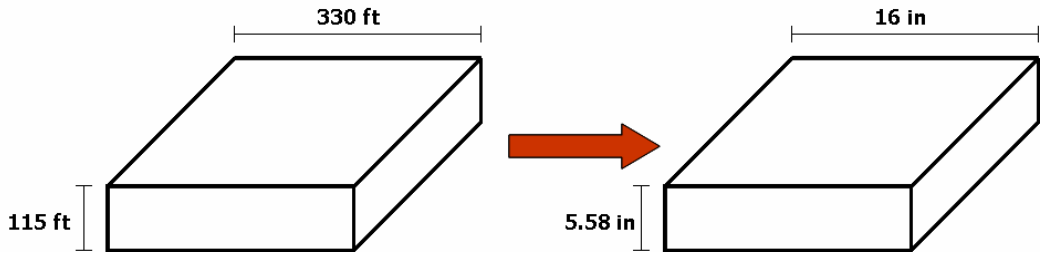

Fig. 3.1- Geometric scaling of the pattern.

The steam injection rate (CWE, cold water equivalent) is scaled using the following dimensionless group:

$$\frac{W_{st}\,\mu_w}{\rho_w\,K\,\Delta p\,h} \tag{3.3}$$

This dimensionless number should be the same in the prototype and in the model, therefore:

$$\left[\frac{W_{st}\,\mu_w}{\rho_w\,K\,\Delta p\,h}\right]_M = \left[\frac{W_{st}\,\mu_w}{\rho_w\,K\,\Delta p\,h}\right]_P \tag{3.4}$$

For a typical pattern steam injection rate of 450 STBW/D (CWE) for San Ardo, the steam injection rate for the model can be calculated as:

$$W_{stM} = W_{stP}\left[\frac{h_M}{h_P}\right] = \frac{450\ \text{bbl/day}}{4}\left[\frac{0.4646\ \text{ft}}{115\ \text{ft}}\right] = 50.2\ \text{cm}^3/\text{min} \tag{3.5}$$

The time is scaled using the square of the geometric factor. For every year in the prototype, we can calculate its equivalent in the model as:

$$t_M = \frac{t_P}{a^2} = \frac{1\ \text{year}}{(247.5)^2} = 8.58\ \text{min per year} \tag{3.6}$$

The use of direct geometrical scaling for the wells is not practical. For instance, a typical 12 in. diameter well will scale down to a model diameter of 0.048 in. (using a = 247.5).

To overcome this limitation, numerous well scaling techniques have been proposed in the literature.[38,39] For this work, the approach proposed by Kimber[40] will be used.

In Kimber's technique, the area open for flow in a well in the prototype is scaled down, and then the well in the model is represented with a slit having this scaled area (**Fig. 3.2**). This will allow maintaining the same pressure differential in the prototype as in the model.

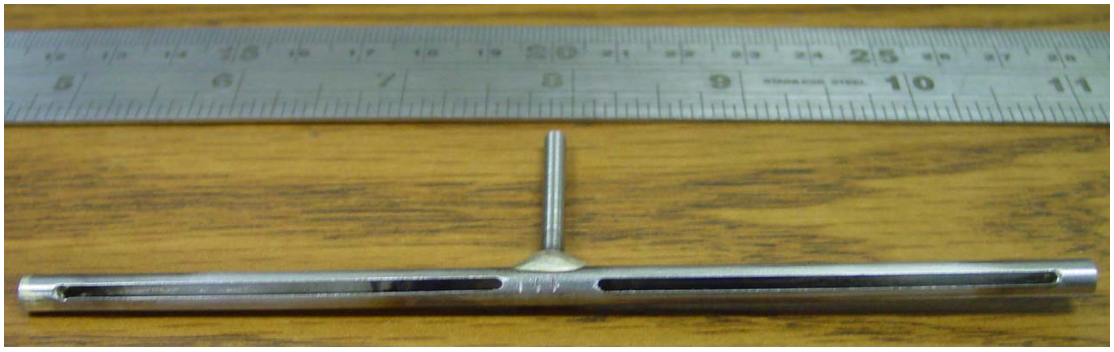

Fig. 3.2- Well section showing scaled area open to flow.

The following dimensionless group is used to scale the area open to flow in a vertical well:

$$\left[\frac{A_{iw}}{L\,h}\right]_M = \left[\frac{A_{iw}}{L\,h}\right]_P \tag{3.7}$$

$$A_{iwM} = A_{iwP}\frac{L_M h_M}{L_P h_P} = \pi\, d_{wP} h_P \frac{L_M h_M}{L_P h_P} = \pi\, d_{wP}\frac{L_M h_M}{L_P} \tag{3.8}$$

Assuming a prototype well diameter, d_{wP}, of 6 in. (0.5 ft.), we have

$$A_{iwM} = \pi\,(0.5\text{ ft})\frac{(16\text{ in})\,(5.58\text{ in})}{330\text{ ft}} = 0.425\text{ in}^2 \tag{3.9}$$

The vertical well is completed along the whole interval, therefore, the slit width can be calculated as:

$$w_M = \frac{A_{iwM}}{h_M} = \frac{0.4255\,\text{in}^2}{5.58\,\text{in}} = 0.076\,\text{in} \tag{3.10}$$

Since horizontal wells penetrate in a horizontal fashion, the scaled area open to flow for the smart well is calculated as follows:

$$A_{iwM} = A_{iwP}\frac{L_M h_M}{L_P h_P} = \pi\, d_{wP} L_P \frac{L_M h_M}{L_P h_P} = \pi\, d_{wP}\frac{L_M h_M}{h_P} \tag{3.11}$$

Assuming a prototype well diameter, d_{wP}, of 6 in. (0.5 ft.), we obtain

$$A_{iwM} = \pi\,(0.5\,\text{ft})\frac{(16\,\text{in})\,(5.58\,\text{in})}{115\,\text{ft}} = 1.219\,\text{in}^2 \tag{3.12}$$

The horizontal well is completed along the total length of the symmetry element; therefore, the slit width can be obtained as follows:

$$w_M = \frac{A_{iwM}}{L_M} = \frac{1.219\,\text{in}^2}{16\,\text{in}} = 0.076\,\text{in} \tag{3.13}$$

The following parameters remain unchanged after the scaling process: temperature, pressure, permeability, porosity and fluid saturations.

3.1 Scaling of heat losses

Surrounding formations are simulated using concrete blocks placed on top and below the cell (**Fig. 3.3**). Due to the shape of the pressure jacket, the concrete blocks vary in thickness from 5 to 8 inches.

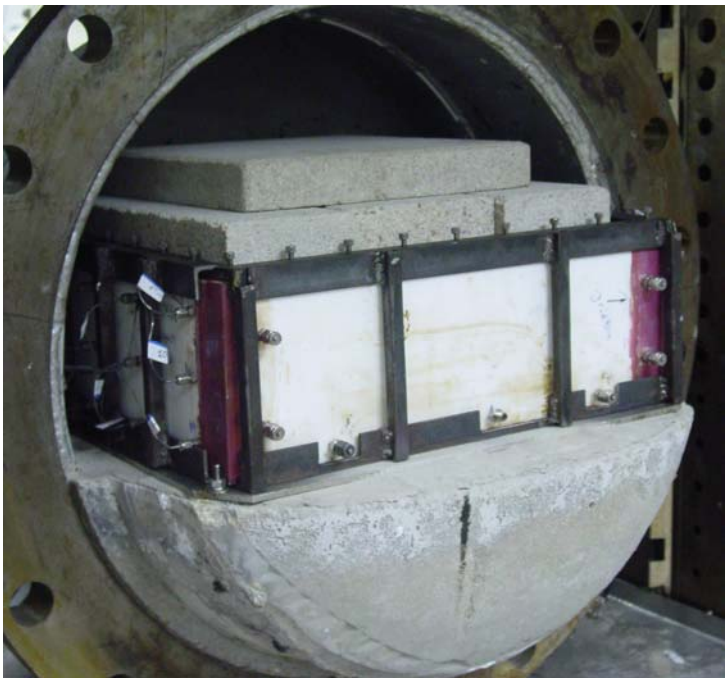

Fig. 3.3- Concrete slabs placed on top and bottom of the physical model to simulate heat losses.

To determine whether the use of finite concrete slabs will cause errors introduced by boundary effects, the corresponding cumulative heat losses are calculated and then compared to the heat losses for a hypothetical infinite concrete block.

Cumulative heat loss to an infinite concrete slab that has had its temperature at the inner boundary raised by ΔT is described by:

$$Q_{\infty} = \frac{2\,\kappa_c\,\Delta T\sqrt{t}}{\sqrt{\pi\,\alpha_c}} \tag{3.14}$$

The corresponding cumulative heat loss to a concrete slab of thickness h_c, for which the external boundary is held at the original temperature, is represented as:

$$Q_f = \frac{2\,\kappa_c\,\Delta T\sqrt{t}}{\sqrt{\pi\,\alpha_c}}\left[1 + 2\sqrt{\pi}\sum_{n=1}^{\infty}\text{ierfc}\left(\frac{n\,h_c}{\sqrt{\alpha_c\,t}}\right)\right] \tag{3.15}$$

Where α_c is the thermal diffusivity of the concrete, which is defined as:

$$\alpha_c = \frac{\kappa_c}{\rho_c C_c} \tag{3.16}$$

The properties for concrete are as follows:

$$C_c = 0.37 \frac{\text{Btu}}{\text{lb}\,^\circ\text{F}}$$

$$\kappa_c = 0.607 \frac{\text{Btu}}{\text{h ft}\,^\circ\text{F}}$$

$$\rho_c = 150 \frac{\text{lb}}{\text{ft}^3}$$

The initial reservoir temperature is 128ºF, and the steam injection temperature is around 400ºF, therefore, the maximum ΔT experienced by the surrounding formations is around 270ºF. The maximum expected run time for any experiment is around three hours. With all this information, the error introduced by boundary effects is calculated using:

$$\xi = \frac{Q_f - Q_\infty}{Q_\infty} 100 \tag{3.17}$$

A plot of the error vs. run time for various concrete block thicknesses is presented in **Fig. 3.4.**

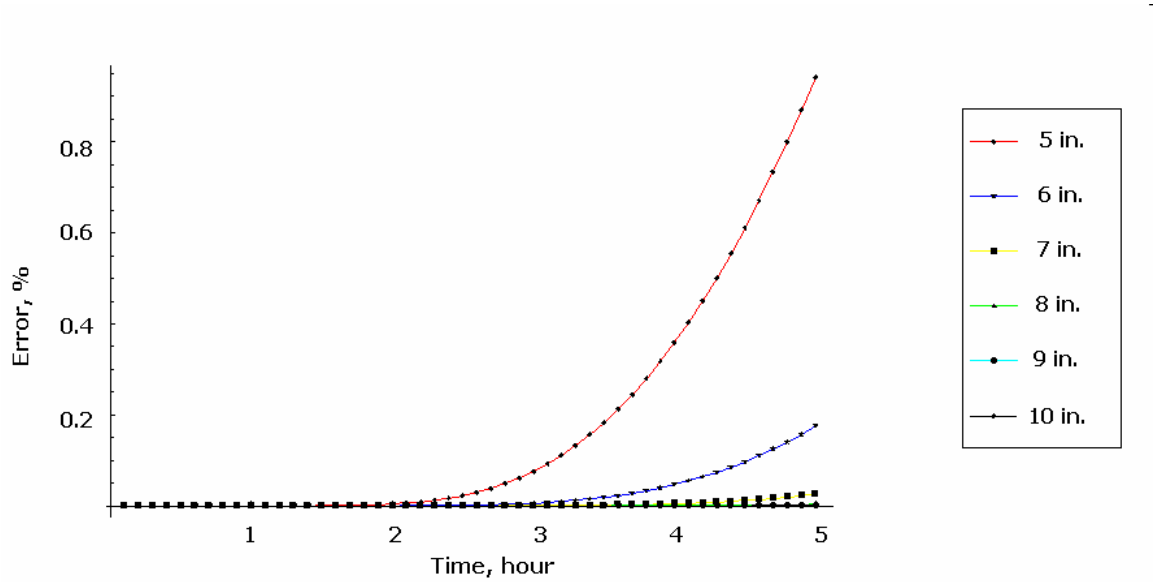

Fig. 3.4- Heat loss error introduced by boundary effects caused by the use of finite surrounding formations.

The plot shows that the thinnest parts of the concrete blocks (around 5 in.) will only introduce very small errors (less than 0.1%) for the maximum expected experimental run time.

CHAPTER IV

EXPERIMENTAL APPARATUS

The experimental setup was designed and specially constructed to conduct this research. The apparatus is comprised of four different systems: (1) physical model (shown in **Fig. 4.1**); (2) steam injection system; (3) propane injection system; (4) fluid production system; and (5) data measurement and recording system.

A schematic diagram showing the entire experimental setup is presented in **Fig. 4.2**.

4.1 Physical model

The methodology used to calculate the dimensions of the physical model has been presented in the Chapter III. The resulting internal dimensions of the cell are 16 in. long by 16 in. wide by 5.58 in. high. The walls of the cell are constructed of 0.75 in. thick Teflon PTFE sheets. Since the walls of the cell should represent a no-flow boundary for mass and energy, Teflon was chosen because of its low thermal conductivity, high operating temperature rating and compressive strength. A picture of the cell is show in **Fig. 4.1**.

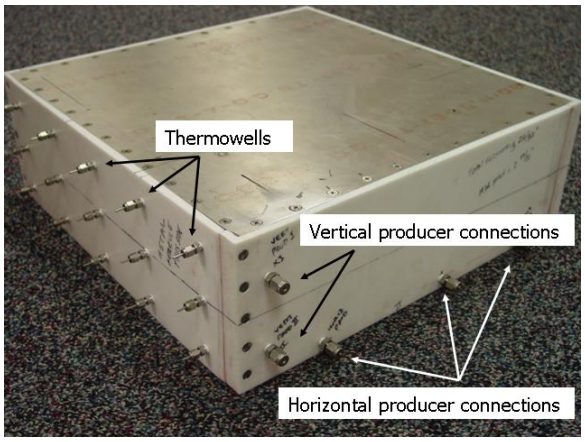

Fig. 4.1- Teflon and aluminum cell used for the physical model.

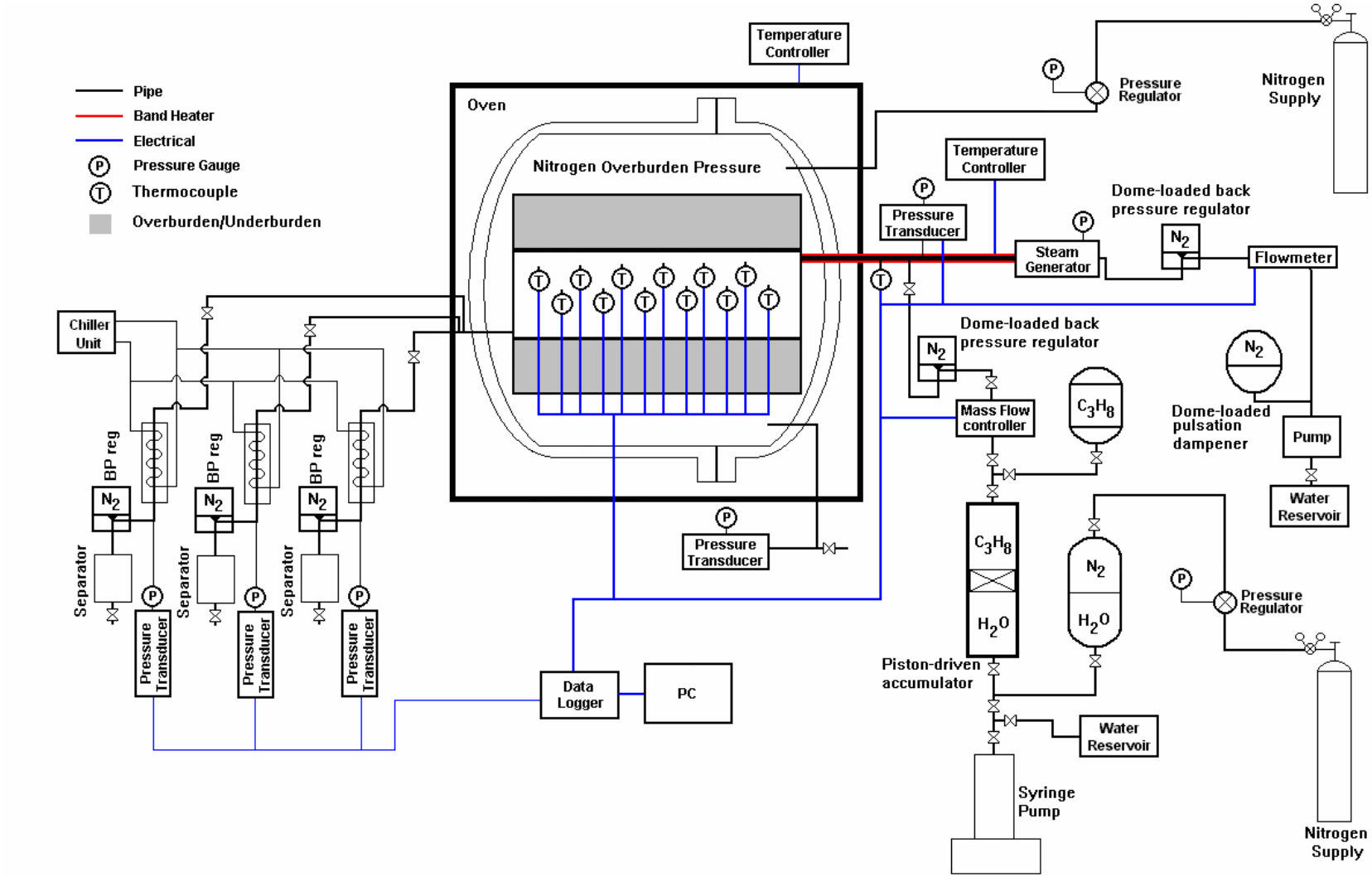

Fig. 4.2- Schematic diagram showing experimental apparatus.

The bottom and top of the cell are made of aluminum alloy plate. The bottom of the cell is affixed to the walls while the top is removable. The metal will allow heat losses to occur to the overburden and underburden of the model. In theory, the boundaries at the top and at the bottom of the cell should only conduct heat in a vertical fashion (*z* direction). However, in reality, heat is conducted both in the vertical (*z*) and horizontal directions (*x* and *y*), along the entire area of the aluminum plates. To minimize heat conduction in the horizontal directions (*x* and *y*), the cross section of the aluminum plate should be reduced as much as possible. The only way to accomplish this is to use the minimum allowable plate thickness to construct the top and bottom of the cell. It was found that the thinnest practical aluminum plate was 0.09 in. thick.

The seal of the removable top aluminum cover with the Teflon walls is facilitated by the use of a high-temperature silicon gasket compound. Thirty-four Allen screws are used to secure the aluminum plate to the cell. The screws are mounted in four brackets (one for each side of the model) at evenly spaced intervals (see **Fig. 4.3**).

The surrounding formations are simulated using concrete (see **Fig. 4.3**). The thickness of the overburden and underburden are scaled so boundary effects do not have influence on the heat losses during the time the experiment lasts (see section 3.1).

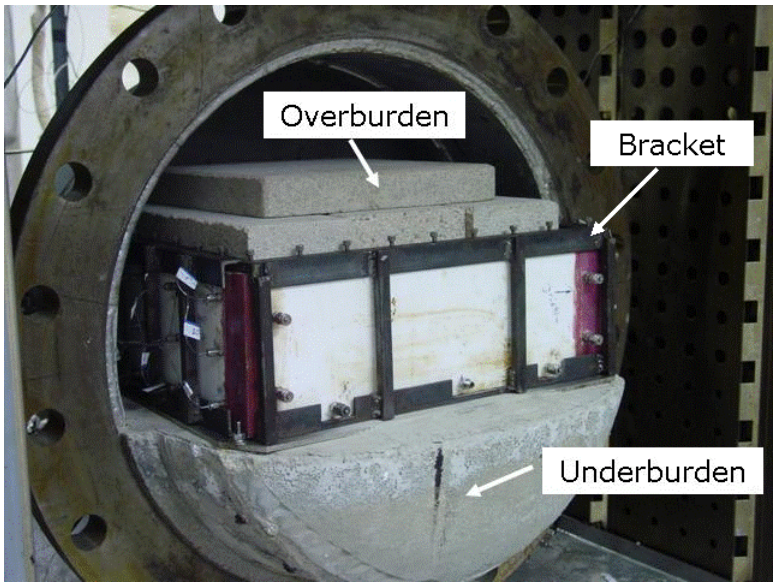

Fig. 4.3- Surrounding formations are simulated using concrete on top and at the bottom of the cell.

In order to monitor the steam front profile during the experiments, 15 thermowells are placed across the cell. They are arranged in three rows of five thermowells each (see **Fig. 4.1**). The thermowells are constructed of 304 stainless steel tubing with an outer diameter of 0.072 in. and 0.009 in. wall thickness. These dimensions can easily accommodate five 20/1000 in. thermocouples in order to measure temperature at evenly spaced intervals. A total of 75 thermocouples (3 layers of 25 thermocouples each) are used to register temperature at various locations inside the model. **Fig. 4.4** shows a schematic diagram with plan and front views of the cell depicting the location of the thermocouple measuring points.

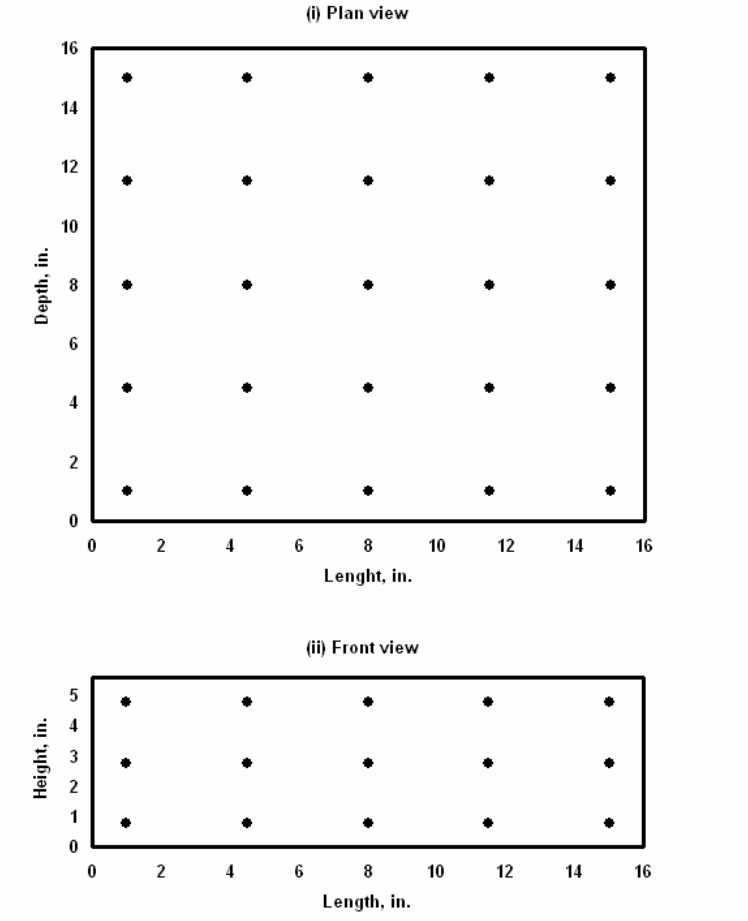

Fig. 4.4- Location of the thermocouple measuring points inside the cell. (i) Top view. (ii) Front view.

The Teflon cell is not able to withstand internal pressure; therefore, in order to conduct the experiments at field conditions, the cell is encapsulated inside a pressure jacket (**Fig. 4.5**) that allows application of a confining pressure always in excess of the internal cell pressure. This overburden pressure will be supplied using nitrogen, which is injected via a pressure regulator. The confining pressure has to be manually controlled during the run and is adjusted according to the cell injection pressure. A pressure transducer installed in the jacket allows the automatic monitoring and recording of the overburden pressure.

The pressure jacket was designed using the ASME boiler and pressure vessel code with a pressure rating of 600 psi. The internal diameter of the jacket is 24 in. with a wall thickness of 0.33 in. The jacket has two hemispherical-shaped ends and the cover is attached to the main body by using a 150# ISO flange. Modifications had to be made to the jacket to allow the passage of the connections for the injector and producer wells and the thermocouples.

Fig. 4.5- Pressure jacket used to subject the cell to overburden pressure.

In order to simulate reservoir temperature conditions (55ºC), the pressure jacket is placed inside an oven (**Fig. 4.6**) whose frame has been reinforced to withstand the weight of the physical model assembly (in excess of 1500 lb). The rear end of the oven was modified to open a window that allows access to the back of the pressure jacket.

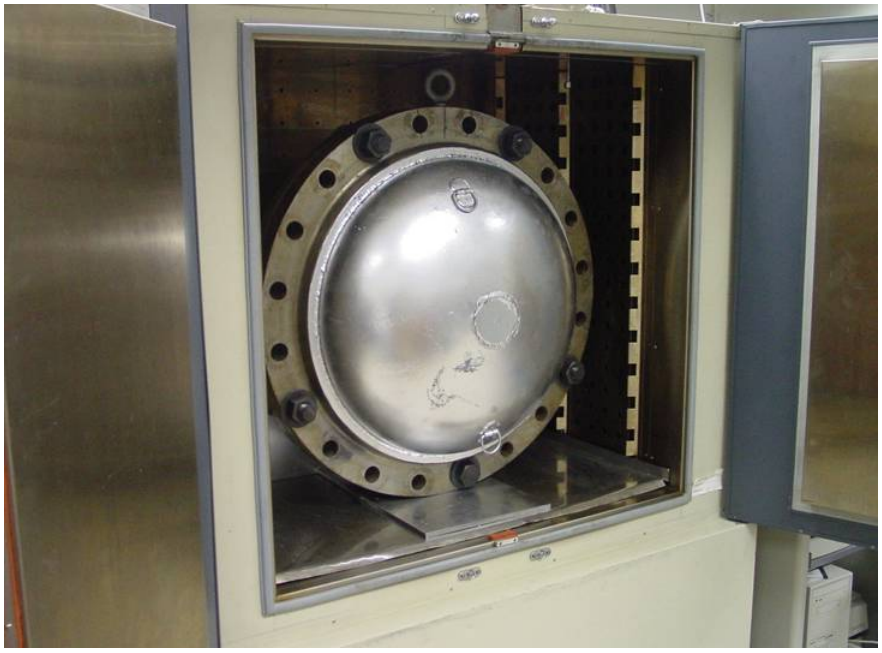

Fig. 4.6- Pressure jacket inside oven used to represent reservoir temperature.

The physical model incorporates one vertical injector, three vertical producers and a horizontal well. The vertical wells are located in the corners of the cell, while the horizontal well is located at the bottom of the cell, running parallel to the side of the cell opposite to the injector. The horizontal well is divided into three sections. The location of the wells is shown in **Fig. 4.7**. Each well is fabricated using stainless steel tubing with an outer diameter of 0.1875 in. A mill is used to cut a slit of a predetermined thickness along the tubing to form the area open to flow in the well (see **Fig. 3.2**). Chapter III explains the methodology used to calculate the slit thickness. Each one of the well sections is closed at both ends using 0.1275 in. steel rod with soldering. In order to connect the well to the outside of the cell, a hole is drilled in the center of the section and a 0.1275 in. OD tubing is soldered to the hole (see **Fig. 3.2**). The well section is wrapped in a steel screen designed to keep sand out. A finished well section is shown in **Fig. 4.8**. The

implementation of the vertical injector-smart horizontal well system (see **Fig. 2.2**) requires that the steam has to be injected only in the top section of the vertical injector. To accomplish this in the physical model, all the vertical wells (the producers as well as the injector) are divided into two sections. In **Fig. 4.9**, it can be observed how a typical vertical well (vertical producer # 1) is comprised of two identical sections, one in the top half of the cell and the other occupying the bottom half of the model.

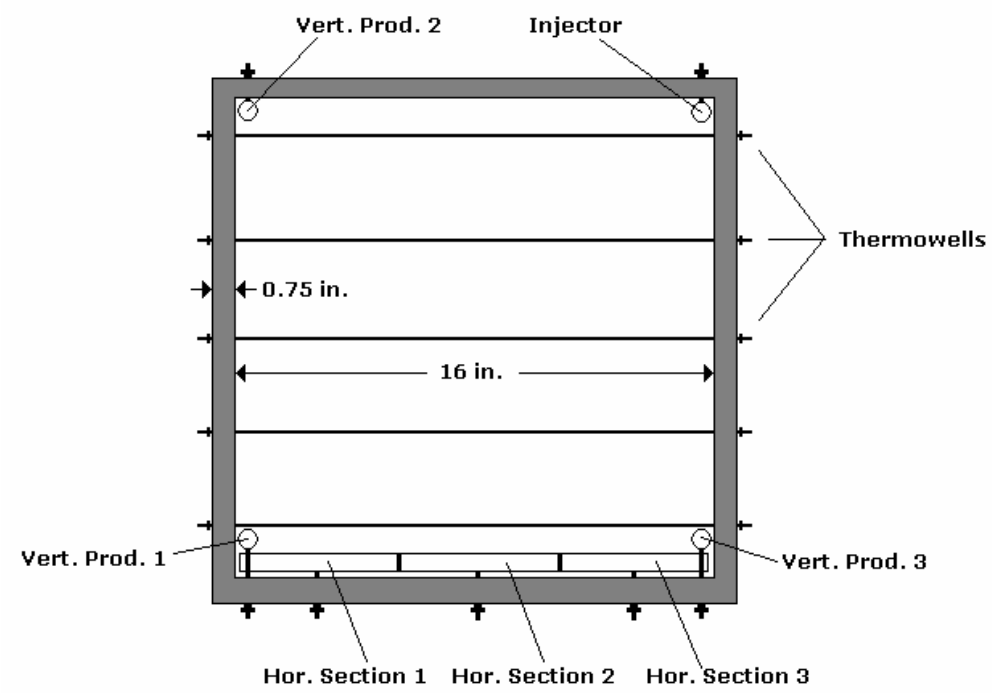

Fig. 4.7- Schematic drawing showing a plan view of the cell. The location of the wells and thermowells is shown.

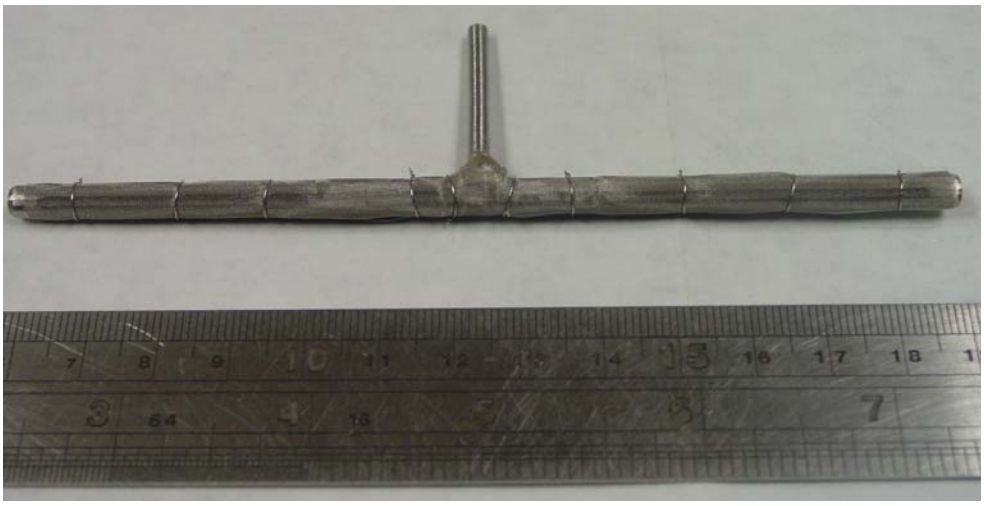

Fig. 4.8- Finished well section (horizontal section 1) wrapped in steel screen. 1/8" tubing soldered to the well is used to provide a connection to the outside of the cell.

To provide a connection for the well to the outside of the cell, a hole is drilled on the Teflon wall and the 01275 in. tubing is passed through it. The seal is provided by inserting the tubing in a fitting that has previously been attached to the wall of the cell. **Fig. 4.9** shows how the wells are installed inside the cell.

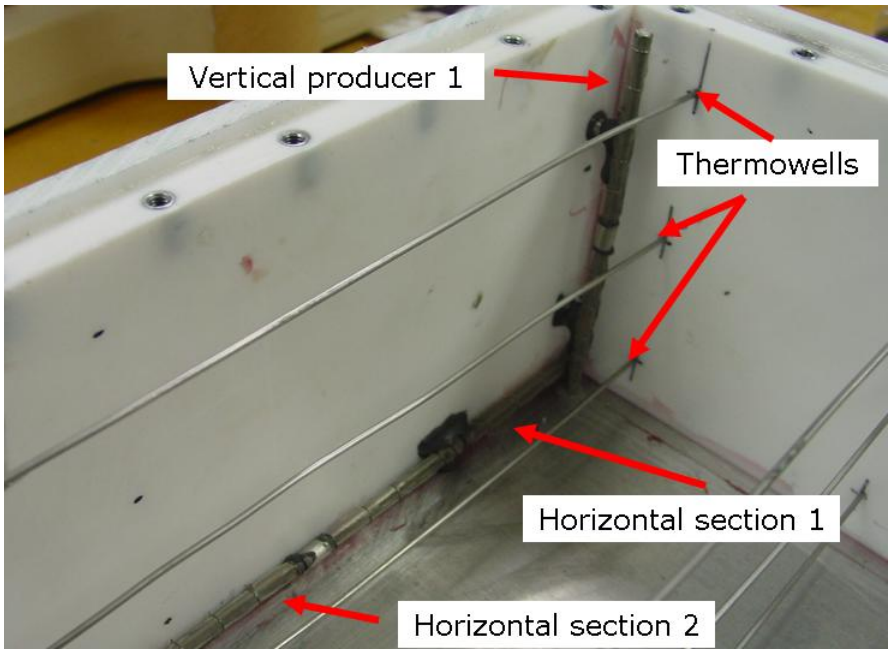

Fig. 4.9- Horizontal well sections and vertical producer 1 are shown inside the cell. The thermowells are also depicted.

4.2 Steam injection system

A diaphragm metering pump (**Fig. 4.10**) is used to inject water at a fixed rate. At the outlet of the pump, a dome-loaded pulsation dampener is installed to help mitigate the pressure surges produced by the pumping action. The delivery rate of a diaphragm pump is heavily influenced by the delivery pressure; therefore, to minimize this effect and insure a consistent delivery rate during the run, a dome-loaded backpressure regulator was installed at the outlet of the pump. The regulator setting point is much higher than the maximum pressure expected during the experiment, thus insuring a consistent delivery rate. In order to measure water injection rate, a turbine flowmeter (see **Fig. 4.11**) was installed between the outlet of the pump and the backpressure regulator.

An 11,000W custom-made steam generator (**Fig. 4.12**) is used to produce superheated steam (220ºC and 150 psig). A series of computer-controlled flexible heaters wrapped around the injection line are used to compensate for heat losses and maintain the superheated conditions of the injected steam. Just upstream of the injection well, a pressure transducer was installed to record the injection pressure as close as possible to the cell. A thermocouple was also placed inside the injection line to register the steam temperature at the injection well.

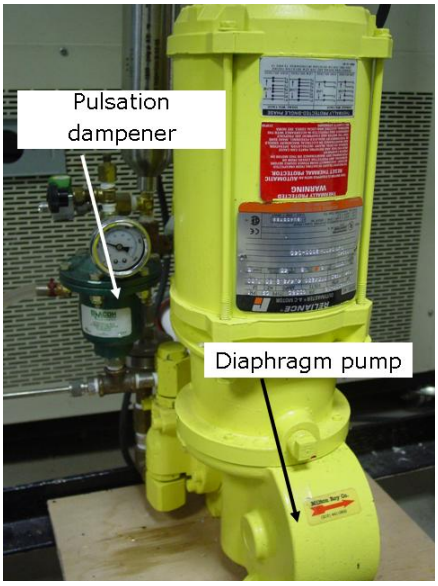

Fig. 4.10- Metering pump with pulsation dampener.

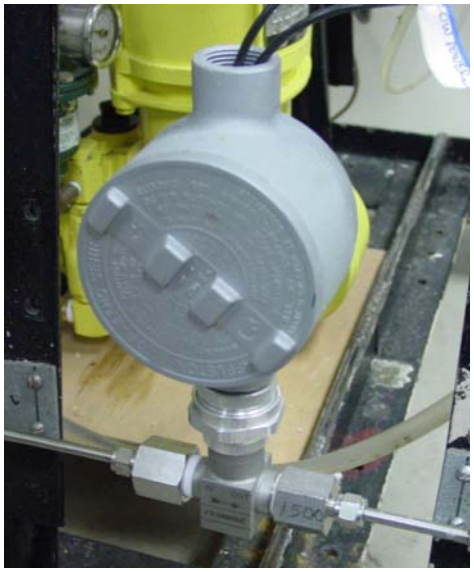

Fig. 4.11- Turbine flowmeter.

Fig. 4.12- Steam generator.

4.3 Propane injection system

The experimental conditions require that propane be injected in liquid form. To accomplish this, an assembly consisting of a piston-driven accumulator (see **Fig. 4.13**) and a syringe pump is used to pressurize the propane at 350 psi (see diagram in **Fig. 4.2**). Once the propane is in liquid form inside the accumulator, it is delivered to a mass flow controller where the rate is regulated and measured. A dome-loaded backpressure regulator (**Fig. 4.14**) set at 300 psi is placed downstream of the flow controller in order to maintain the propane in liquid conditions at all times. To maintain a constant pressure differential across the flow controller, the piston in the accumulator is pushed at constant pressure using nitrogen and water (see **Fig. 4.2**).

Fig. 4.13- Accumulator used to store and inject propane in liquid phase.

Fig. 4.14- Backpressure regulator, syringe pump and flow controller demodulator used to control the propane injection rate.

4.4 Fluid production system

Once fluids are produced out of the cell, they are cooled by using a condenser fed by a chiller unit. The flowing pressure for all the producing wells is set at 50 psig, which is accomplished by using a dome-loaded backpressure regulator capable of handling multiphase flow (see **Fig. 4.15**). The fluids are then collected in 500 ml graduated cylinders, separated and measured. Each well stream is fitted with a pressure transducer that allows the measurement and recording of the flowing production pressures. For safety purposes, when propane runs are conducted, the process of fluid collection is performed in an enclosure fitted with a suction hose connected to the laboratory fume hood system. This allows the evacuation of combustible gases out of the laboratory in a safe manner.

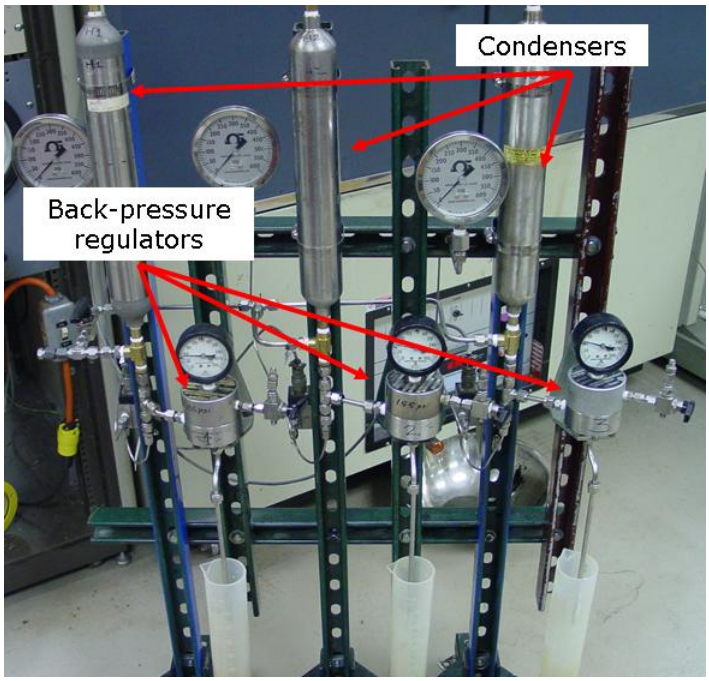

Fig. 4.15- Condensers and backpressure regulators in the fluid production system.

4.5 Data measurement and recording system

A special data logging program was written using the Lab-View programming language to measure and record the following parameters every 30 seconds (a total of 84 channels):

1. Elapsed run time in the experiment.
2. Temperature profile inside the cell by recording 75 thermocouple measurements.
3. Injection temperature.
4. Injection pressure.
5. Overburden pressure.
6. Flowing production pressure for each well by recording the signal from three pressure transducers.
7. Steam injection rate, CWE (Cold Water Equivalent).

8. Propane injection rate.

The program also displays parameters such as: overburden pressure, injection pressure and water injection rate every 5 seconds. These parameters require more frequent monitoring as they can change very rapidly during the experiment and will require immediate adjustment. In the case of the overburden and injection pressures, the program emits an audible alarm whenever the difference between them is below 20 psig. This alert is designed to help maintain an overburden pressure in excess of the cell's pressure at all times during the run.

The data collection is performed by using two data loggers connected to a personal computer using the GPIB 488.2 protocol.

CHAPTER V

EXPERIMENTAL PROCEDURE

To simulate the reservoir rock and fluids, the physical model is packed with a mixture of sand, oil and water. After conducting several tests with different saturations, it was decided to carry out the experiments using 40% oil, 40% water and 20% gas saturations. The mixture is prepared beforehand with pre-calculated proportions using 20/40 mesh Ottawa sand, San Ardo crude oil and distilled water. The methodology used to calculate the mixture proportions in shown in Appendix A.

The mixture is carefully tamped into the cell always attempting to pack it with the same amount of mixture for each run to ensure consistent conditions for each experiment. **Fig. 5.1** shows a composite picture depicting the packing of the mixture in the stage before and after the installation of the top layer of thermowells.

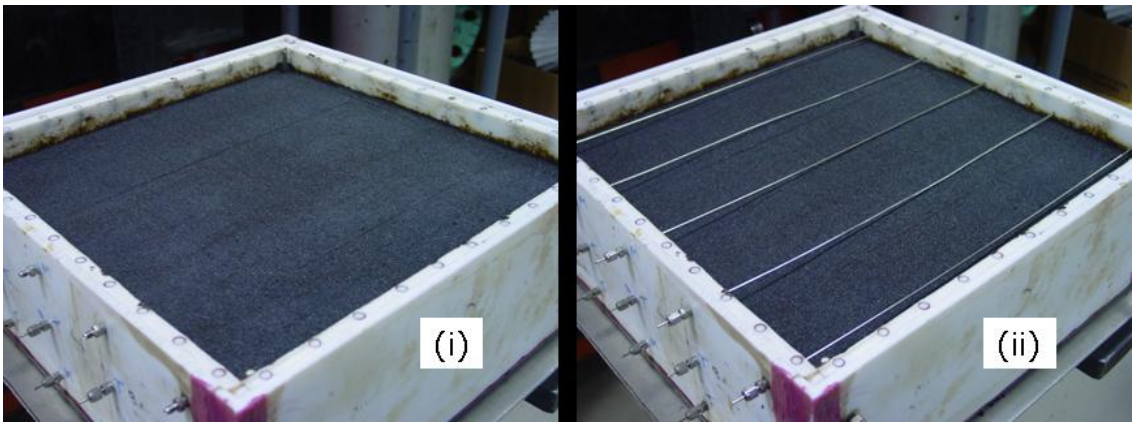

Fig. 5.1- Packing process of the physical model. Packed cell before (i) and after (ii) the installation of the top thermowell layer.

After the cell is packed, the top aluminum cover is installed and sealed using a high-temperature silicon gasket compound. The compound is left to cure for 48 hours and the cell is tested for leaks using vacuum.

The cell is introduced into the pressure jacket using a forklift (see **Fig. 5.2**). As the cell is introduced in the jacket, the thermocouples are progressively inserted in the thermowells, starting with those located towards the back end of the cell (see **Fig. 5.3**).

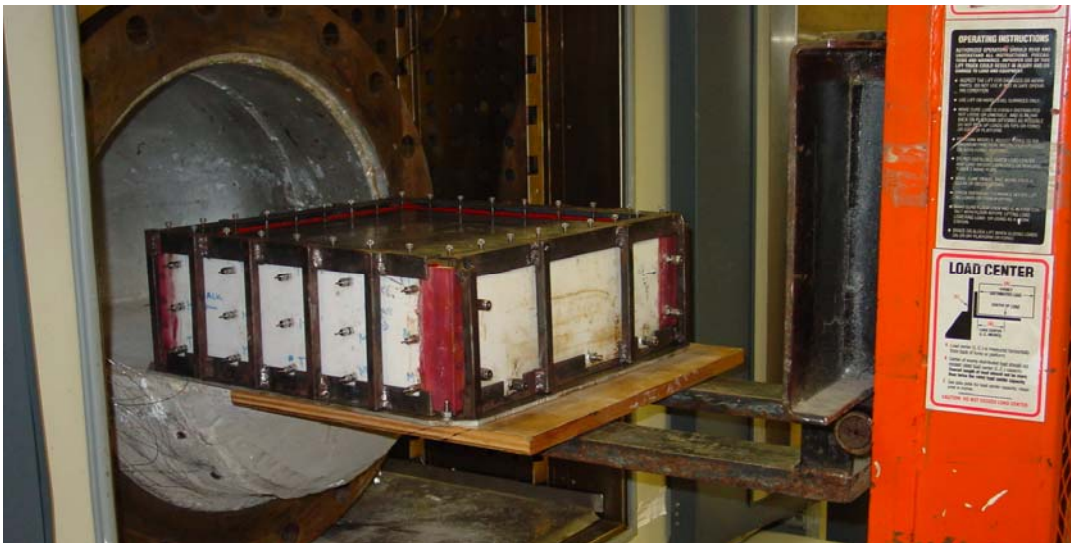

Fig. 5.2- Forklift used to introduce the cell in the pressure jacket.

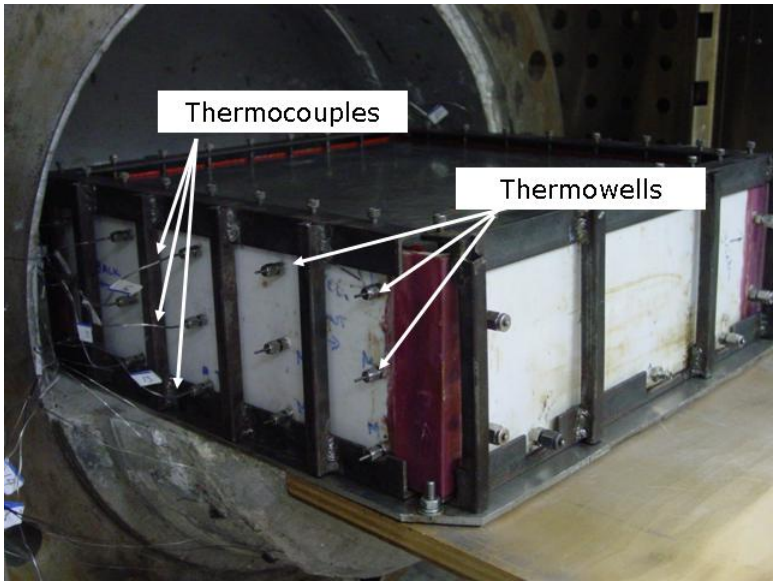

Fig. 5.3- Thermocouples are installed in the thermowells as the cell is being introduced in the pressure jacket.

After the pressure jacket is closed, the production wells are connected to the production system and the injection well is attached to the steam generator. After the oven is turned on, it takes about 48 hours to reach a uniform initial reservoir temperature (55ºC) throughout the cell.

Before the start of each experiment, the steam generator is set at 240ºC with a backpressure of 50 psig. The steam is bypassed around the cell in order to stabilize the pressure and temperature before injection to the physical model can occur. The cell is charged with nitrogen to set an initial reservoir pressure of 50 psig. While the cell is being charged, the overburden pressure is simultaneously increased in order to maintain a confining pressure that is always 20 psi above the cell pressure.

The run is started by closing the steam bypass and opening the injection valve from the steam generator to the physical model. Several parameters are constantly monitored during the run in order to insure that they remain inside the appropriate operational range. These parameters are: injection pressure, overburden pressure, steam injection rate, propane injection rate, injection temperature and flowing production pressures. The injection temperature is controlled so the steam injected is slightly superheated at all times.

The produced stream includes water, oil and an oil-water emulsion. After several tests it was determined that the easiest way to separate the emulsion was to add petroleum distillate, emulsion breaker and a water clarifier to the mixture. It was also found that the addition of sodium chloride was an effective method to increase the water density and in turn facilitate the separation of the oil and water phases. A known amount of petroleum distillate (50 cm^3), the emulsion breaker and the water clarifier are added beforehand to the measuring cylinders. Just after fluid collection, the sodium chloride is added and a magnetic stirrer is used to mix the additives with the produced fluids. The cylinder is then placed in an ultrasonic bath to help the separation by gravity of the fluids. Once the separation is complete, the volumes of water and oil are measured and recorded taking into consideration that the oil volume includes 50 cm^3 of petroleum distillates.

CHAPTER VI

EXPERIMENTAL RESULTS

Five experimental runs were conducted to test the proposed concepts of steam-propane injection and the vertical injector-smart horizontal producer system. The experimental runs are as follows:

- **Runs using the conventional vertical well system**
    - Pure steam injection (Run 2)
    - Steam-propane injection (Run 4)
- **Runs using the smart horizontal well system (Configuration A)**
    - Pure steam injection (Run 3)
    - Steam-propane injection (Run 5)
- **Runs using the smart horizontal well system (Configuration B)**
    - Pure steam injection (Run 6)

The following parameters were kept constant for all the runs:

- Initial pressure: 50 psig
- Well flowing backpressure: 50 psig
- Initial temperature: 55ºC
- Steam injection rate: 48 cm^3/min cold water equivalent (CWE)
- Water saturation of sandpack in cell: 20%

- Oil saturation of sandpack in cell: 40%

In the smart horizontal system, steam is injected only in the top half of the vertical injector, while in the vertical well system, injection takes place along the entire well. This difference in the injection conditions causes the injection pressure to be different in the smart horizontal well system and the vertical well system. Since steam has to be injected under superheated conditions and the saturation temperature depends on pressure, the steam injection temperature will vary from run to run.

It was initially decided to run the experiments for 180 minutes, which corresponds approximately to 20 years in the field (see section 3), a reasonable period for a steamflooding project. However, the experiments were run as long as operationally possible, with the limiting factor being the amount of cylinders available to collect the fluids. The longest experiments ran for more than 240 minutes.

As can be seen in **Fig. 4.7**, the smart horizontal well is divided into three sections of equal length. The idea of dividing the well into three sections is based on the results presented by Sandoval,[10] who tested several configurations for the smart horizontal well and found that dividing the well in three sections was the optimum design. In this research, two different production configurations were used to test the concept of the smart horizontal well, namely configuration A and configuration B.

Configuration A: In this case, the two sections closer to the injector (sections 2 and 3) are opened from the beginning of the run. Twenty six minutes after production starts (about 3 years in the field), section 1 is opened and sections 2 and 3 are closed (see **Fig. 6.1**).

Configuration B: Initially, all the sections are opened to flow. Section 3 is closed 97 minutes after production starts. Section 2 is closed 75 minutes after shutting section 3 (see **Fig. 6.2**).

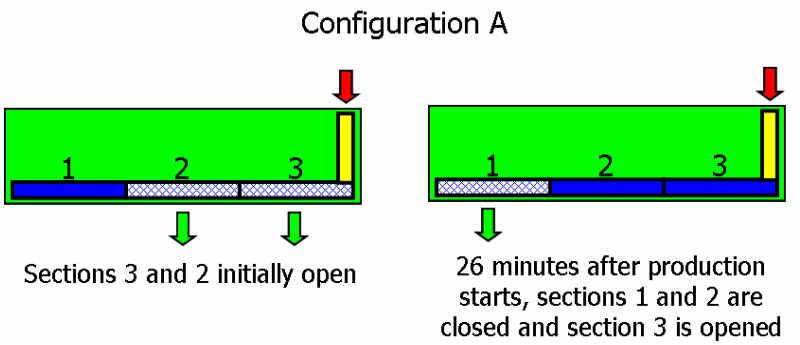

Fig. 6.1- Configuration A for the smart horizontal well.

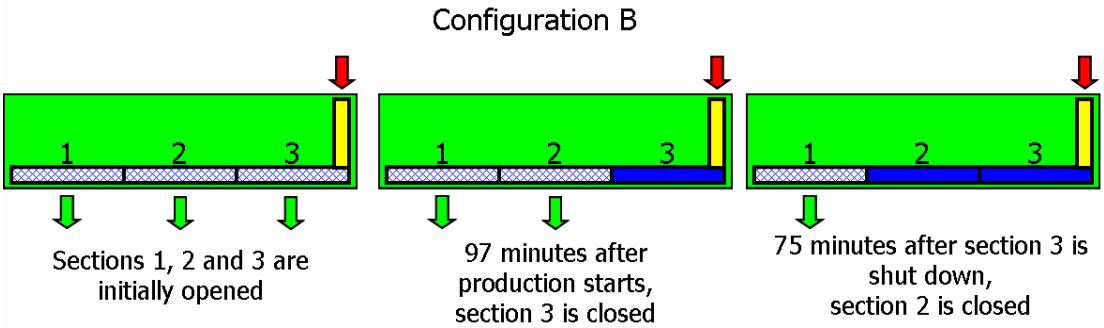

Fig. 6.2- Configuration B for the smart horizontal well.

The properties of the sandpack in the cell in each experiment are presented in **Table 6.1**. The calculation methodology for the sandmix is presented in appendix A.

TABLE 6.1 – SANDMIX PROPERTIES FOR RUNS 2 TO 6

	Run 2	Run 3	Run 4	Run 5	Run 6
Porosity, %	35.2	35.4	35.1	35.7	35.7
Pore volume, cm^3	9398	9368	9420	9327	9328
Water volume inside cell, cm^3	1880	1874	1884	1865	1866
Oil volume inside cell (OOIP), cm^3	3605	3593	3613	3476	3552

6.1 Pure steam injection in the vertical well system (Run 2)

This run constitutes the base case to evaluate the steam-propane process using the vertical well system. In this experiment, one vertical injector and three vertical producers are used (see **Fig. 4.7**). Steam is injected throughout the entire length of the vertical injector. The

entire thickness of the model is also open to production through the vertical producers. This experiment was run for 240 minutes.

Fig. 6.3 shows the steam injection parameters: injection temperature and injection flow rate (Cold Water Equivalent – CWE). The injection temperature ranges between 170 to 175ºC. For reference, the saturation temperature, which depends on the injection pressure, is also shown. It can be noted that superheated steam is injected at all times during the run, as the injection temperature is always higher than the saturation temperature.

The injection and overburden pressures as well as the flowing production pressures for all three vertical producers are plotted in **Fig. 6.4**. Initially, the injection pressure starts around 55 psig. As the experiment progresses, an oil bank forms and the injection pressure starts to gradually increase to a maximum of approximately 80 psig. At about 140 minutes, the injection pressure starts to decrease as the overall oil viscosity in the cell is reduced due to the effect of the increasing temperature. The overburden pressure is manually set during the run to always be above the injection pressure. In this experiment, the difference between the overburden and injection pressures is about 20 to 25 psig.

The backpressure regulators used in the production system are initially set to apply a flowing backpressure of 50 psig to each well. These dome-loaded regulators are ideal for multiphase flow applications, such as the one encountered in this research, where liquid oil and water flow along with propane and water vapor. However, as hot fluids are produced during the run, the temperature of the regulator's dome rises, which in turn causes an increase in the backpressure above the setting point of 50 psig. When the dome pressure increases, a correction of the setting point is required. This correction involves bleeding out some of the nitrogen used to pressurize the dome. Sometimes, too much nitrogen is evacuated and the setting point falls below 50 psig. Such behavior can be observed in the flowing backpressures plotted in **Fig. 6.4**, especially in wells 1 and 3. Despite the fluctuations observed, the flowing pressure for all three wells remain around 45 to 55 psig.

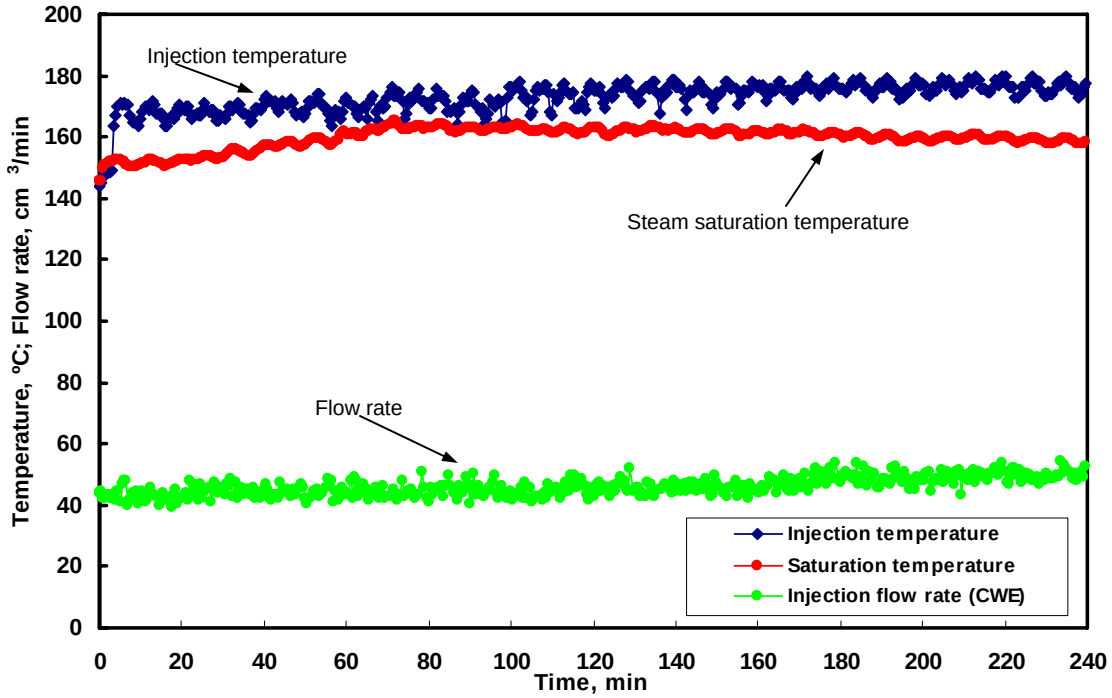

Fig. 6.3- Pure steam injection in the vertical well system (Run 2): Injection temperature and flow rate.

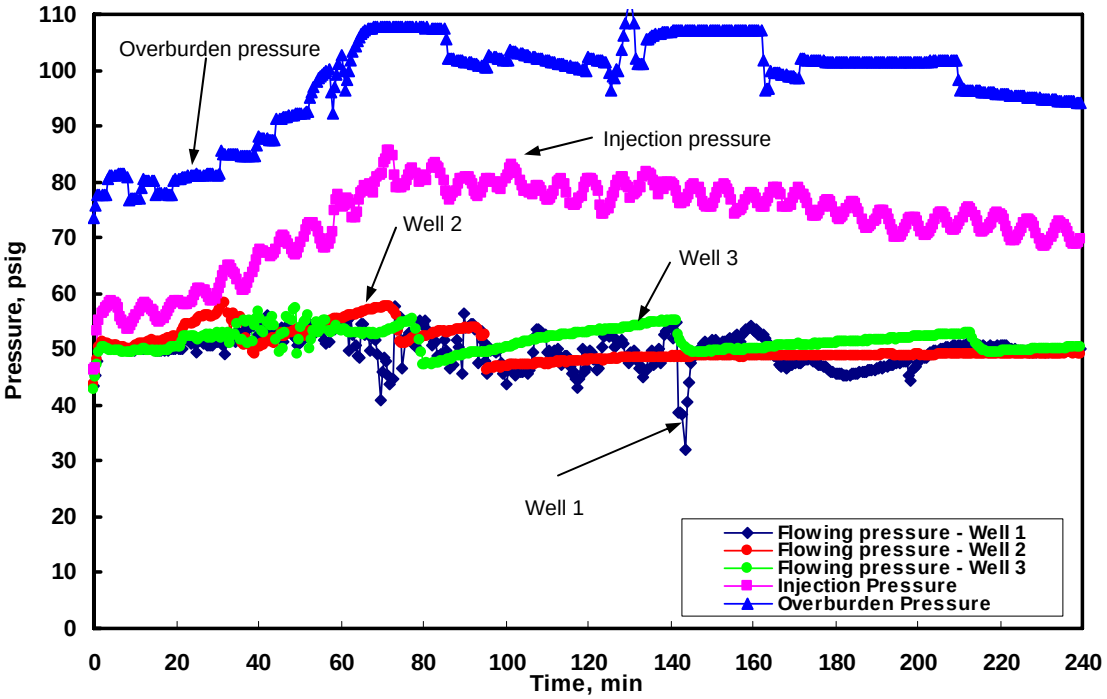

Fig. 6.4- Pure steam injection in the vertical well system (Run 2): Flowing pressure for the three vertical producers, injection pressure and overburden pressure.

Oil and water rates are presented in **Figs. 6.5, 6.6** and **6.7** for wells 1, 2 and 3 respectively. The total oil rate for the entire pattern is shown in **Fig. 6.8**. It can be observed that oil rate peaks at about 100 minutes and a second smaller peak occurs at about 190 minutes. The second peak coincides with the arrival of the steam front in well 1 which brings an instantaneous rise of production to that well (see **Fig. 6.5**).

Cumulative oil production and recovery are depicted in **Figs. 6.9** and **6.10**. At 240 min, oil production totals about 1600 cm^3, which corresponds to about 44% of the OOIP.

Figs. 6.11 through **6.13** show the temperature profiles for this experiment at different times throughout the run. For each instant depicted, there are three temperature profiles shown: at the top, at the middle and at the bottom of the cell. These temperature profiles allow us to monitor the advance of the heated fluids and the steam front along the entire cell. The phenomenon of steam override can be easily identified as the top of the cell is consistently hotter than the rest of the model.

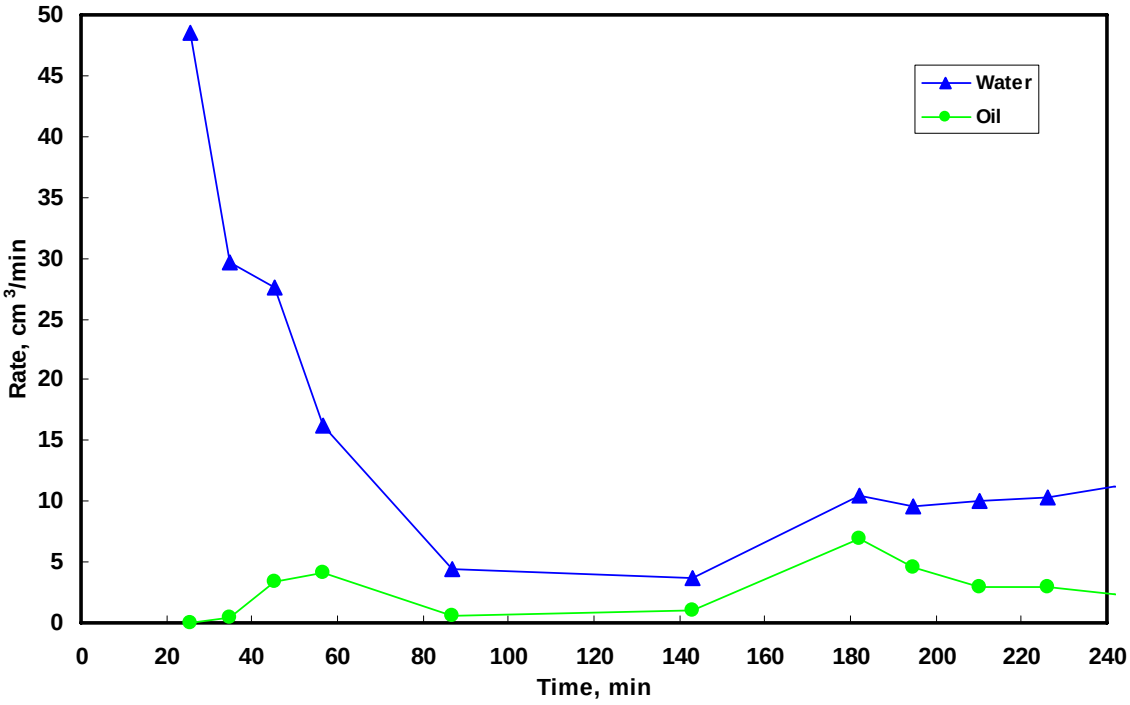

Fig. 6.5- Pure steam injection in the vertical well system (Run 2): Oil and water rates for Well 1.

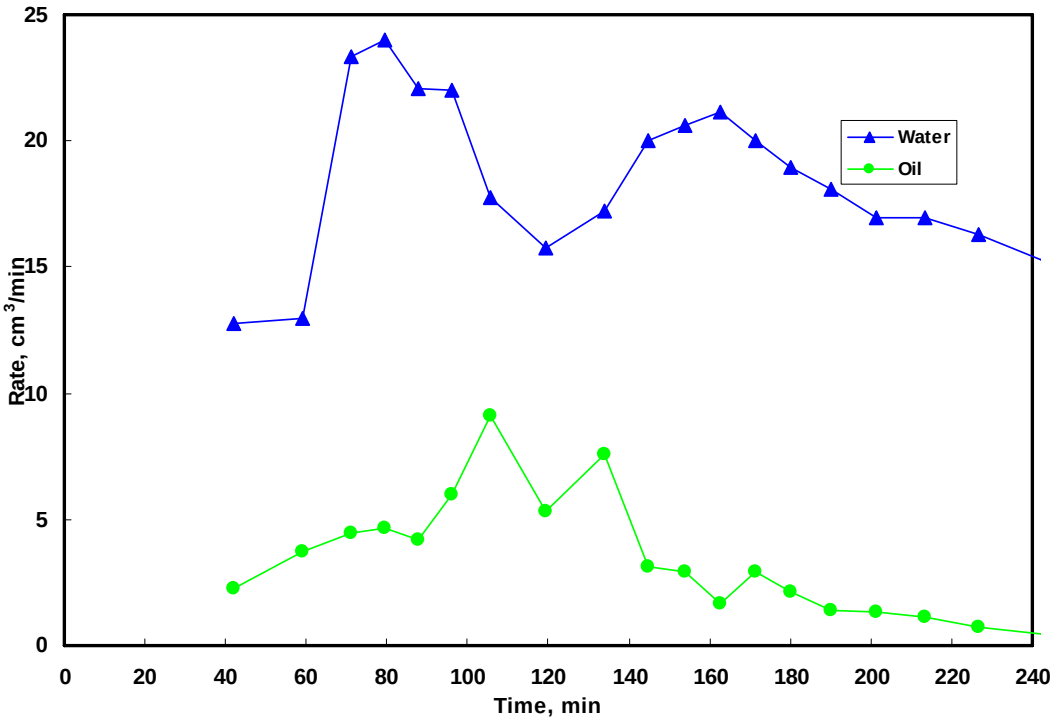

Fig. 6.6- Pure steam injection in the vertical well system (Run 2): Oil and water rates for Well 2.

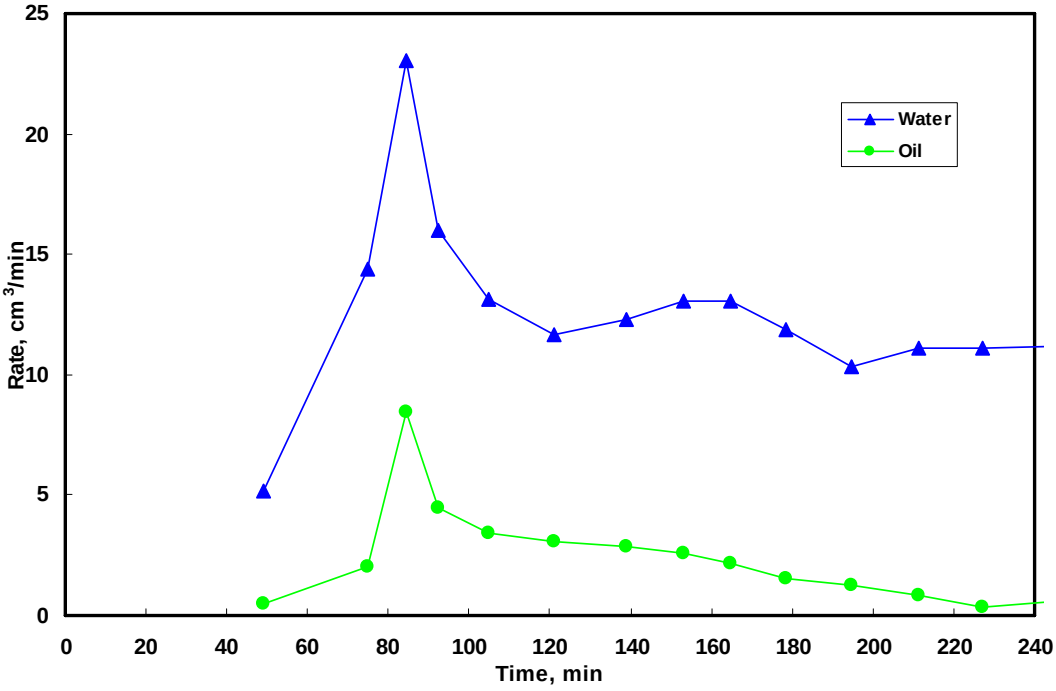

Fig. 6.7- Pure steam injection in the vertical well system (Run 2): Oil and water rates for Well 3.

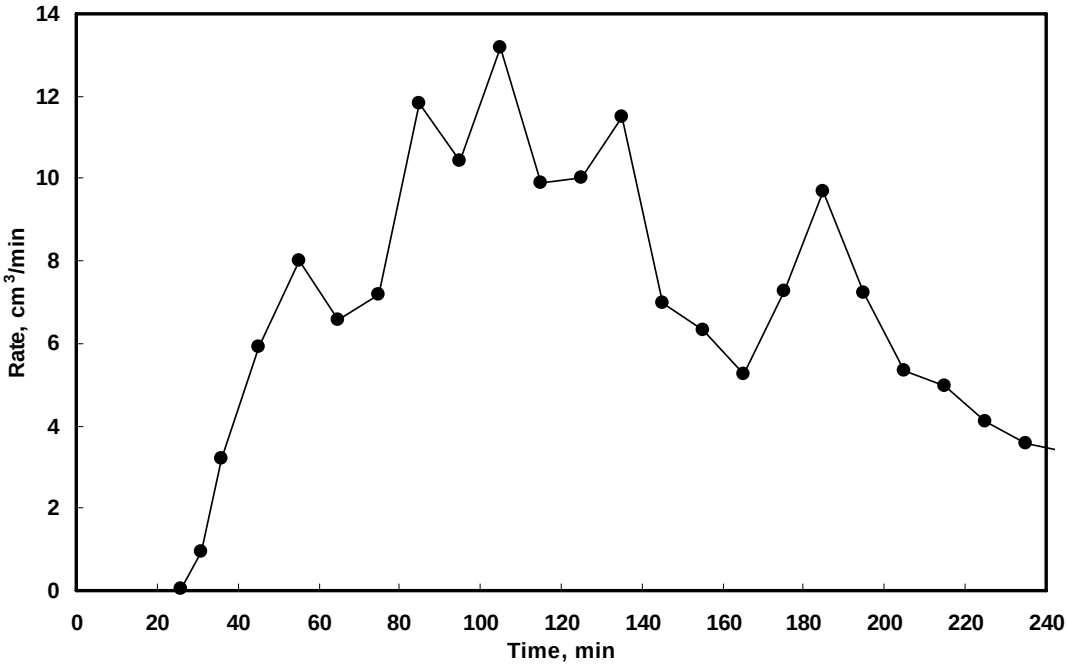

Fig. 6.8- Pure steam injection in the vertical well system (Run 2): Total oil rate production.

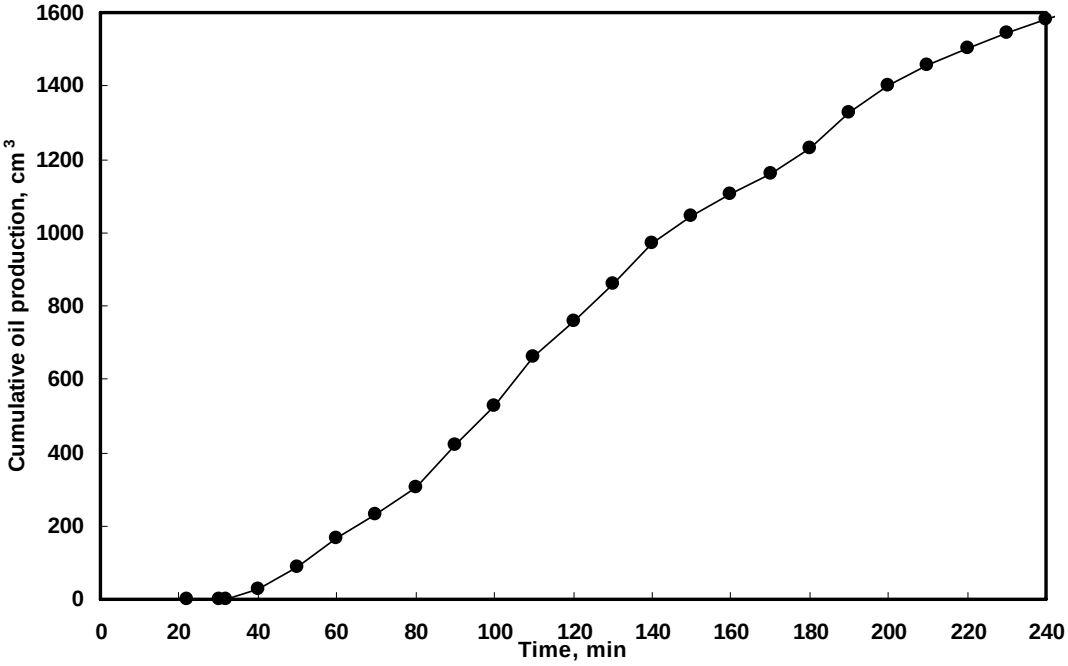

Fig. 6.9- Pure steam injection in the vertical well system (Run 2): Cumulative oil production.

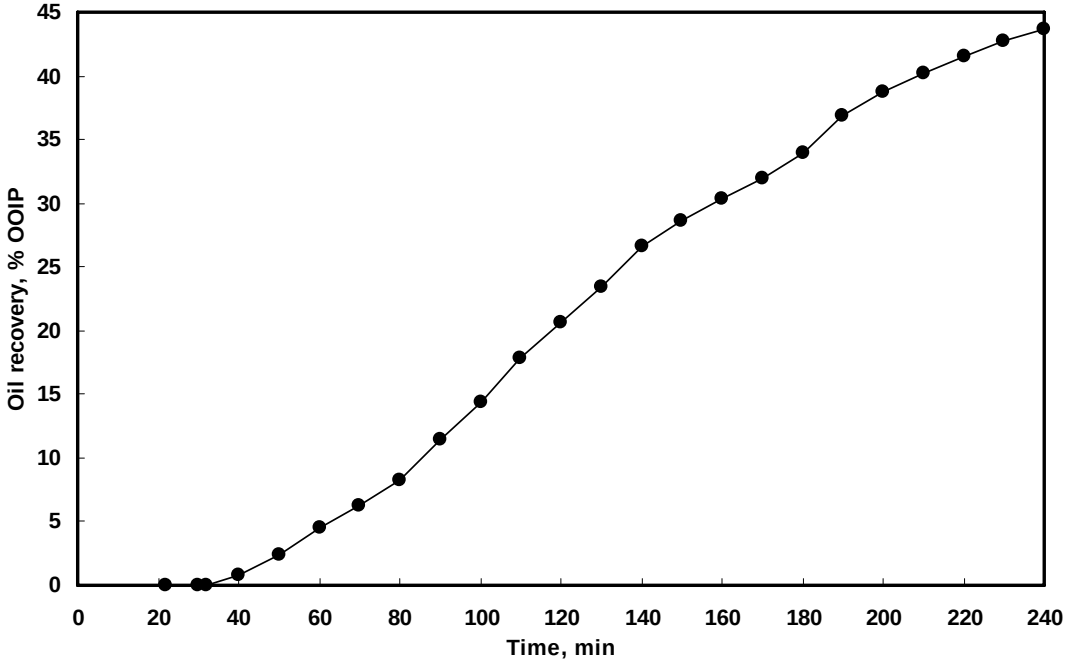

Fig. 6.10- Pure steam injection in the vertical well system (Run 2): Oil recovery.

The temperature profiles shown in this section as well as those presented in the following sections were generated using the temperature measurements collected every 30 seconds in each of the 75 thermocouples distributed along the cell (see **Fig. 4.4**). To create the profiles, the temperature measurements were interpolated to generate temperature contours that were later plotted. All the interpolation and plotting was carried out using the commercial graphing software called Tecplot 360.

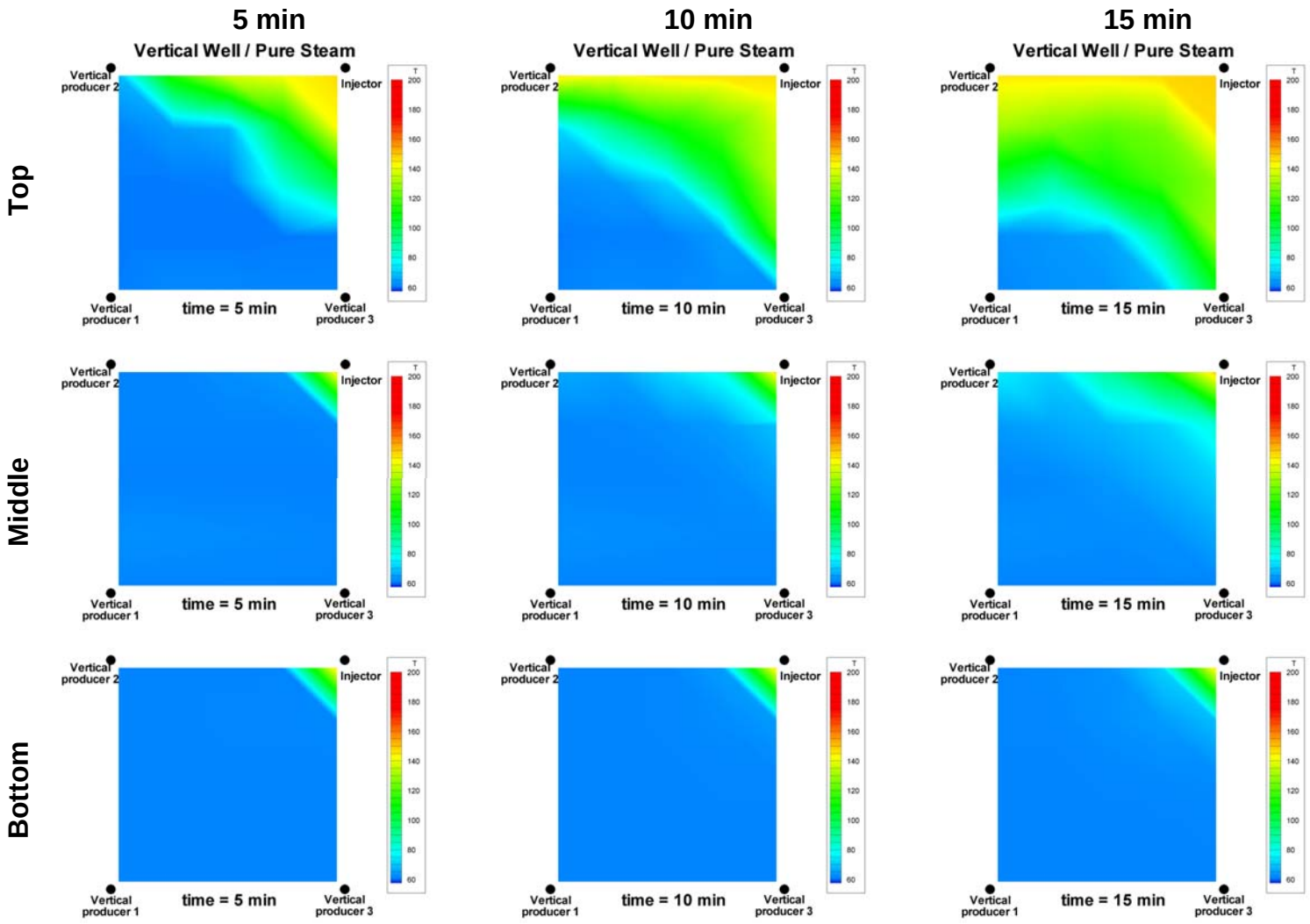

Fig. 6.11- Pure steam injection in the vertical well system (Run 2): Plan view of the temperature profiles in the physical model at 5, 10 and 15 minutes. The top, middle and bottom rows show the profile at the top, middle and bottom of the cell respectively.

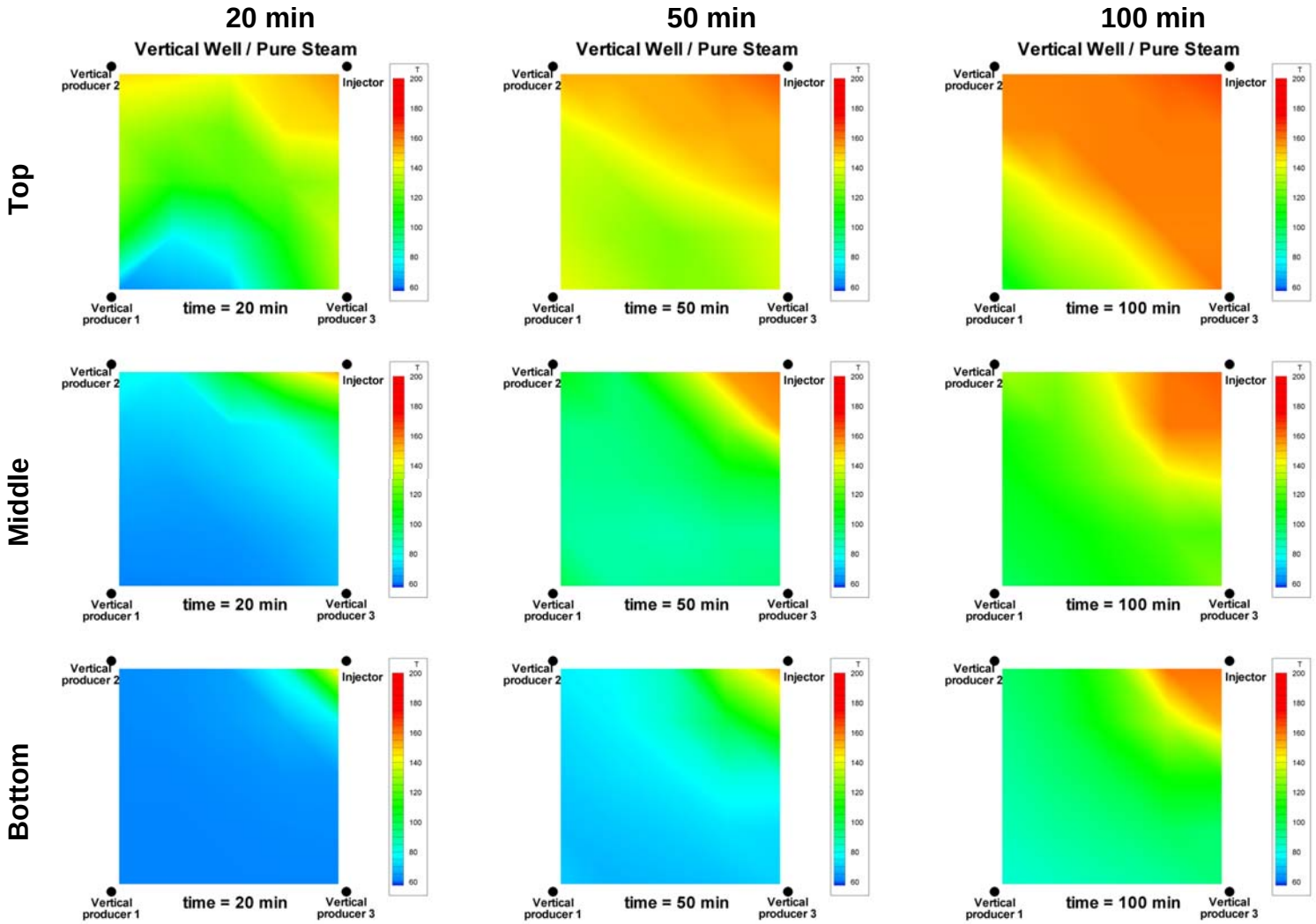

Fig. 6.12- Pure steam injection in the vertical well system (Run 2): Plan view of the temperature profiles in the physical model at 20, 50 and 100 minutes. The top, middle and bottom rows show the profile at the top, middle and bottom of the cell respectively.

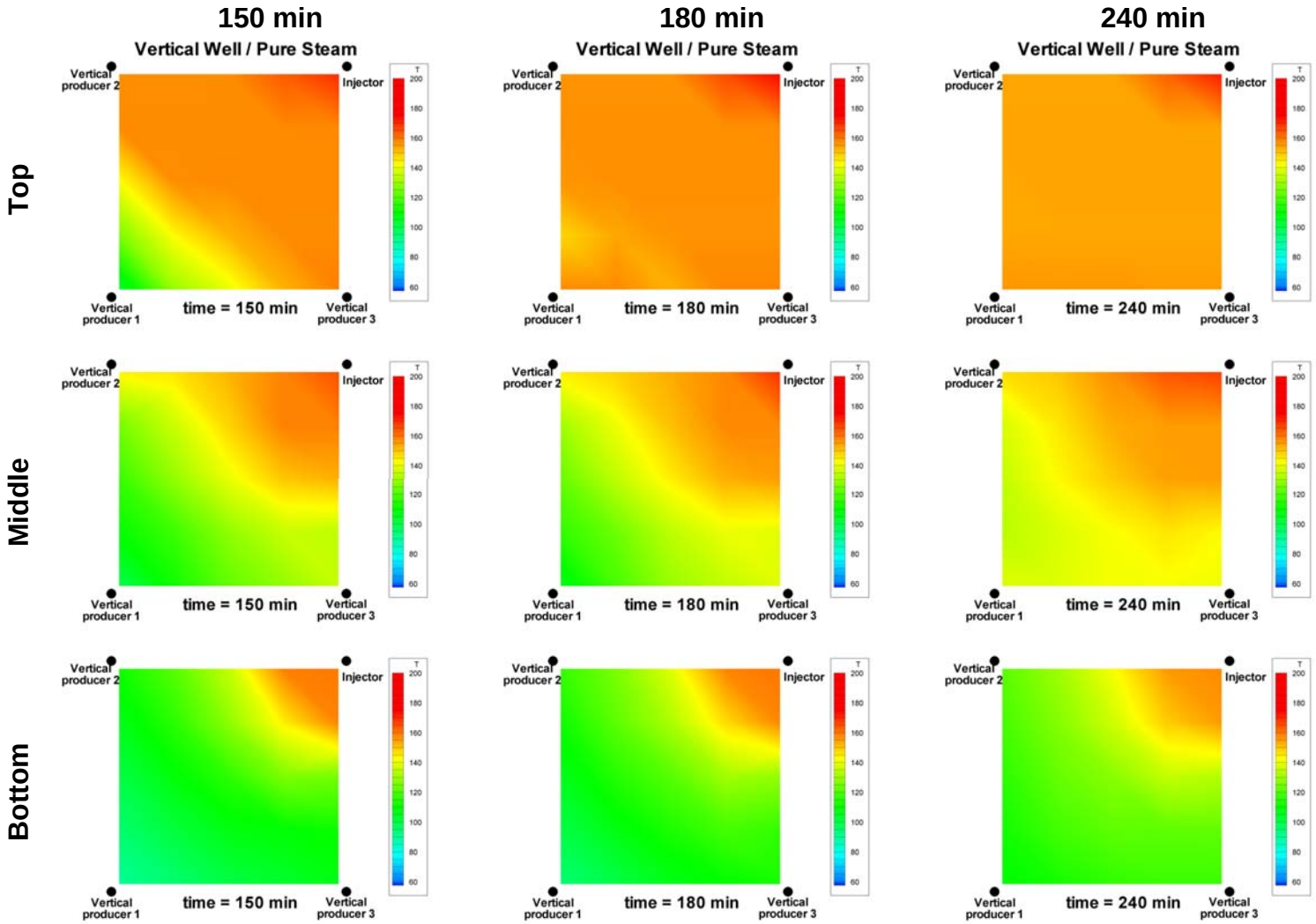

Fig. 6.13- Pure steam injection in the vertical well system (Run 2): Plan view of the temperature profiles in the physical model at 150, 180 and 240 minutes. The top, middle and bottom rows show the profile at the top, middle and bottom of the cell respectively.

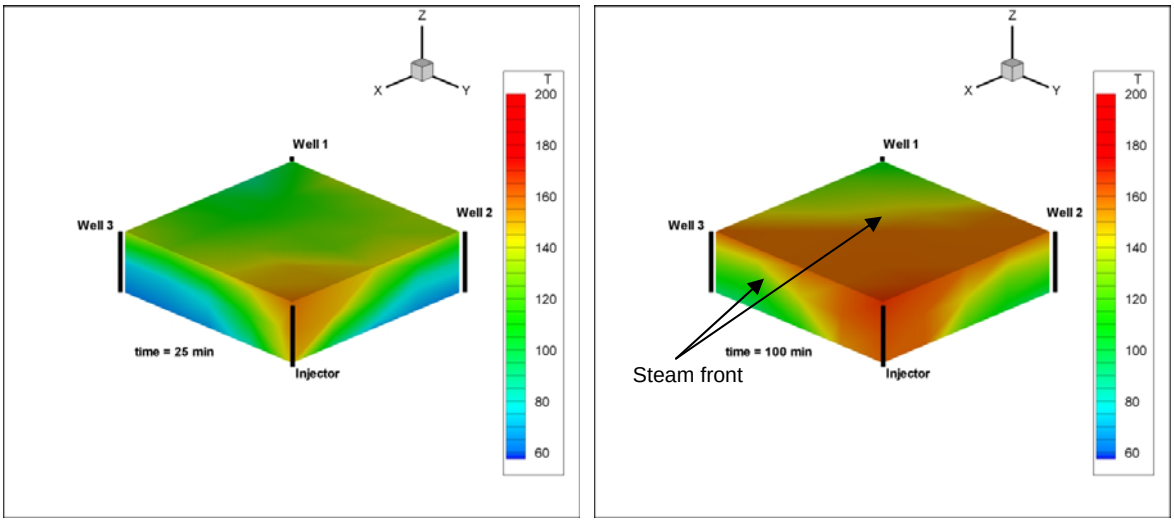

(i) (ii)

Fig. 6.14- Pure steam injection in the vertical well system (Run 2): Temperature profile in isometric view showing steam override at (i) 25 minutes and (ii) 100 minutes

Taking the injection pressure as a reference (80 psig), the steam saturation temperature is 162ºC, which is represented by an orange tone in the profile. From 5 to 15 minutes (top profiles in **Fig. 6.11**) the steam being injected condenses immediately because of heat transfer by conduction and convection to the relatively cold sandpack. At about 20 minutes (**Fig. 6.12**), we start to see a small steam zone in the cell. At 100 minutes, the steam zone had already reached the top part of wells 2 and 3 and covered more than 50% of the cell's area. When comparing the temperature profiles at 180 and 240 minutes in **Fig. 6.13**, it can be observed that very little has changed, which is evidence that a steam chest has formed and the steam is being recirculated from the injector to the producers leaving the middle and bottom parts of the cell mostly unswept.

Fig. 6.14 shows an isometric profile seen from the injector's point of view, where more evidence of steam override can be observed. The location of the steam front is easily identifiable in the temperature profiles, where it can be observed that the steam zone concentrates around the injector and the top of the cell.

6.2 Steam-propane injection in the vertical well system (Run 4)

In this run, the amount of steam injected is the same as in run 2 (48 g/min – CWE). Propane is injected at a ratio of 4% by weight, which corresponds to an injection rate of 1.92 g/min. In the same way as run 2, this experiment uses one vertical injector and three vertical producers. Steam and propane are injected in both the top and bottom sections of the injector. Both sections of the vertical producers are also opened for production. Due a limited availability of collection cylinders, this experiment could only be run for 180 minutes.

Throughout the entire run, superheated steam at about 175 ºC is injected (see **Fig. 6.15).** The steam saturation temperature (dependant on injection temperature) ranges from 160 to 170 psig. **Fig. 6.15** also shows the steam injection rate averaging 47.9 cm^3/min.

Fig. 6.16 depicts the injection and overburden pressures as well as the flowing pressures for the vertical producers. The injection pressure fluctuates between 75 and 85 psig. These fluctuations may be caused by changes in the delivery pressure of the steam generator due to variations in the liquid level inside the generator's core. The manually controlled overburden pressure remains about 15 to 25 psia above the injection pressure.

In this experiment, the flowing pressure in the vertical producers (shown in **Fig. 6.16)**, remains fairly constant at around 50 psig. Starting at 70 minutes, it gradually increases to 55 psig but is corrected at about 120 minutes.

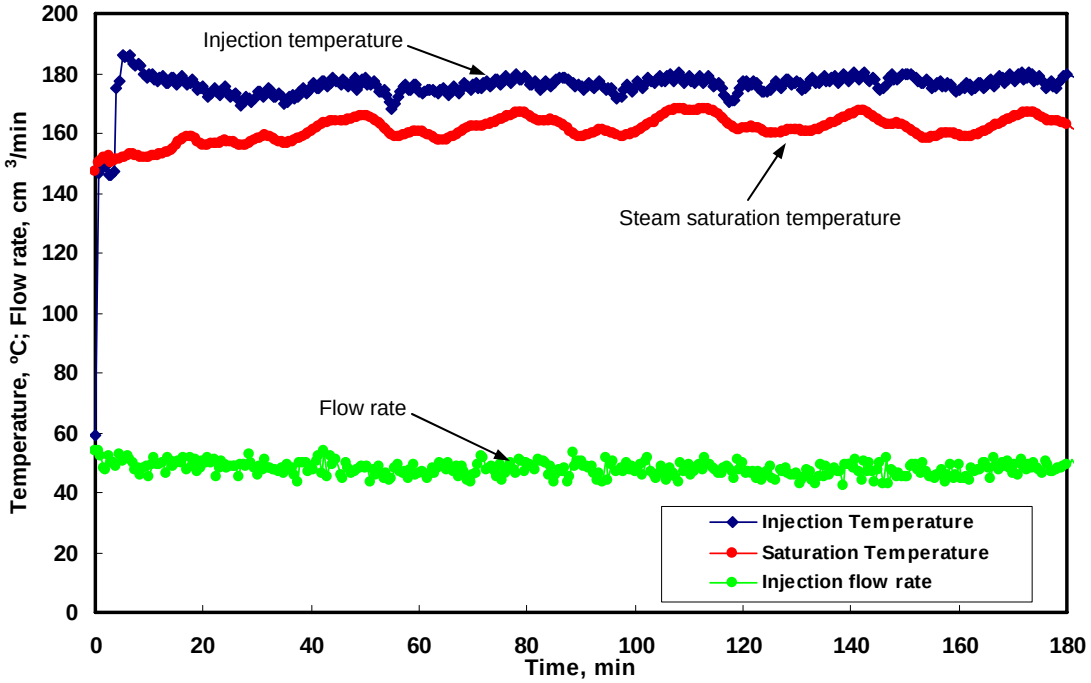

Fig. 6.15- Steam-propane injection in the vertical well system (Run 4): Injection temperature and flow rate.

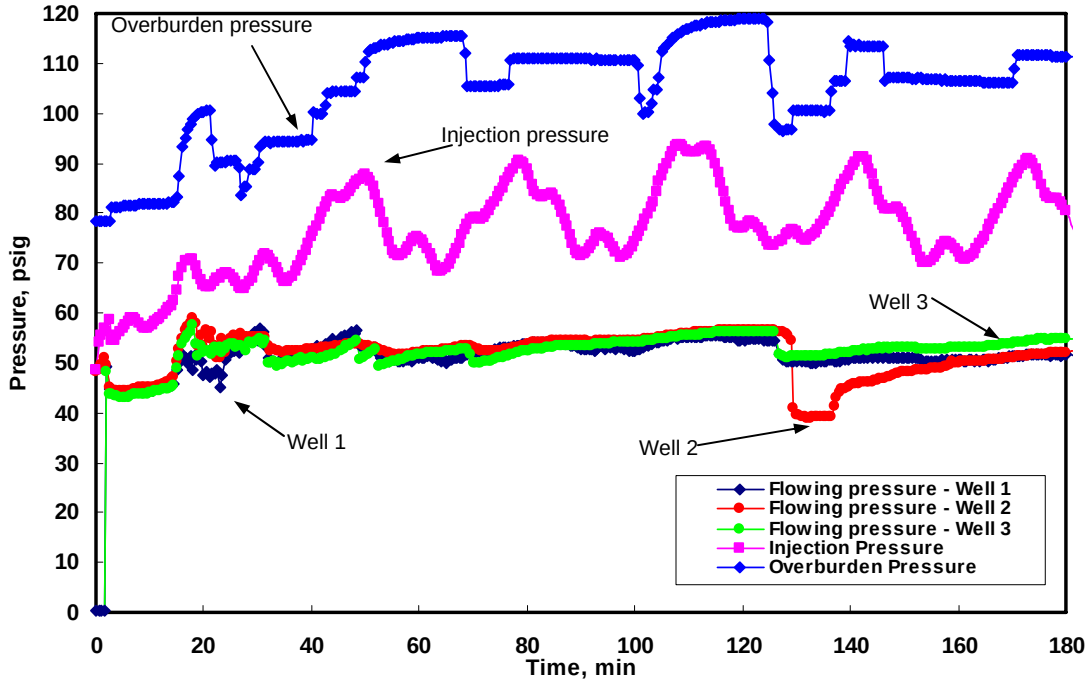

Fig. 6.16- Steam-propane injection in the vertical well system (Run 4): Flowing pressure for the three vertical producers, injection pressure and overburden pressure.

Figs. 6.17 through **6.19** show the water and oil rates for the vertical producers. The total oil rate (shown on **Fig. 6.20)** peaks at around 50 minutes, with 18 cm^3/min.

At 180 min, the cumulative oil produced is around 1530 cm^3 (see **Fig. 6.21**), which amounts to about 41.4% of the OOIP (shown in **Fig. 6.22**).

Temperature profiles at several times during the experiment are shown in **Figs. 6.23** through **6.25**. The profiles show how steam tends to accumulate at the top of the cell, progressively forming a steam chest that creates a path for steam recirculation. When comparing the profiles at 150, 180 and 210 minutes (**Fig. 6.25**), it can be noted that the size of the steam zone does grow significantly, leaving unswept much of the bottom of the cell.

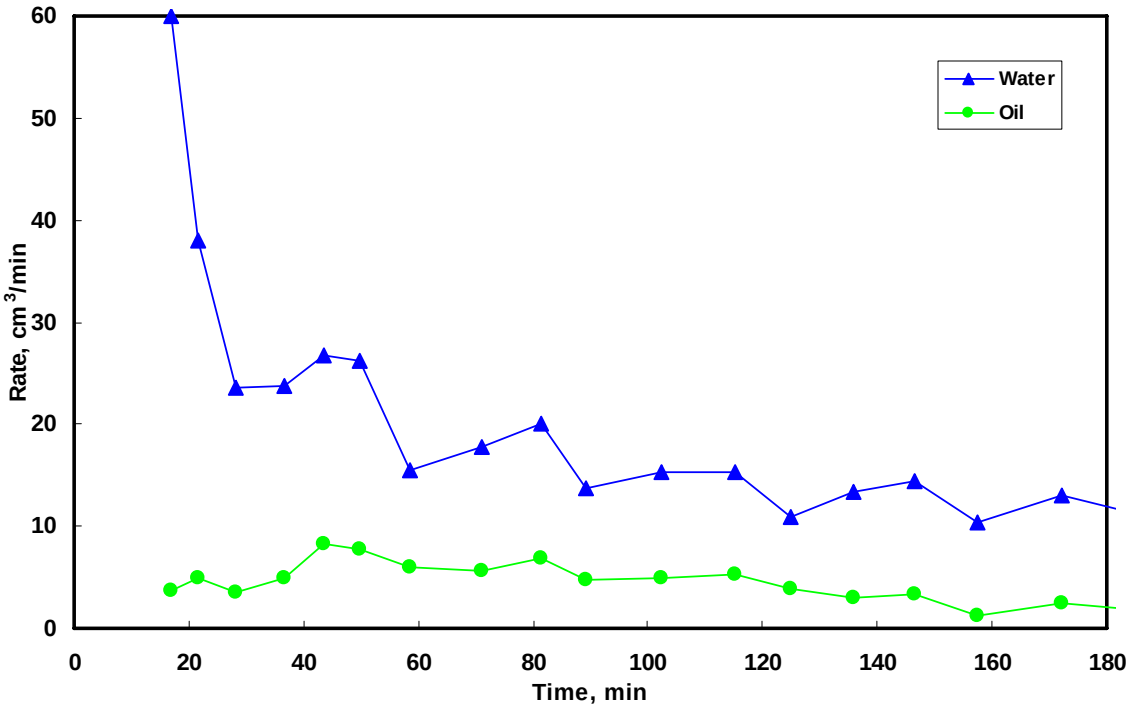

Fig. 6.17- Steam-propane injection in the vertical well system (Run 4): Oil and water rates for Well 1.

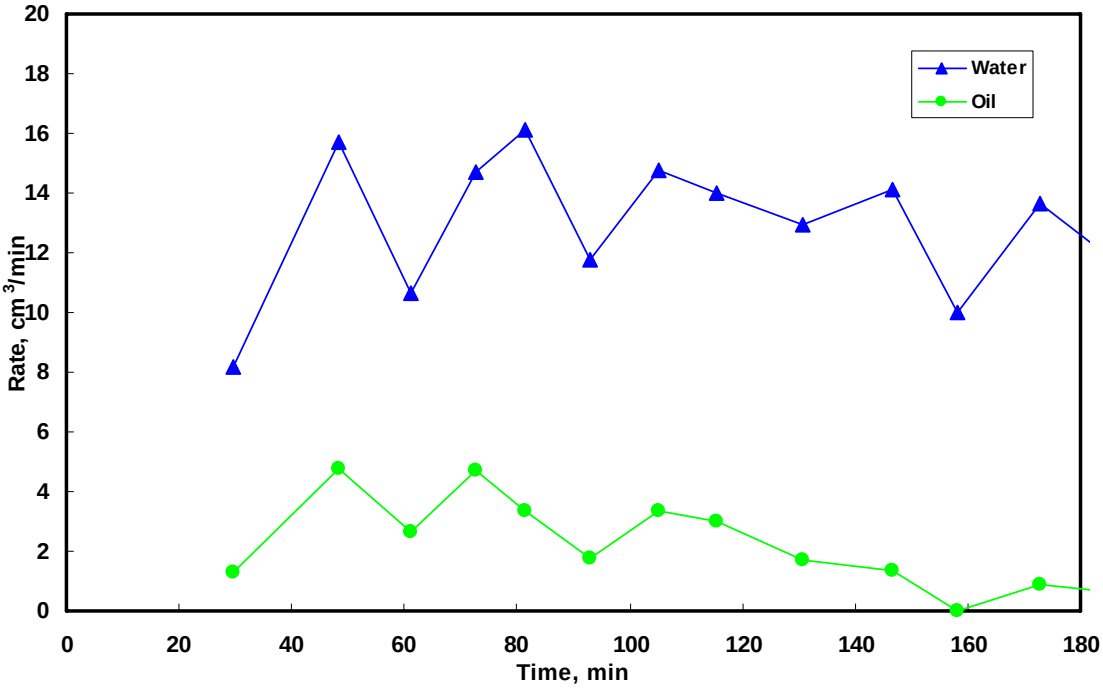

Fig. 6.18- Steam-propane injection in the vertical well system (Run 4): Oil and water rates for Well 2.

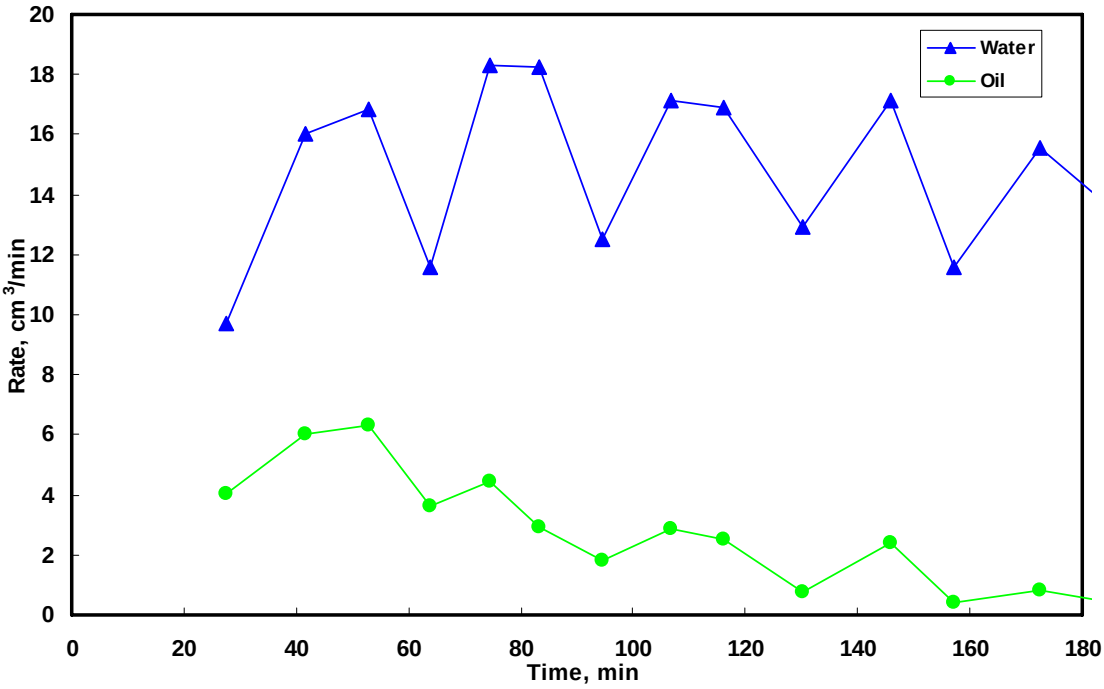

Fig. 6.19- Steam-propane injection in the vertical well system (Run 4): Oil and water rates for Well 3.

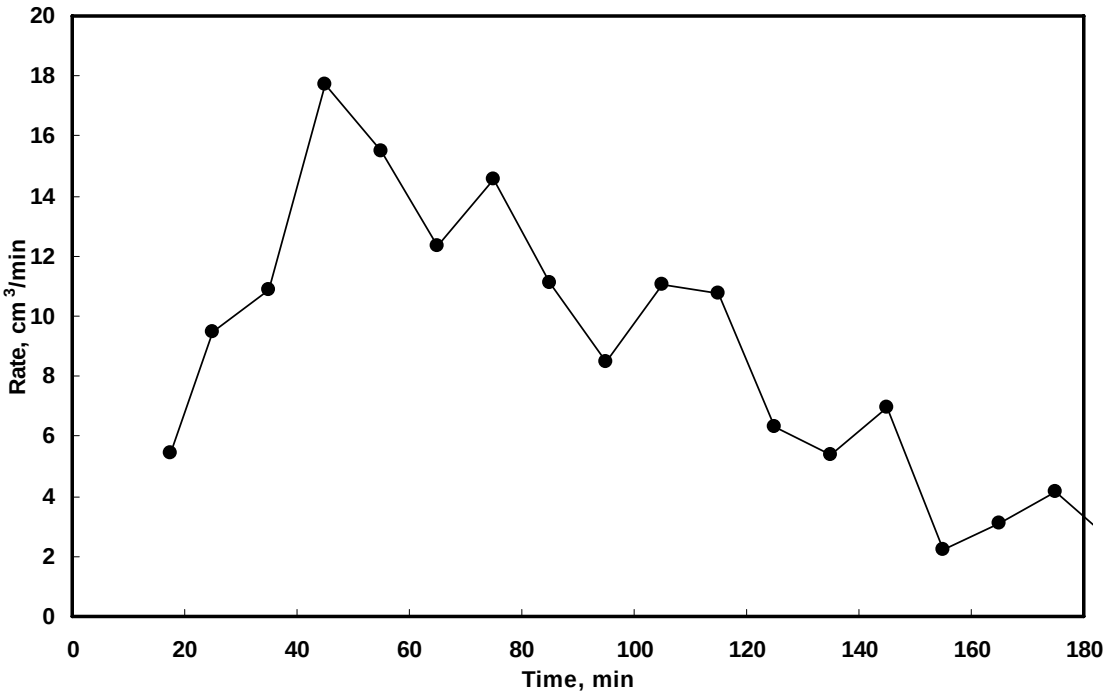

Fig. 6.20- Steam-propane injection in the vertical well system (Run 4): Total oil rate production.

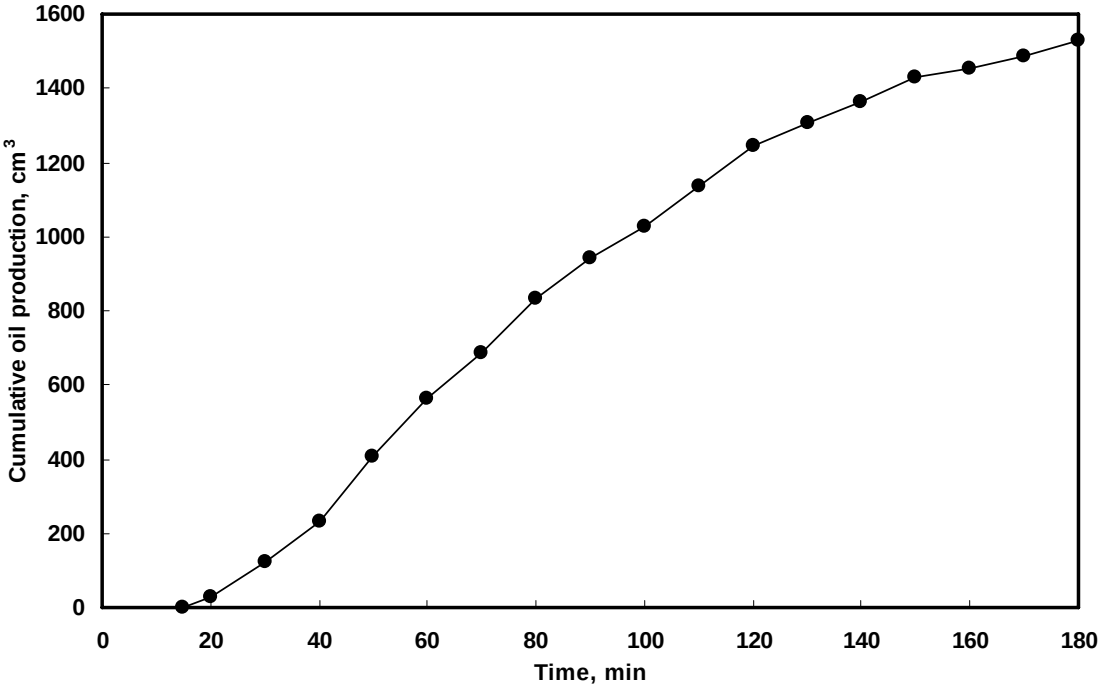

Fig. 6.21- Steam-propane injection in the vertical well system (Run 4): Cumulative oil production.

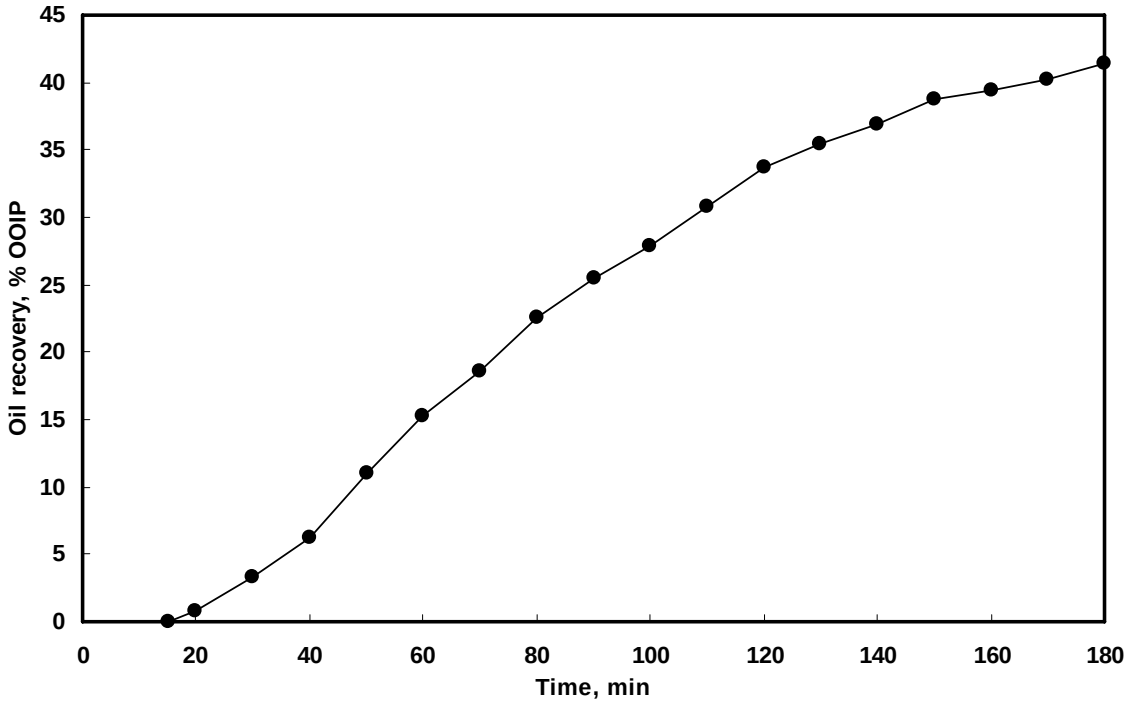

Fig. 6.22- Steam-propane injection in the vertical well system (Run 4): Oil recovery.

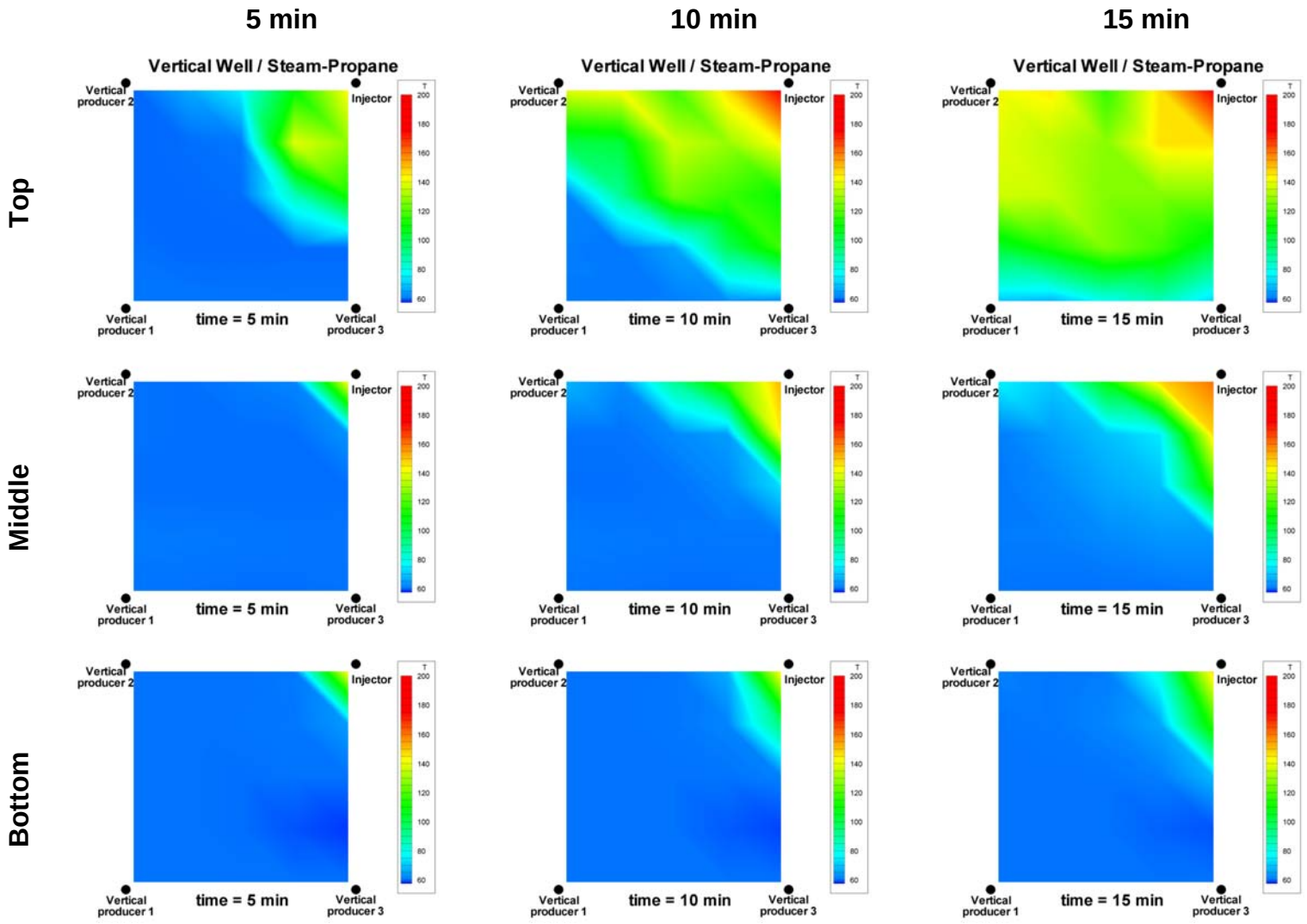

Fig. 6.23- Steam-propane injection in the vertical well system (Run 4): Plan view of the temperature profiles in the physical model at 5, 10 and 15 minutes. The top, middle and bottom rows show the profile at the top, middle and bottom of the cell respectively.

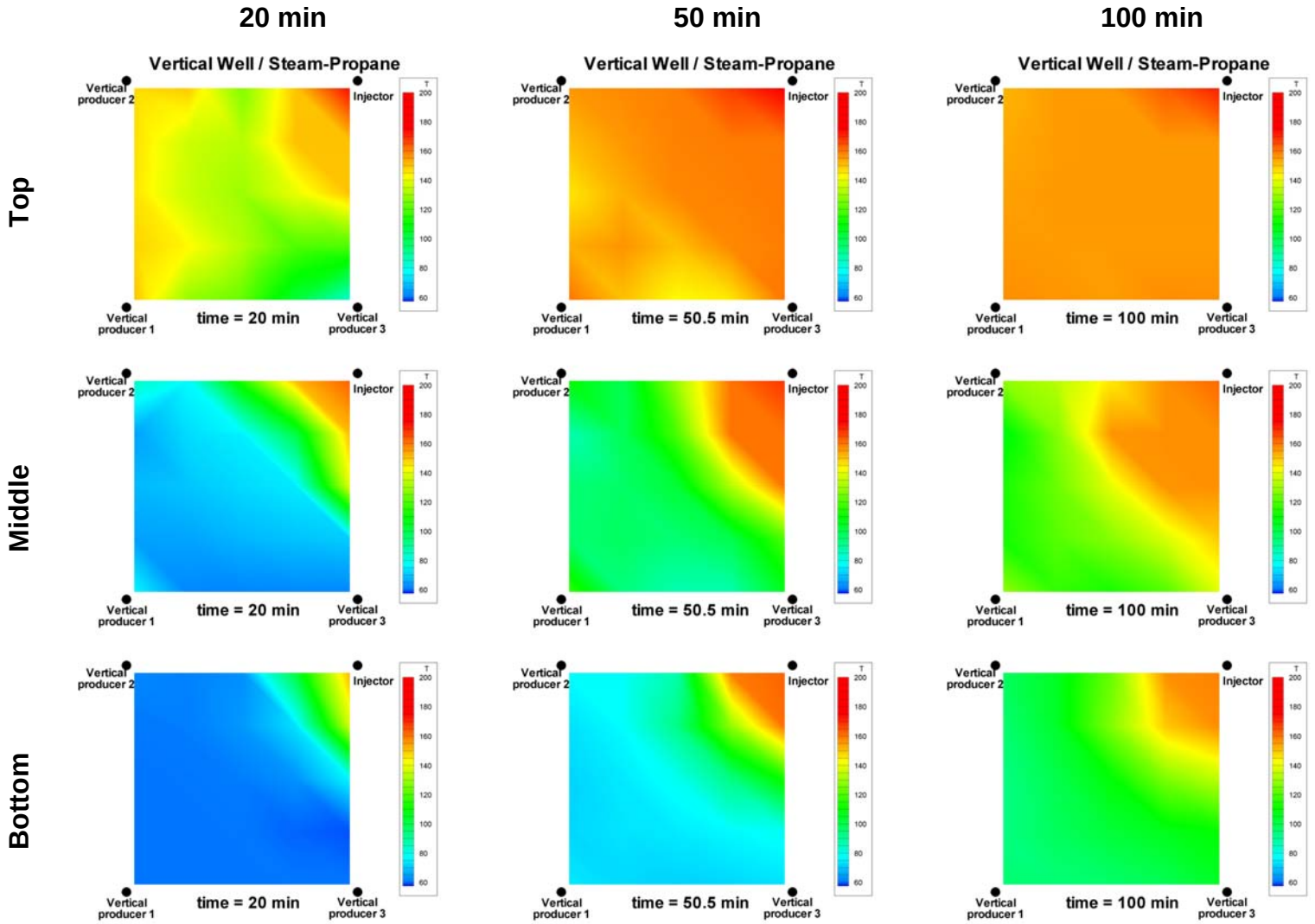

Fig. 6.24- Steam-propane injection in the vertical well system (Run 4): Plan view of the temperature profiles in the physical model at 20, 50 and 100 minutes. The top, middle and bottom rows show the profile at the top, middle and bottom of the cell respectively.

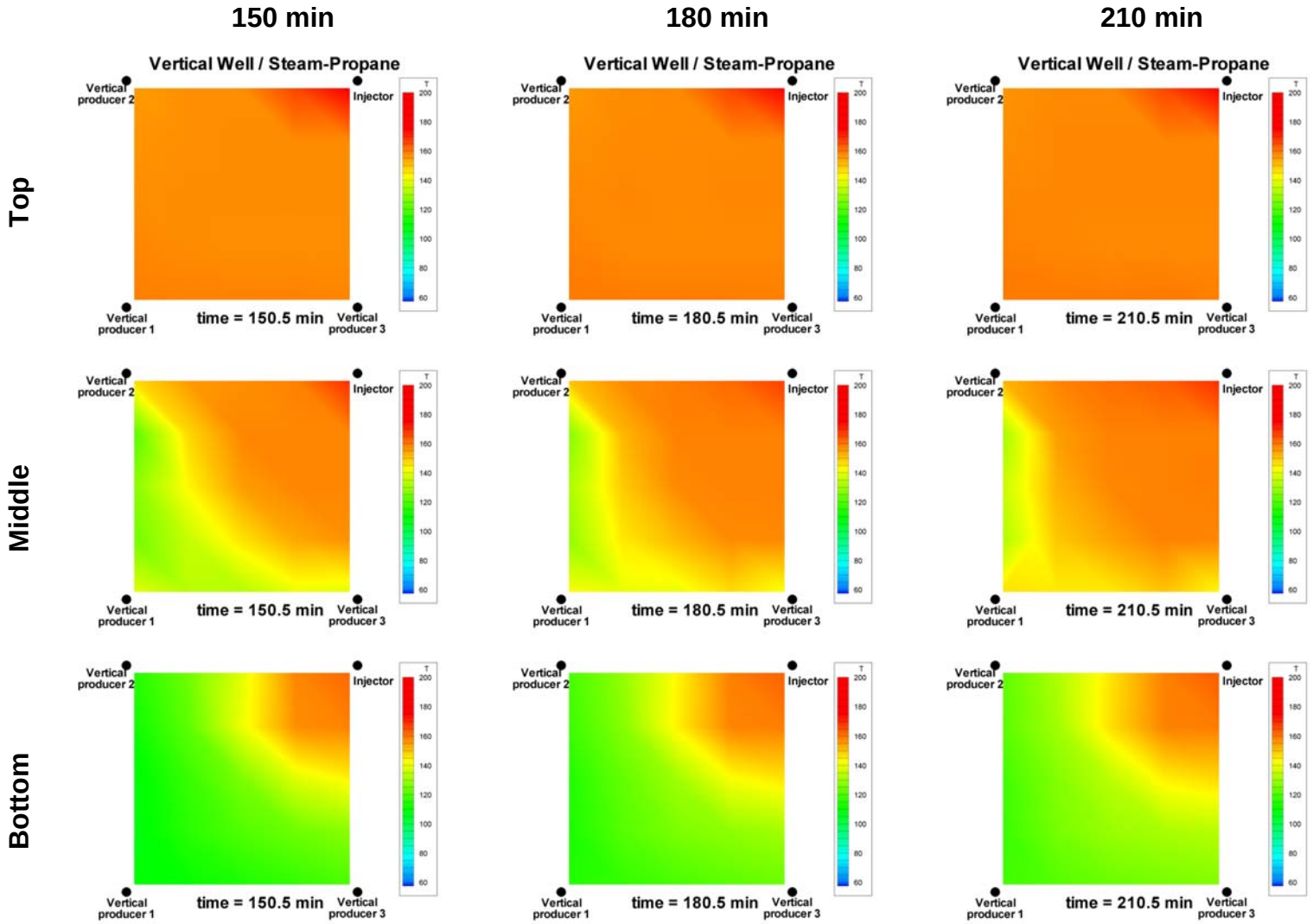

Fig. 6.25- Steam-propane injection in the vertical well system (Run 4): Plan view of the temperature profiles in the physical model at 150, 180 and 210 minutes. The top, middle and bottom rows show the profile at the top, middle and bottom of the cell respectively.

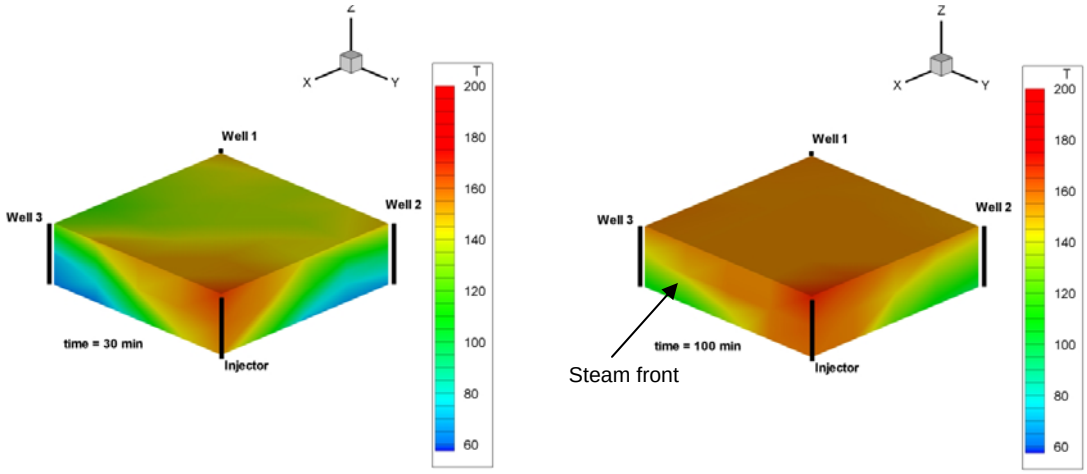

(i) **(ii)**

Fig. 6.26- Steam-propane injection in the vertical well system (Run 4): Temperature profile in isometric view showing steam override at (i) 30 minutes and (ii) 100 minutes.

Temperature profiles in isometric view are shown in **Fig. 6.26** for 30 and 100 minutes. Unlike run 2 (see **Fig. 6.1.12**), the steam zone in this experiment occupies the entire top portion of the cell at 100 minutes. This translates in a better sweep efficiency in the steam-propane case compared to the pure steam case.

6.3 Steam injection in the vertical injector–smart horizontal well system using configuration A (Run 3)

The objective of this experiment is to test the concept of the vertical injector-smart horizontal well system using configuration A (**see Fig. 6.1**). In this configuration, sections 2 and 3 of the horizontal well are opened at the beginning of the experiment and then closed 26 minutes (3 years in field scale) after production starts. In this run, production starts at 24 minutes, therefore, sections 2 and 3 are closed at 50 minutes and at the same time, section 1 is opened.

In this experiment, sections 2 and 3 are produced jointly and they flow together to only one backpressure regulator, after which fluids are collected, separated and measured. Fluids from section 1 flow independently to its own backpressure regulator and production system.

Fig. 6.27 depicts the steam injection temperature, which remains constant around 190ºC (about 10ºC superheated). The average injection flow rate (see **Fig. 6.27**) is 48.4 cm^3/min.

Due to the requirements of the vertical injector-smart horizontal well system, steam is injected only using the top section of the vertical injector. This is in contrast to the vertical well system experiments previously discussed, in which both sections of the injector are employed. Using only half of the interval for injecting the steam will cause an increase in the injection pressure when compared to the vertical well system. Additionally, at any given time in this run, the total area open to flow for production (one or two horizontal sections) is smaller than the area open to flow in the previous vertical well system runs (three vertical producers). This also contributes to the higher injection pressures observed, which in turn causes increased injection temperatures. In this experiment, the steam injection pressure (see **Fig. 6.28**) increases gradually during the first 60 minutes, and then it fluctuates between 120 and 130 psig. In contrast, the pressured registered in run 2 (**Fig. 6.1.2**) varies between 70 and 80 psig.

Fig. 6.28 also shows the flowing pressures for the producing sections of the horizontal well. During its production period (0 to 50 minutes), the combined sections 2 and 3 exhibit a constant backpressure with an average of 53 psig. Since section 1 is closed from 0 to 50 minutes, its flowing pressure is zero. After section 1 is opened, its backpressure increases gradually up to 70 psig and then it is corrected to a setting point close to 50 psig.

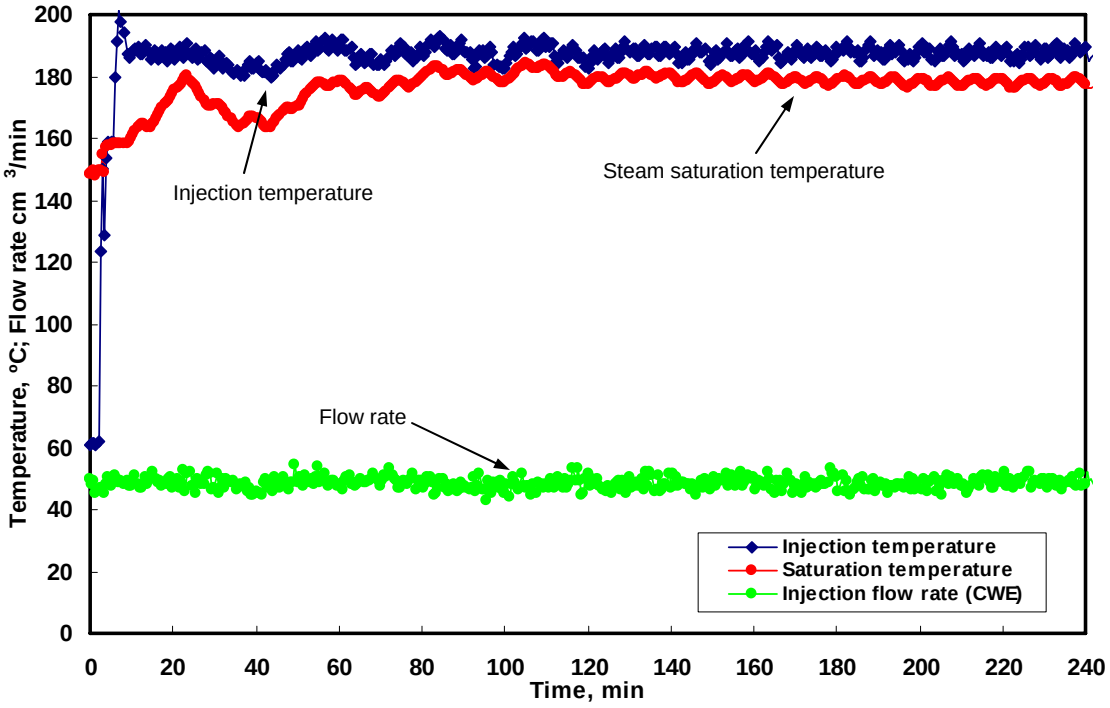

Fig. 6.27- Steam injection in the vertical injector-smart horizontal well system (Run 3 – Configuration A): Injection temperature and flow rate.

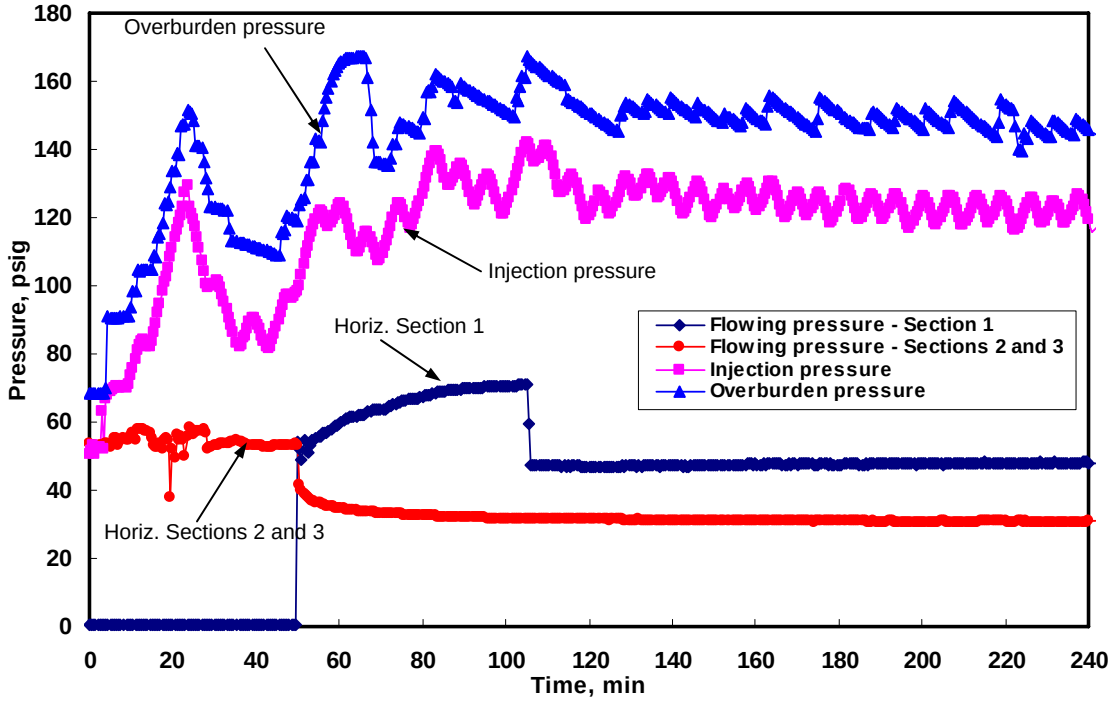

Fig. 6.28- Steam injection in the vertical injector-smart horizontal well system (Run 3 – Configuration A): Flowing pressure for the horizontal sections; injection pressure and overburden pressure.

Water and oil rates for all three horizontal sections are plotted in **Fig. 6.29.** Fluid production up to 50 minutes is owed to sections 2 and 3. From 50 minutes onward, section 1 is the sole contributor to fluid production. Oil rate is plotted by itself in **Fig. 6.30**. Oil production totals 1400 cm^3 after 240 minutes of run time (**Fig. 6.31**). This corresponds to about 38% of the OOIP (see **Fig. 6.32**).

Figs. 6.33 through **6.36** show temperature profiles at different times during the run. At 30 minutes (**Fig. 6.34**), steam already occupies the entire area at the top of the cell. At 40 minutes, a significant increase in temperature is observed in the area adjacent to the horizontal sections open to production (2 and 3). At 50 minutes (**Fig. 6.35**), the steam front can be observed around the middle portion of the cell in the area around the open sections. At the same time, section 1 is opened and sections 2 and 3 are closed. The steam front then starts to move from the area around sections 2 and 3 towards the area around section 1. At 100 minutes, the steam front can be clearly identified around the active producing section.

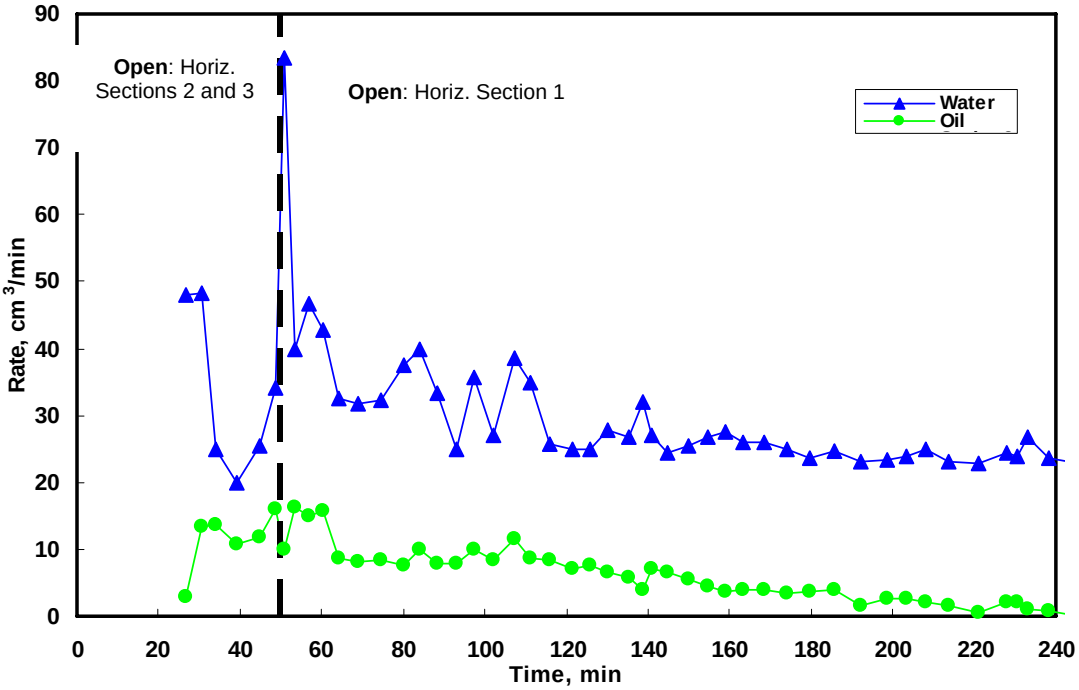

Fig. 6.29- Steam injection in the vertical injector-smart horizontal well system (Run 3 – Configuration A): Oil and water rates for horizontal sections 1, 2 and 3.

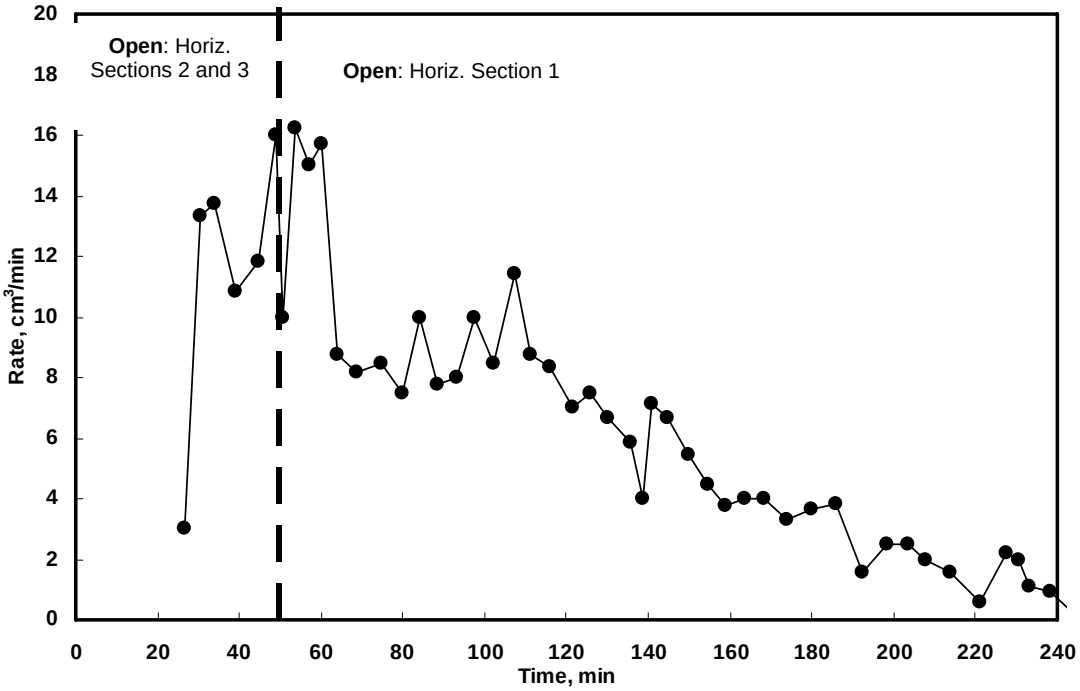

Fig. 6.30- Steam injection in the vertical injector-smart horizontal well system (Run 3 – Configuration A): Total oil rate production.

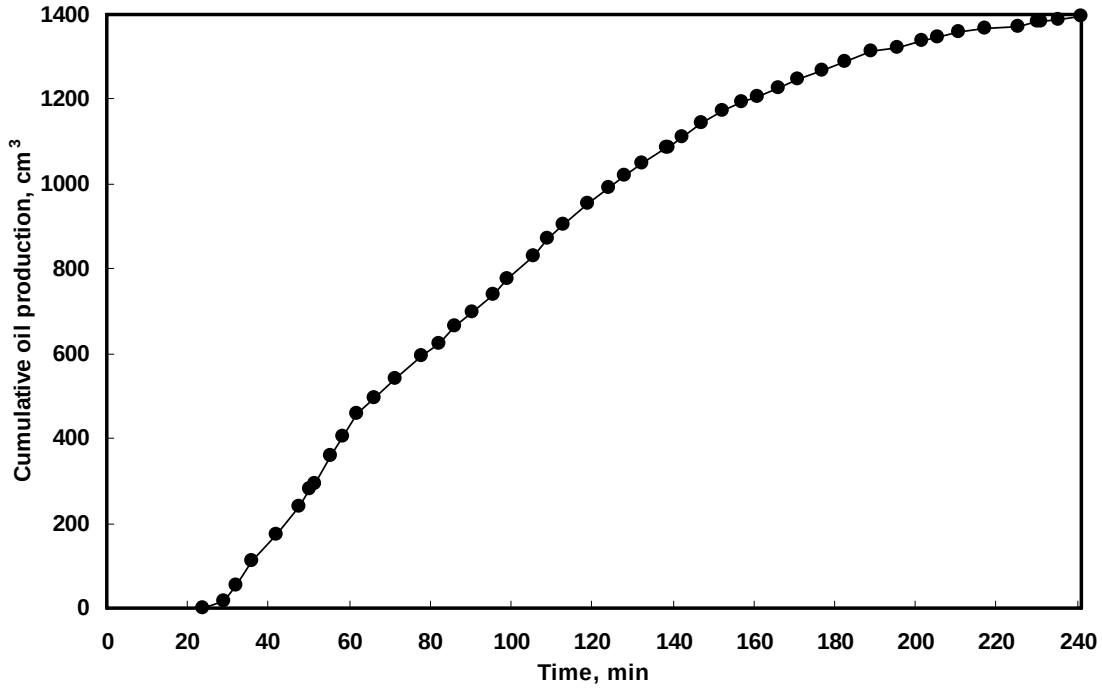

Fig. 6.31- Steam injection in the vertical injector-smart horizontal well system (Run 3 – Configuration A): Cumulative oil production.

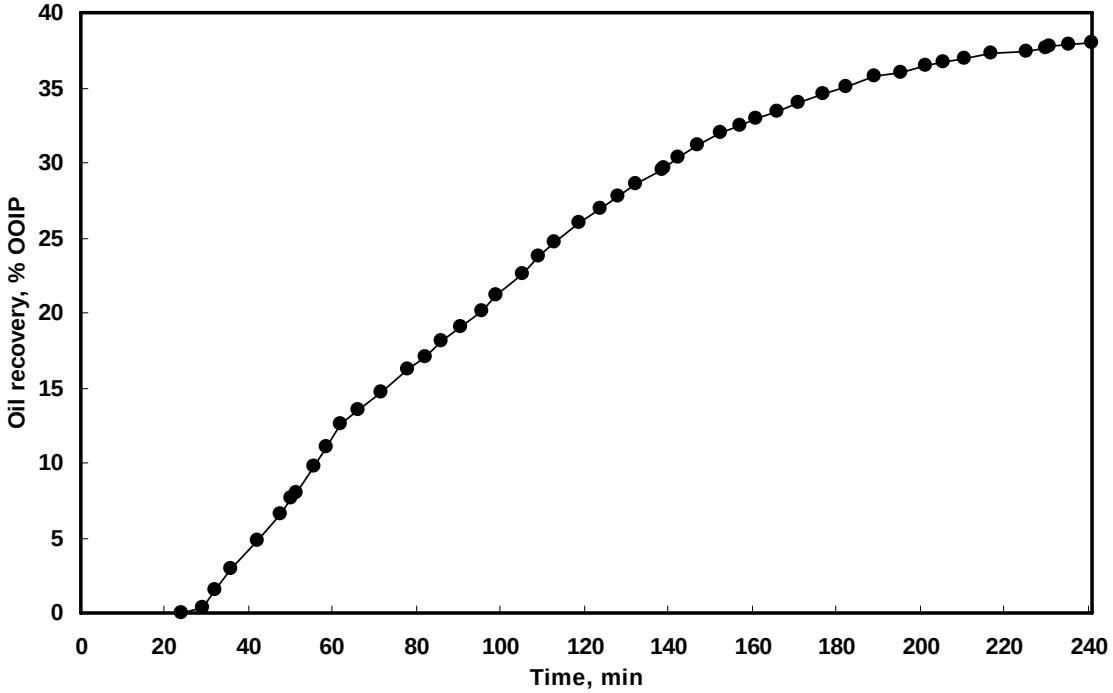

Fig. 6.32- Steam injection in the vertical injector-smart horizontal well system (Run 3 – Configuration A): Oil recovery.

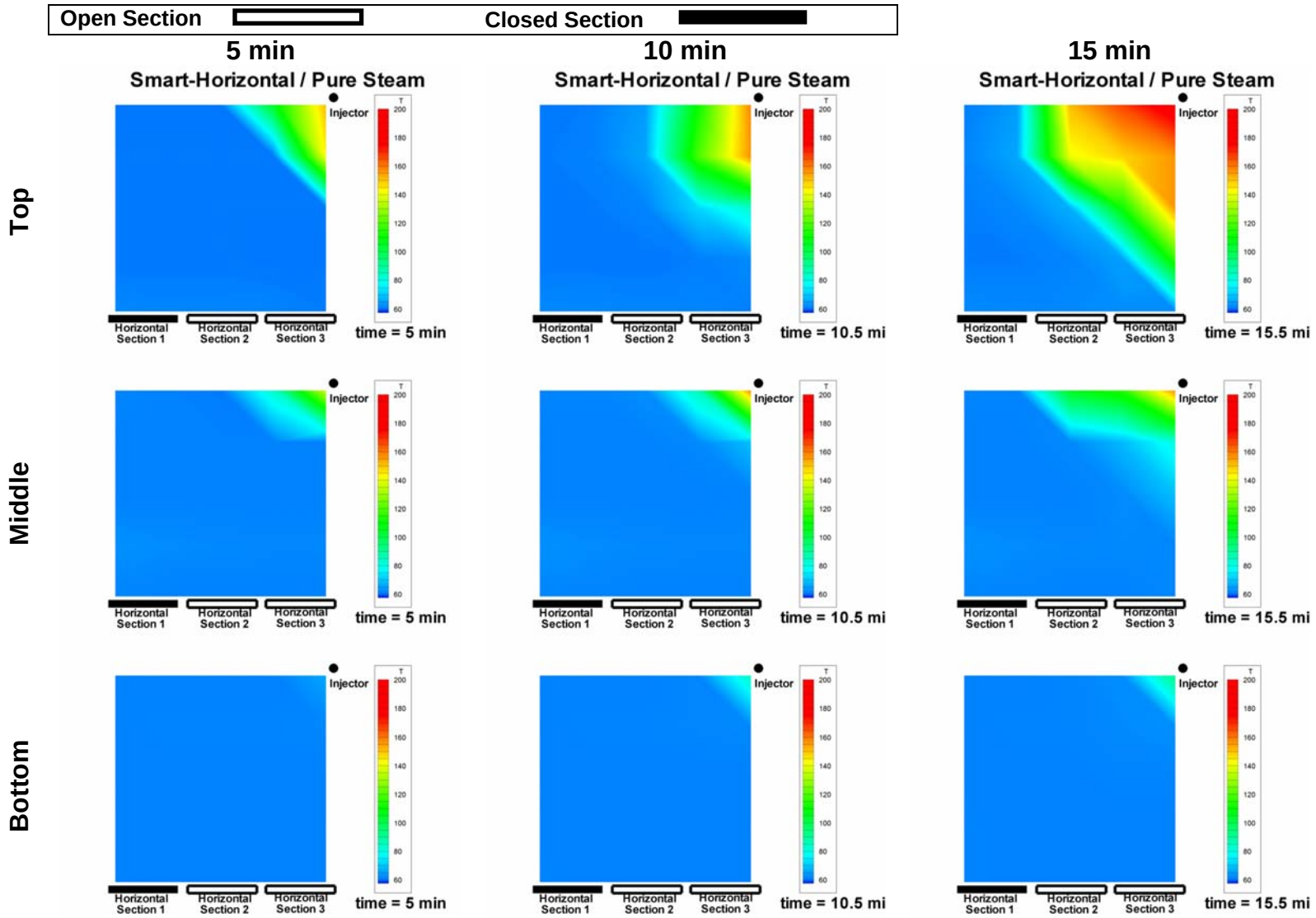

Fig. 6.33- Steam injection in the vertical injector-smart horizontal well system (Run 3 – Configuration A): Plan view of the temperature profiles in the physical model at 5, 10 and 15 minutes. The top, middle and bottom rows show the profile at the top, middle and bottom of the cell respectively.

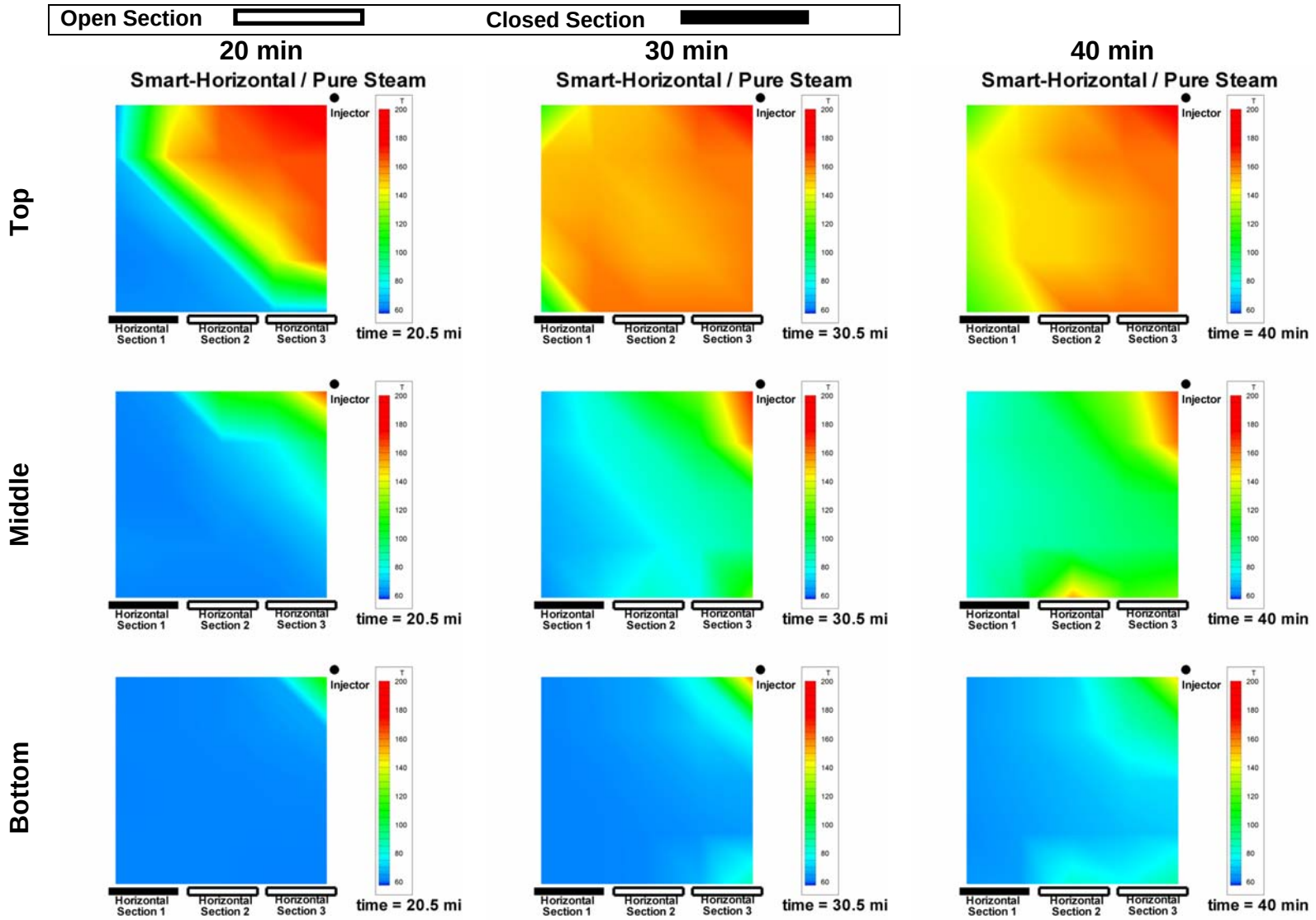

Fig. 6.34- Steam injection in the vertical injector-smart horizontal well system (Run 3 – Configuration A): Plan view of the temperature profiles in the physical model at 20, 30 and 40 minutes. The top, middle and bottom rows show the profile at the top, middle and bottom of the cell respectively.

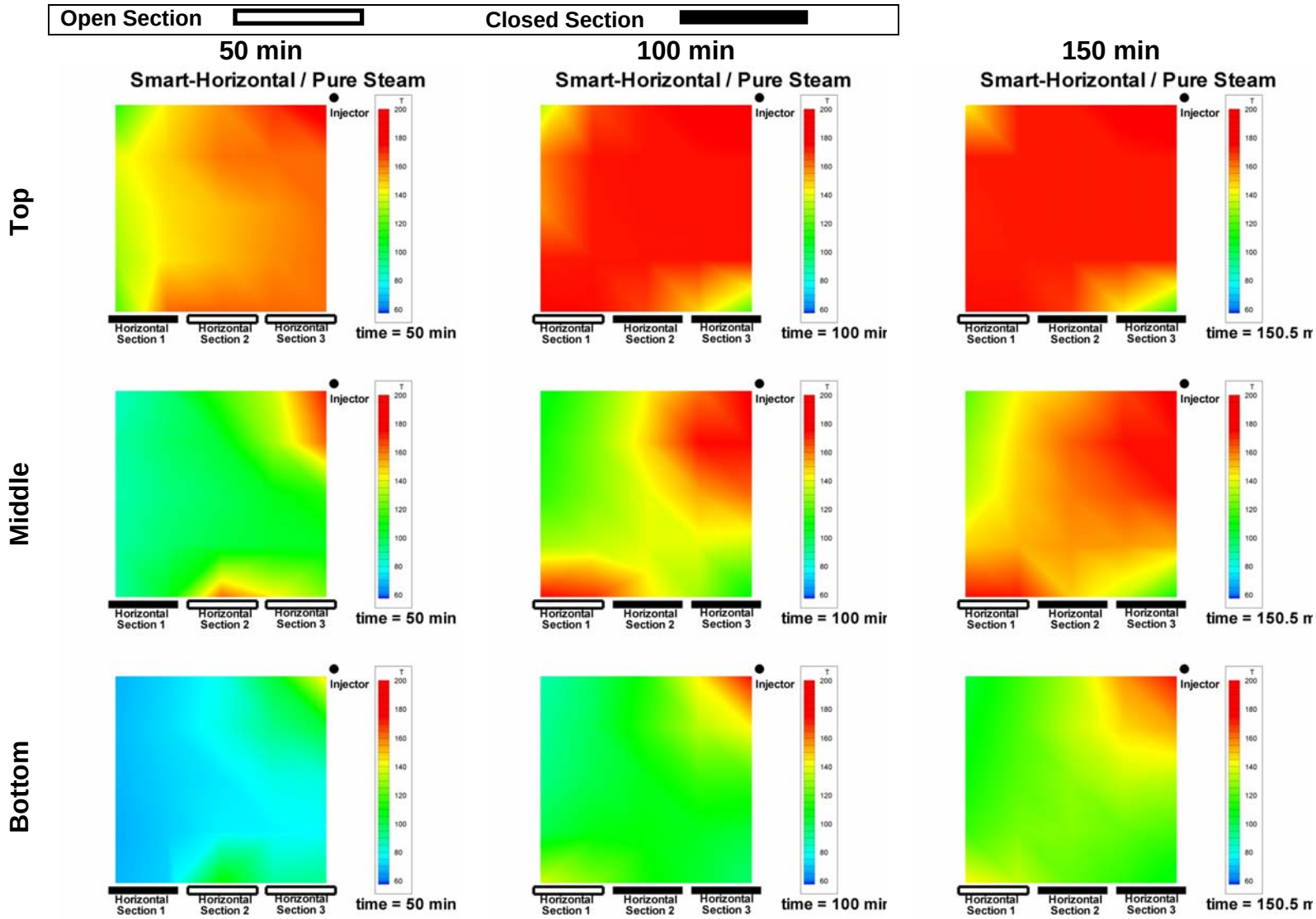

Fig. 6.35- Steam injection in the vertical injector-smart horizontal well system (Run 3 – Configuration A): Plan view of the temperature profiles in the physical model at 50, 100 and 150 minutes. The top, middle and bottom rows show the profile at the top, middle and bottom of the cell respectively.

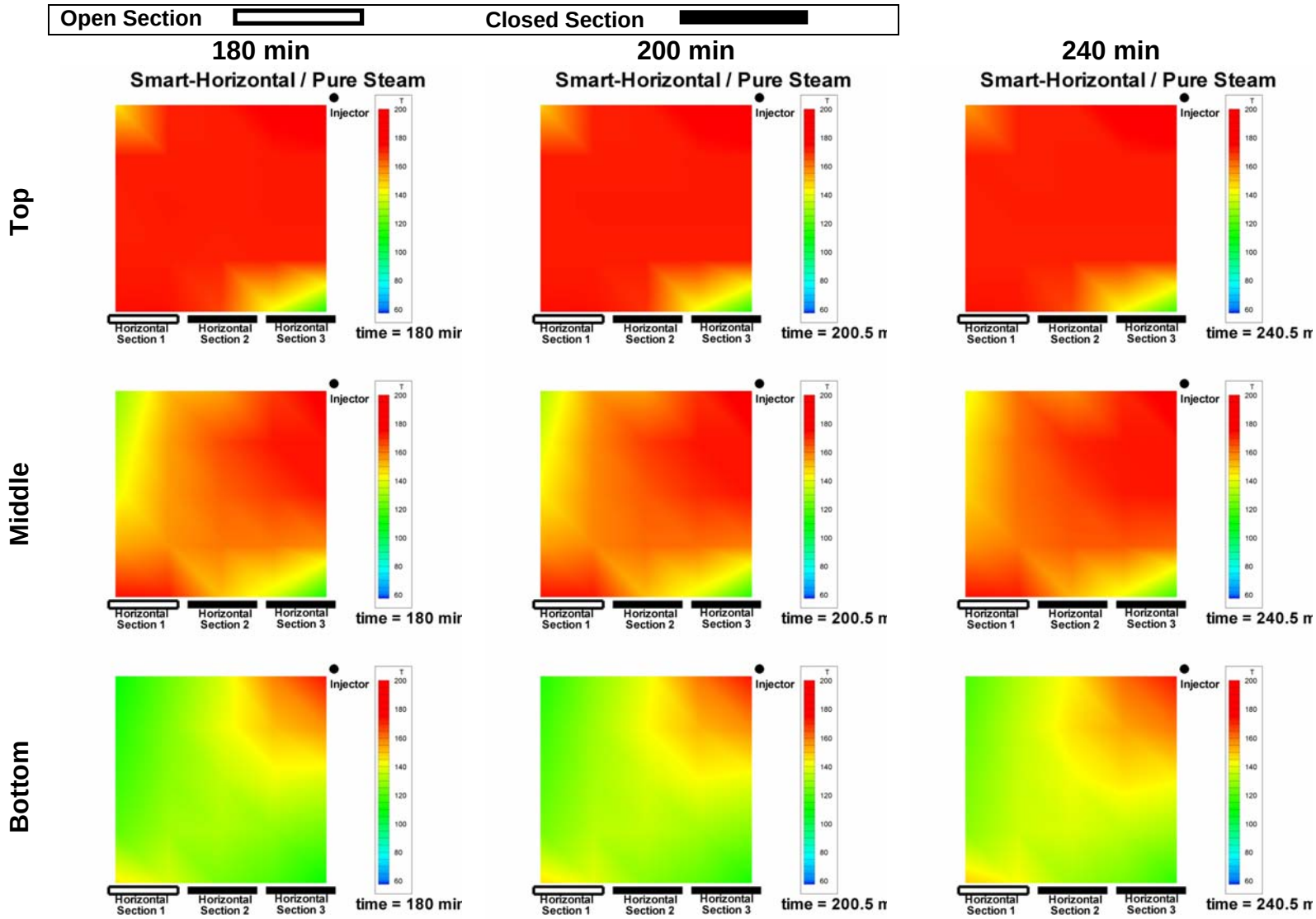

Fig. 6.36- Steam injection in the vertical injector-smart horizontal well system (Run 3 – Configuration A): Plan view of the temperature profiles in the physical model at 180, 200 and 240 minutes. The top, middle and bottom rows show the profile at the top, middle and bottom of the cell respectively.

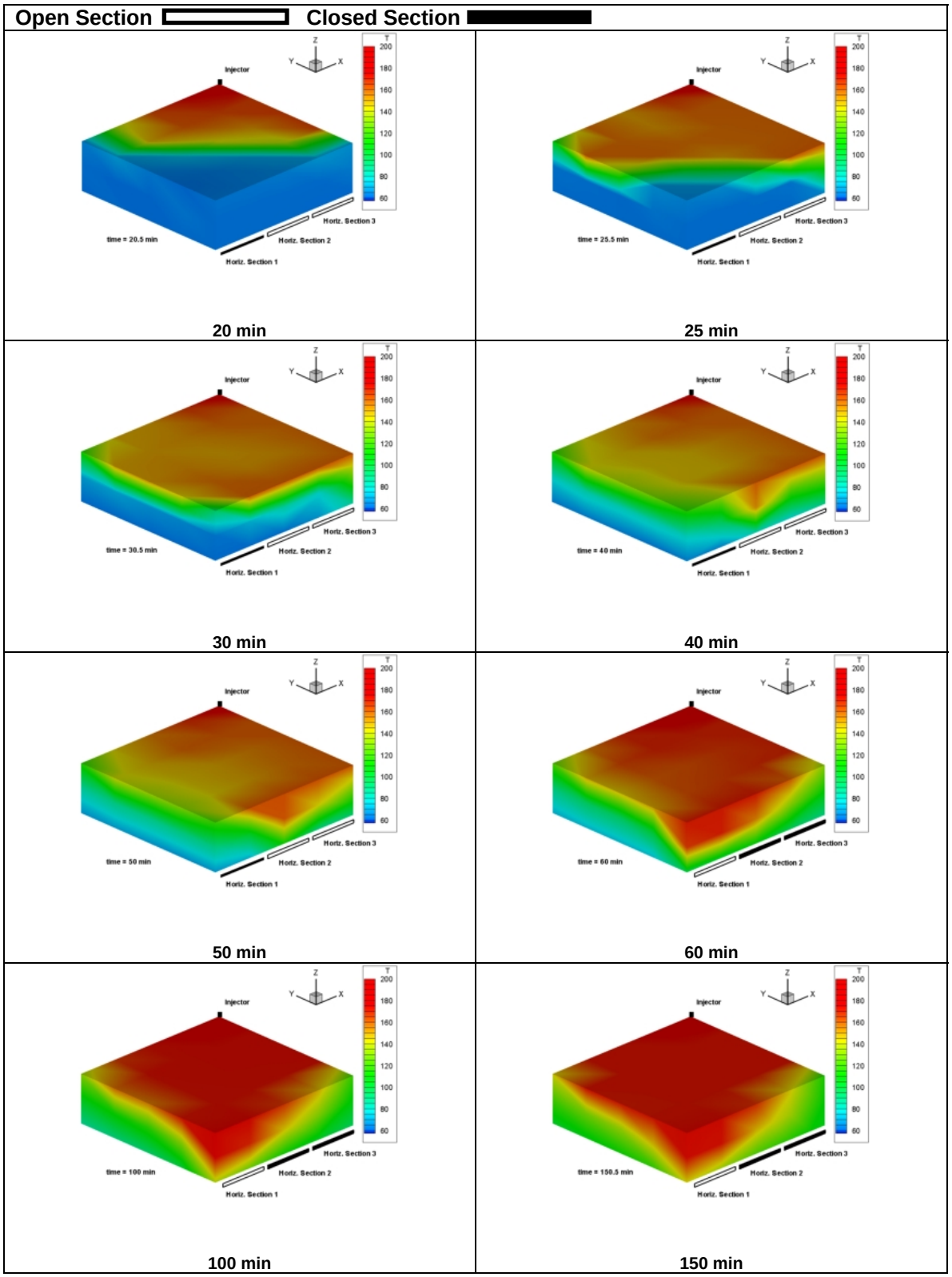

Fig. 6.37- Steam injection in the vertical injector-smart horizontal well system (Run 3 – Configuration A): Temperature profiles in isometric view seen from the front of the cell.

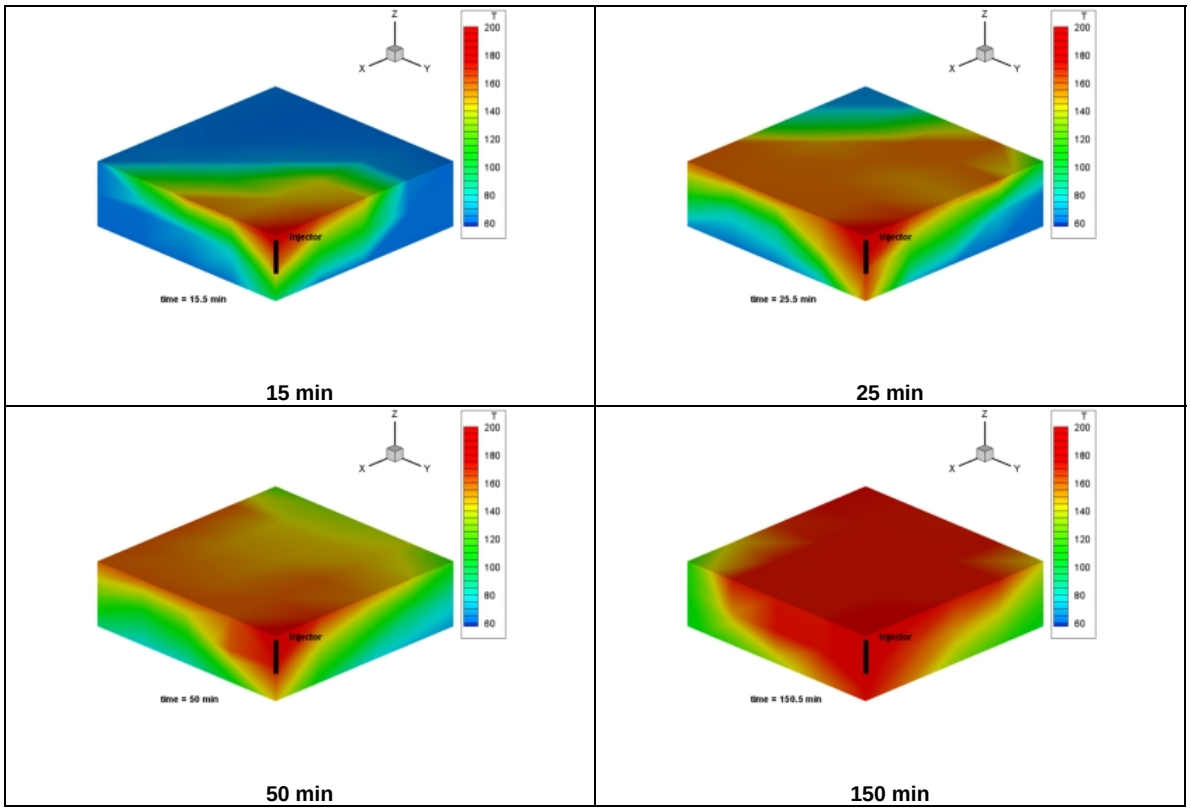

Fig. 6.38- Steam injection in the vertical injector-smart horizontal well system (Run 3 – Configuration A): Temperature profiles in isometric view seen from the back of the cell.

Fig. 6.37 shows a composite of several temperature profiles seen from the producers' point of view. The progress of the steam front at the top of the cell can be observed at 20, 25 and 30 minutes. At 40 minutes, steam starts to channel towards sections 2 and 3. At 50 minutes, a defined steam crest can be observed around the active producing sections. Once section 1 is opened, the crest advances from section 2 and 3 towards section 1.

A series of three-dimensional profiles oriented from the injector's point of view can be observed in **Fig. 6.38**. Given that steam is injected only through the top half of the vertical injector, the steam initially (15 and 20 minutes) accumulates mostly at the top of the cell. As injection progresses, steam tends to occupy lower parts of the physical model. The profile at 50 minutes shows the instant in which the change in producing sections occurs.

6.4 Steam-propane injection in the vertical injector–smart horizontal well system using configuration A (Run 5)

This experiment was carried out to test the efectiveness of combining the process of steam-propane injection with the concept of the smart horizontal well system. In the same way as run 3, configuration A (**see Fig. 6.1**) was employed in this experiment. Production starts at 15.5 minutes, consequently, sections 2 and 3 are closed 26 minutes later at 41.5 minutes of run time.

The steam injection temperature (**Fig. 6.39**) starts with superheated conditions at around 180ºC, however, as the injection pressure increases (**Fig. 6.40**), the saturation temperatures rises and for a brief period of time, the injection temperature falls below saturation. This situation is immediately corrected and for the remainder of the run, the injection temperature is kept 15 to 20ºC superheated. The average injection flow rate (see **Fig. 6.39**) is 49.2 cm^3/min and remains fairly constant during the run.

The delivery pressure of the steam generator creates fluctuations in the injection pressure which oscillate between 120 and 170 psig (see **Fig. 6.40**). At about 15 minutes, the flowing pressure of sections 2 and 3 increases above the setting point, however, the dome-loaded regulator was adjusted and the backpressure was brought back to its intended value (50 psig). Starting at 41.5 minutes, section 1 flows at a constant 50 psig.

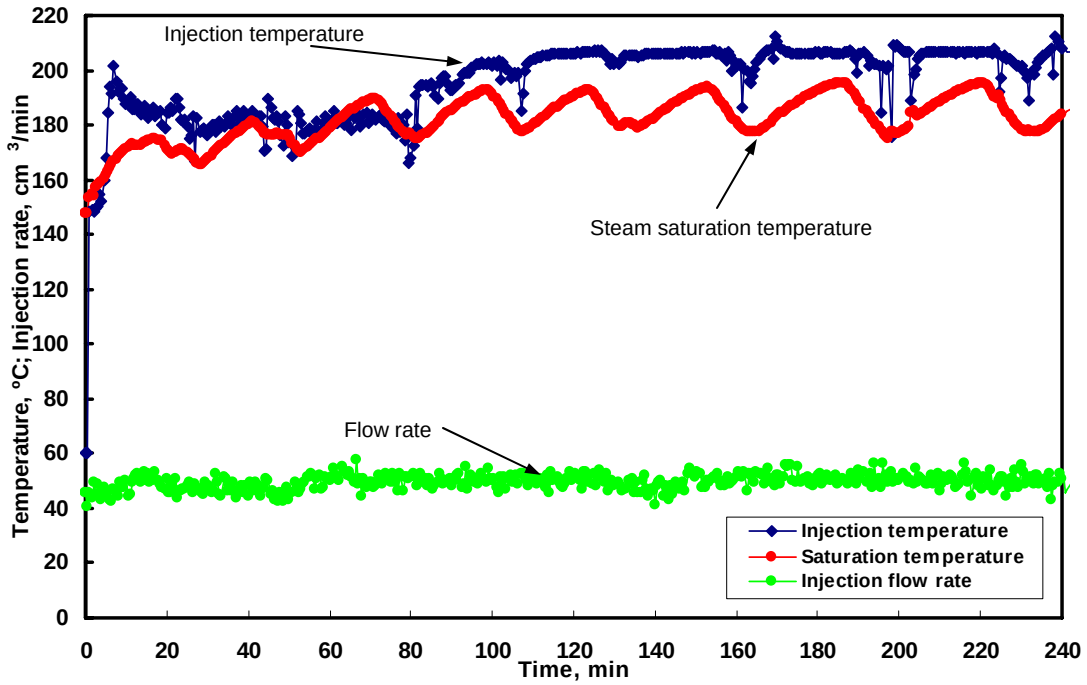

Fig. 6.39- Steam-propane injection in the vertical injector-smart horizontal well system (Run 5 – Configuration A): Injection temperature and flow rate.

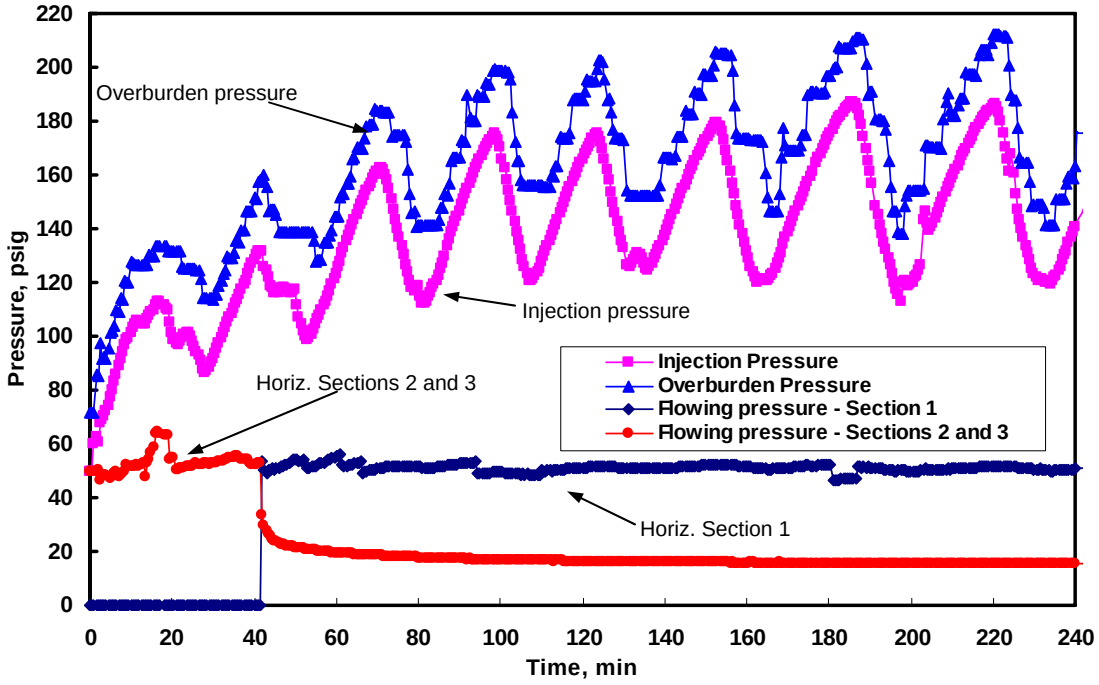

Fig. 6.40- Steam-propane injection in the vertical injector-smart horizontal well system (Run 5 – Configuration A): Flowing pressure for the horizontal sections; injection pressure and overburden pressure.

Fig. 6.41 and **6.42** show the water and oil rates for all the sections open to flow. At 41.5 minutes, sections 2 and 3 are shut and section 1 is opened to flow. At the end of the run (240 minutes), the cumulative oil production reaches about 1100 cm^3 (**Fig. 6.43)**, which is equivalent to approximately 32% of the OOIP (see **Fig. 6.44**).

Temperature profiles at different moments during the run are shown in **Figs. 6.45** through **6.48**. Starting at 30 minutes (**Fig. 6.46**), the steam override phenomenon can be identified in the profile. At this time, the temperature at the top of the cell is significantly higher than the initial temperature. Additionally, the mid and bottom profiles show the first signs of heating around the area of sections 2 and 3. This heating in the middle and bottom portions of the cell becomes more evident at 41.5 min. However, at that time, the active horizontal sections (2 and 3) are shut down before a sufficient temperature increase could be achieved in that area. At 50 minutes (**Fig. 6.47**), it is evident that the steam front has already started to flow towards section 1, and at 100 minutes, the front can be clearly identified around the active producing section. Towards the end of the run (**Fig. 6.48**), the middle section of the cell shows a colder area in the center, which corroborates the classical steam override profile.

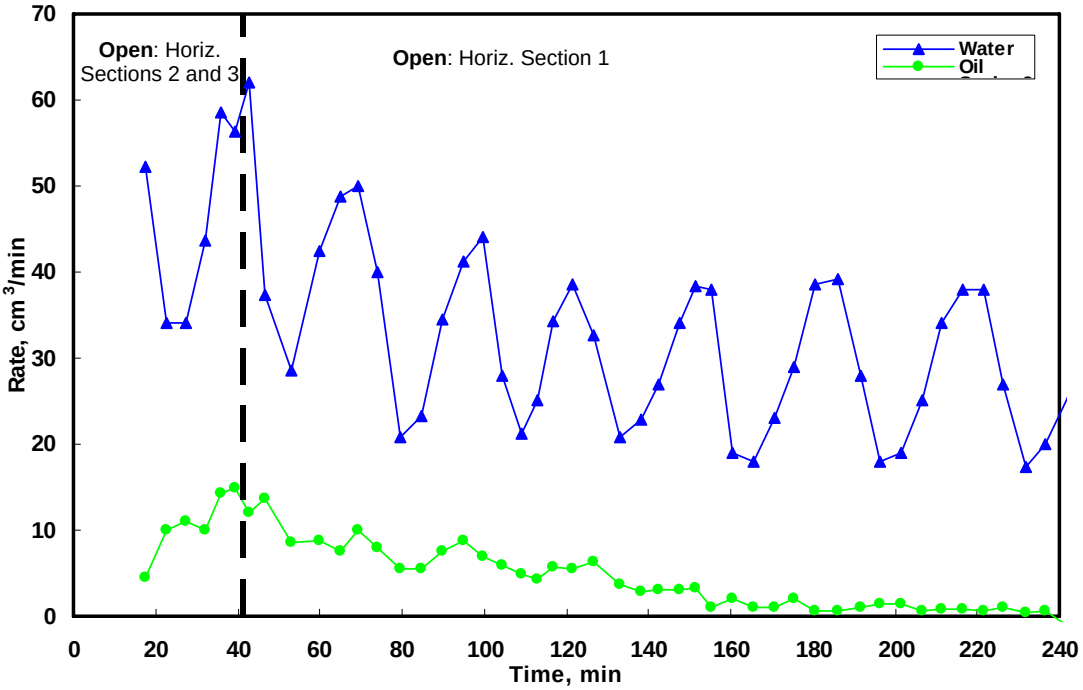

Fig. 6.41- Steam-propane injection in the vertical injector-smart horizontal well system (Run 5 – Configuration A): Oil and water rates for the horizontal sections.

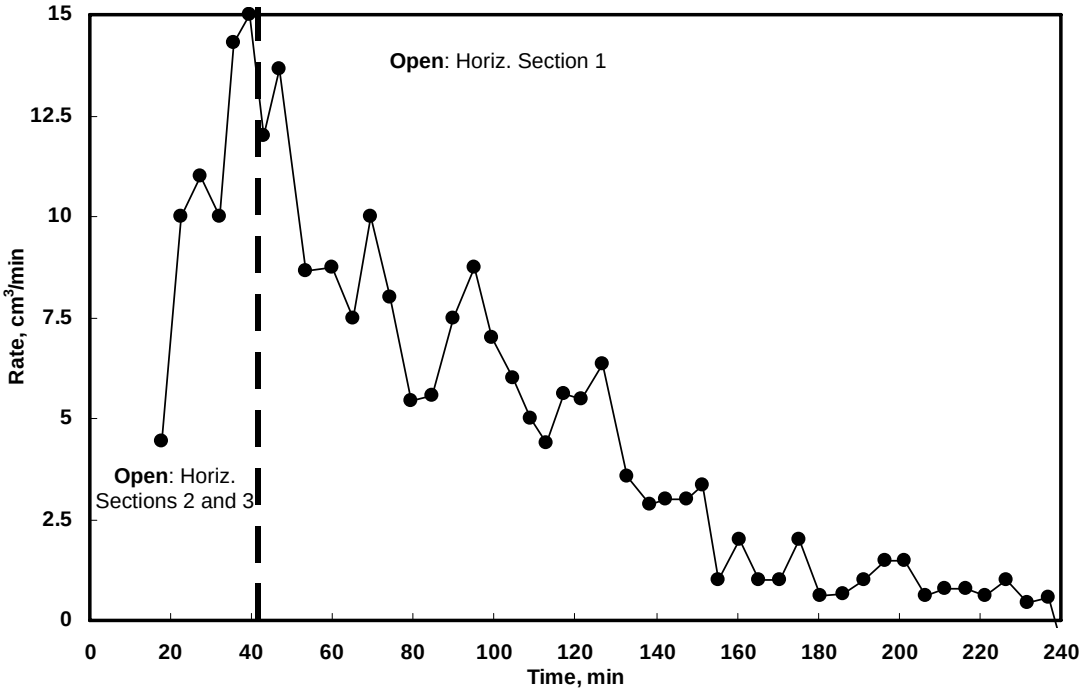

Fig. 6.42- Steam-propane injection in the vertical injector-smart horizontal well system (Run 5 – Configuration A): Total oil rate production.

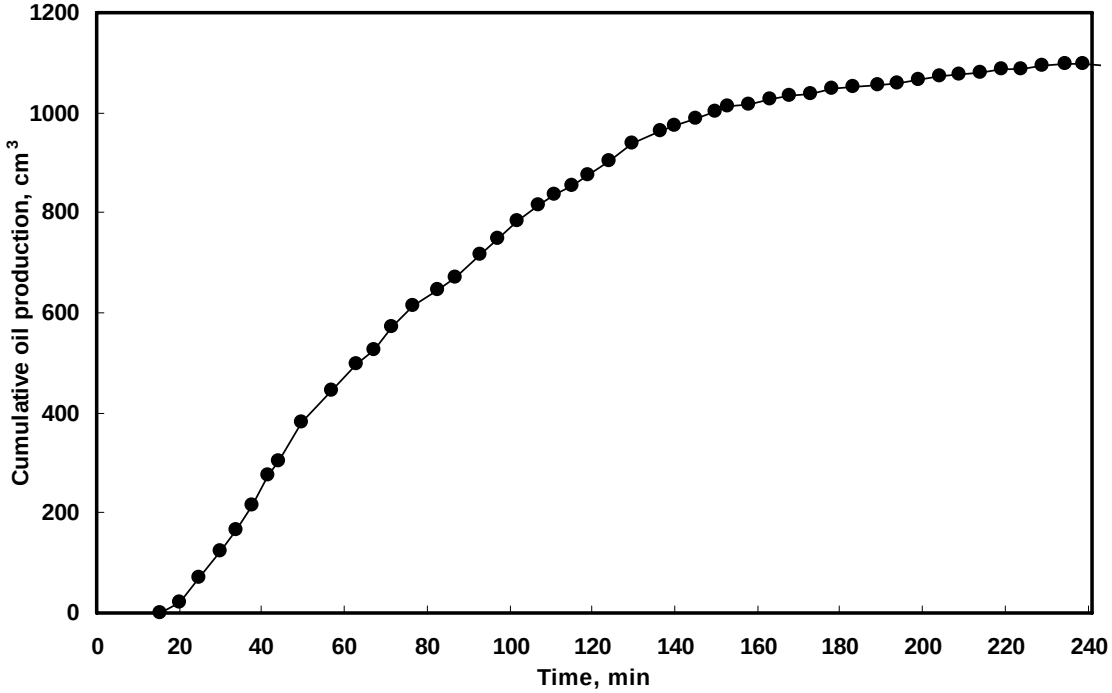

Fig. 6.43- Steam-propane injection in the vertical injector-smart horizontal well system (Run 5 – Configuration A): Cumulative oil production.

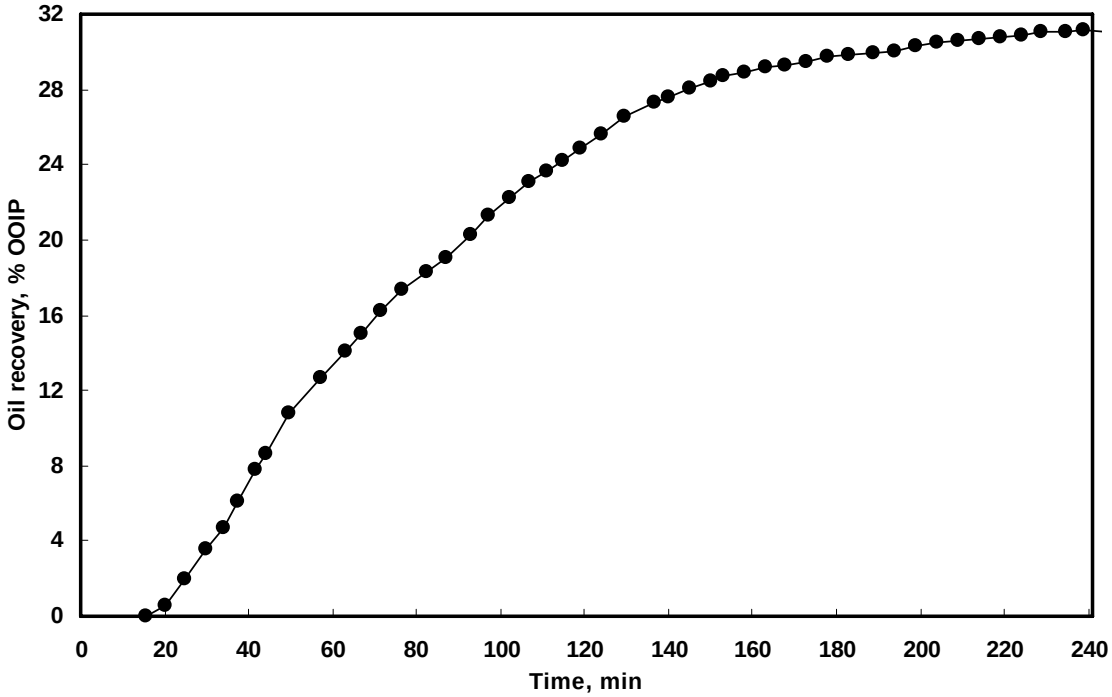

Fig. 6.44- Steam-propane injection in the vertical injector-smart horizontal well system (Run 5 – Configuration A): Oil recovery.

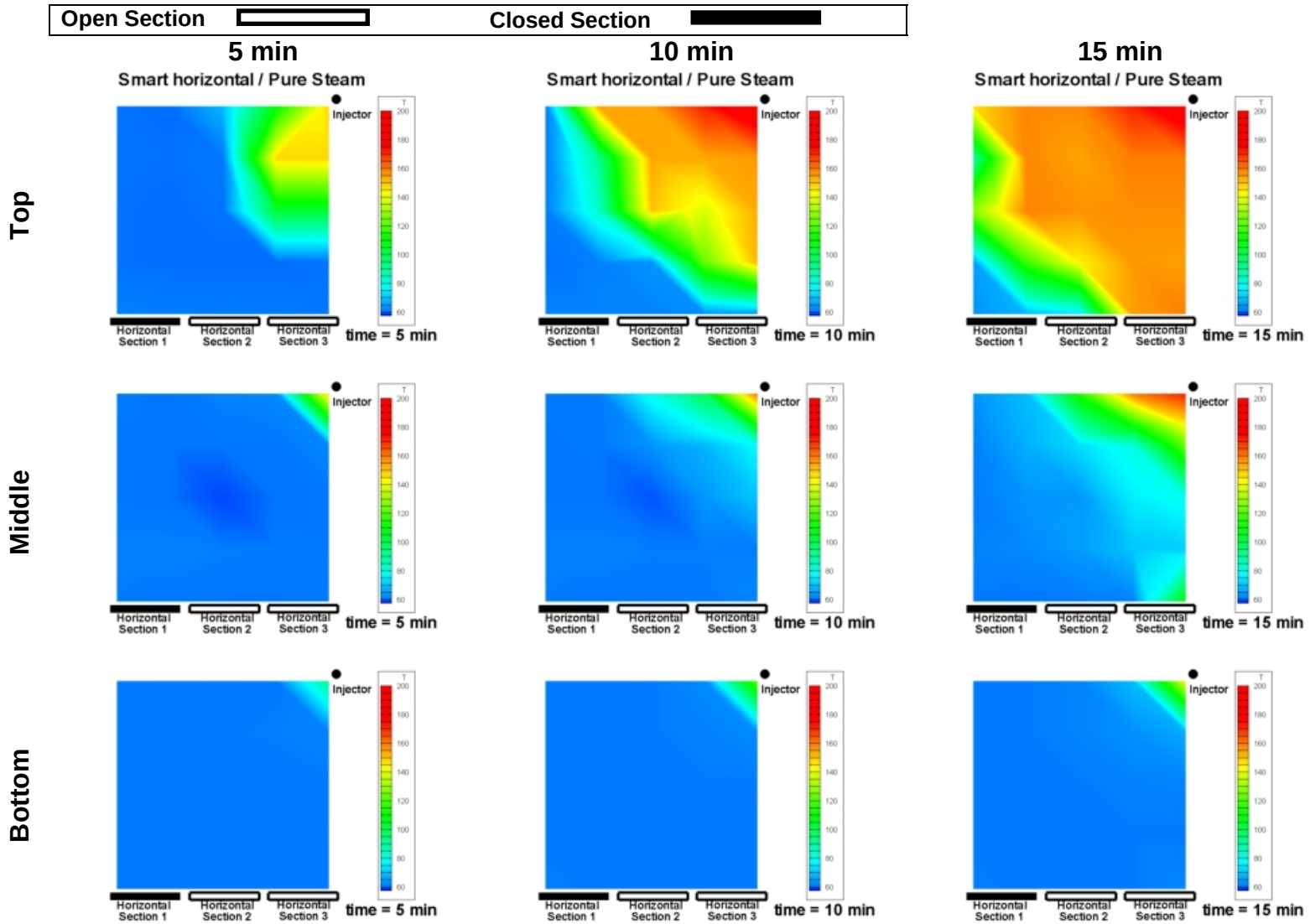

Fig. 6.45- Steam-propane injection in the vertical injector-smart horizontal well system (Run 5 – Configuration A): Plan view of the temperature profiles in the physical model at 5, 10 and 15 minutes. The top, middle and bottom rows show the profile at the top, middle and bottom of the cell respectively.

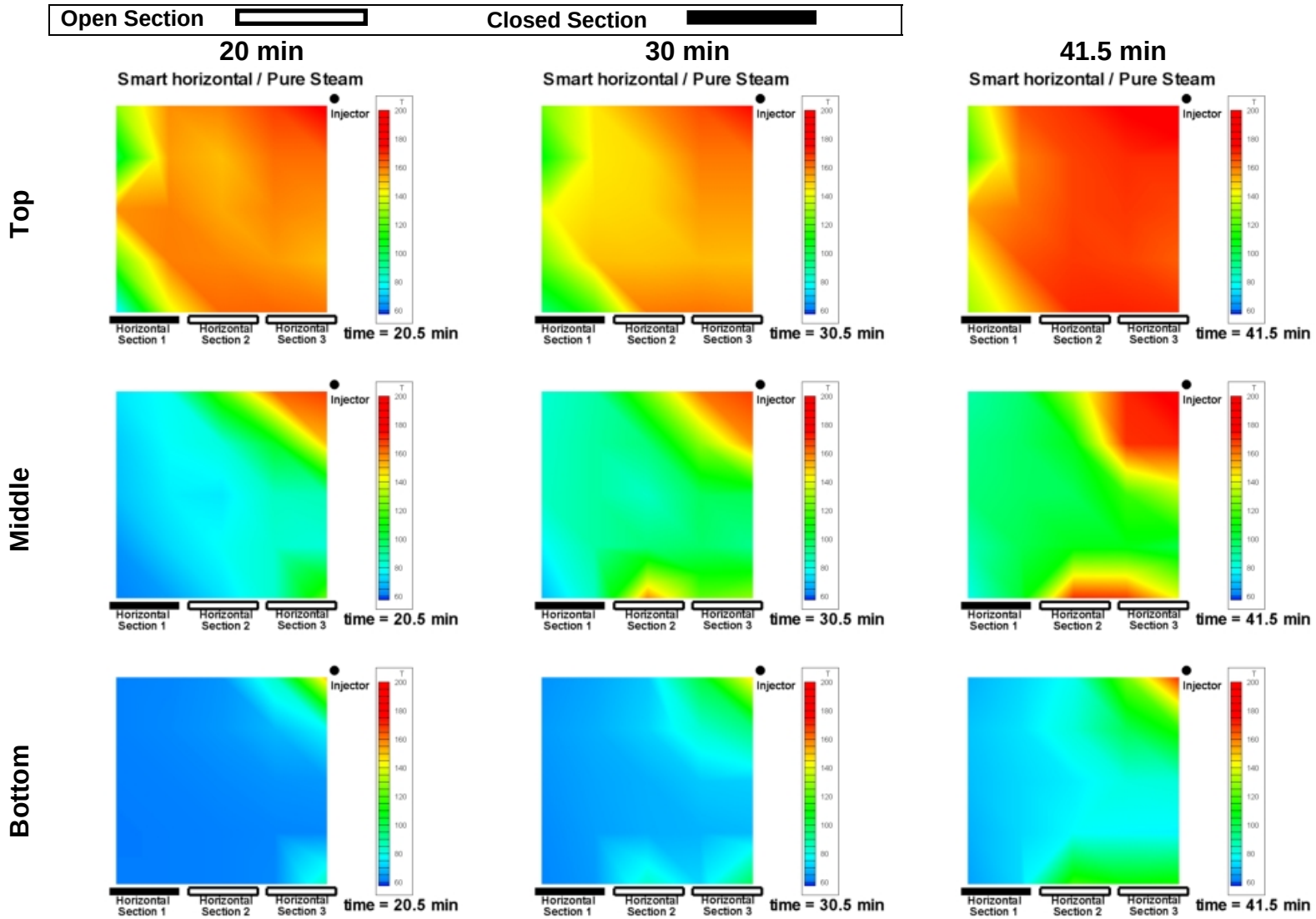

Fig. 6.46- Steam-propane injection in the vertical injector-smart horizontal well system (Run 5 – Configuration A): Plan view of the temperature profiles in the physical model at 20, 30 and 41.5 minutes. The top, middle and bottom rows show the profile at the top, middle and bottom of the cell respectively.

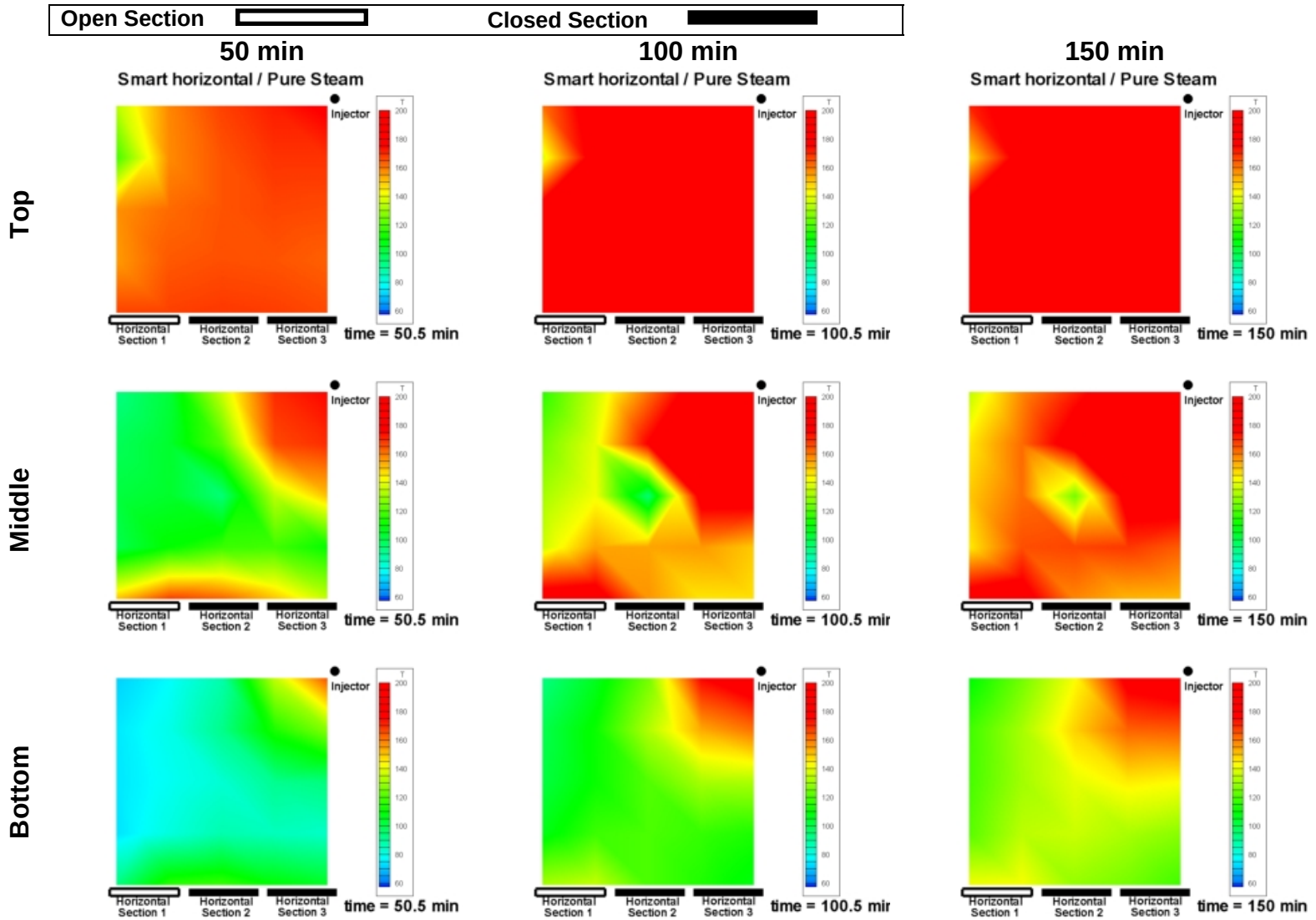

Fig. 6.47- Steam-propane injection in the vertical injector-smart horizontal well system (Run 5 – Configuration A): Plan view of the temperature profiles in the physical model at 50, 100 and 150 minutes. The top, middle and bottom rows show the profile at the top, middle and bottom of the cell respectively.

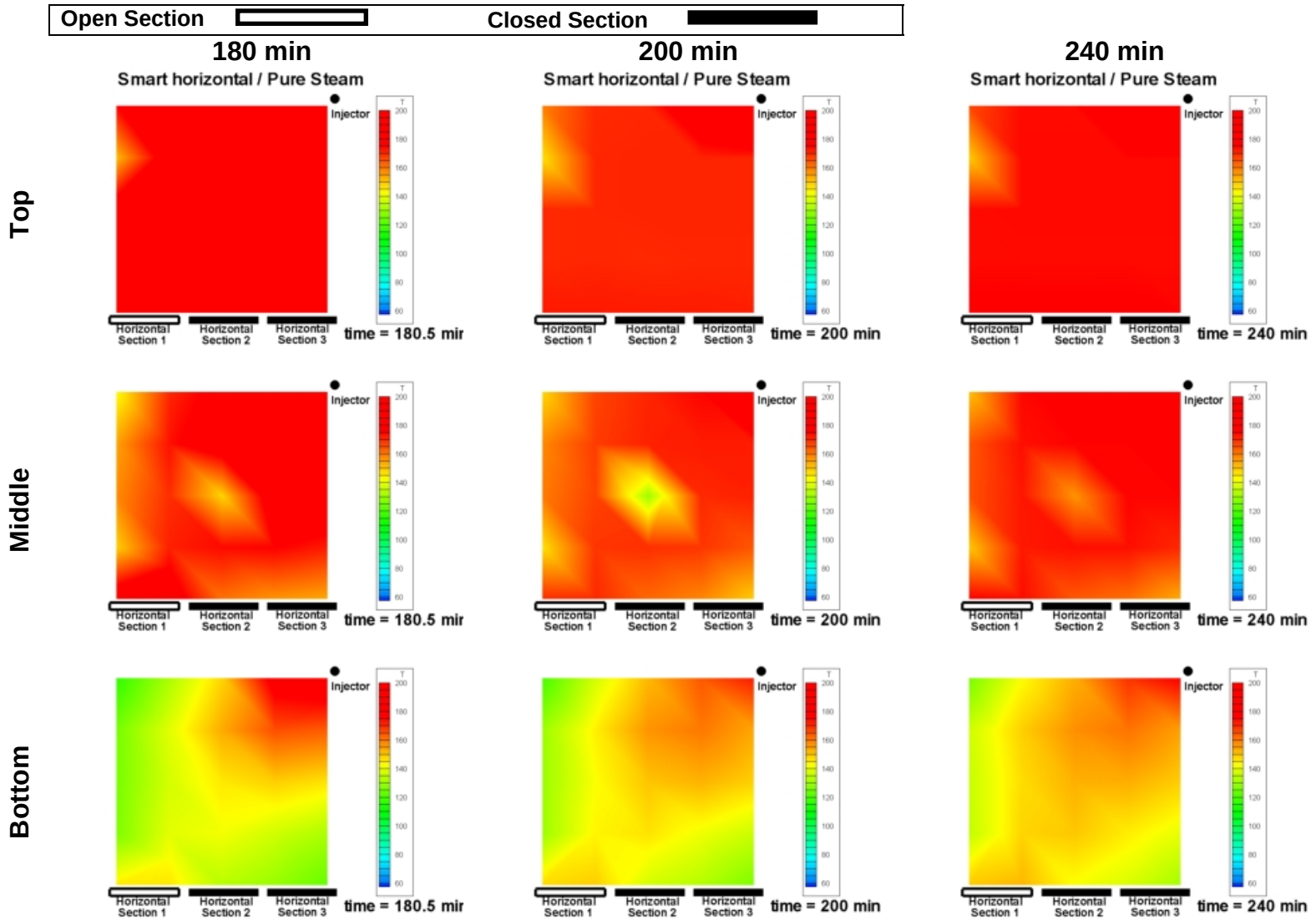

Fig. 6.48- Steam-propane injection in the vertical injector-smart horizontal well system (Run 5 – Configuration A): Plan view of the temperature profiles in the physical model at 180, 200 and 240 minutes. The top, middle and bottom rows show the profile at the top, middle and bottom of the cell respectively.

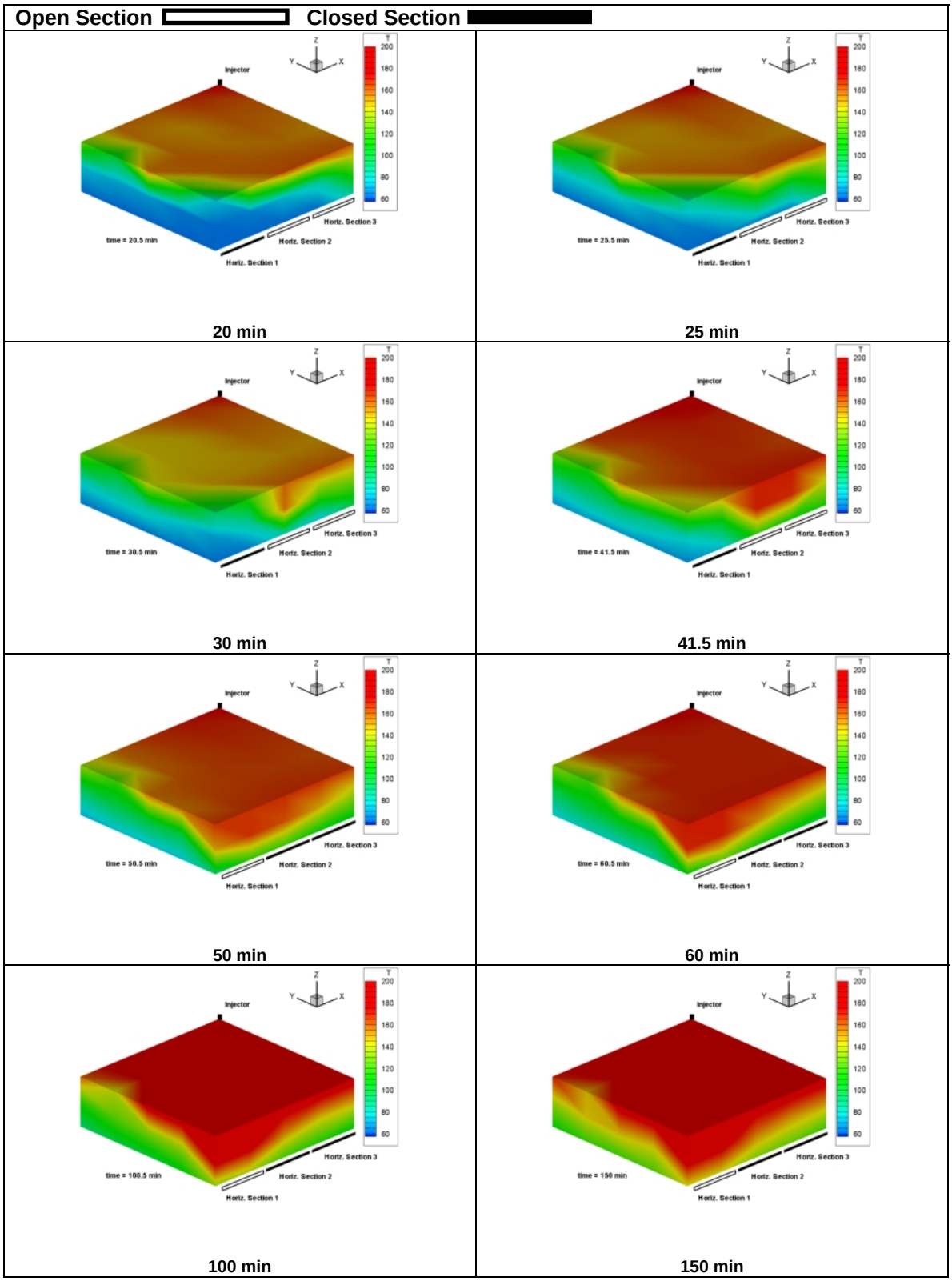

Fig. 6.49- Steam-propane injection in the vertical injector-smart horizontal well system (Run 5 – Configuration A): Temperature profiles in isometric view seen from the front of the cell.

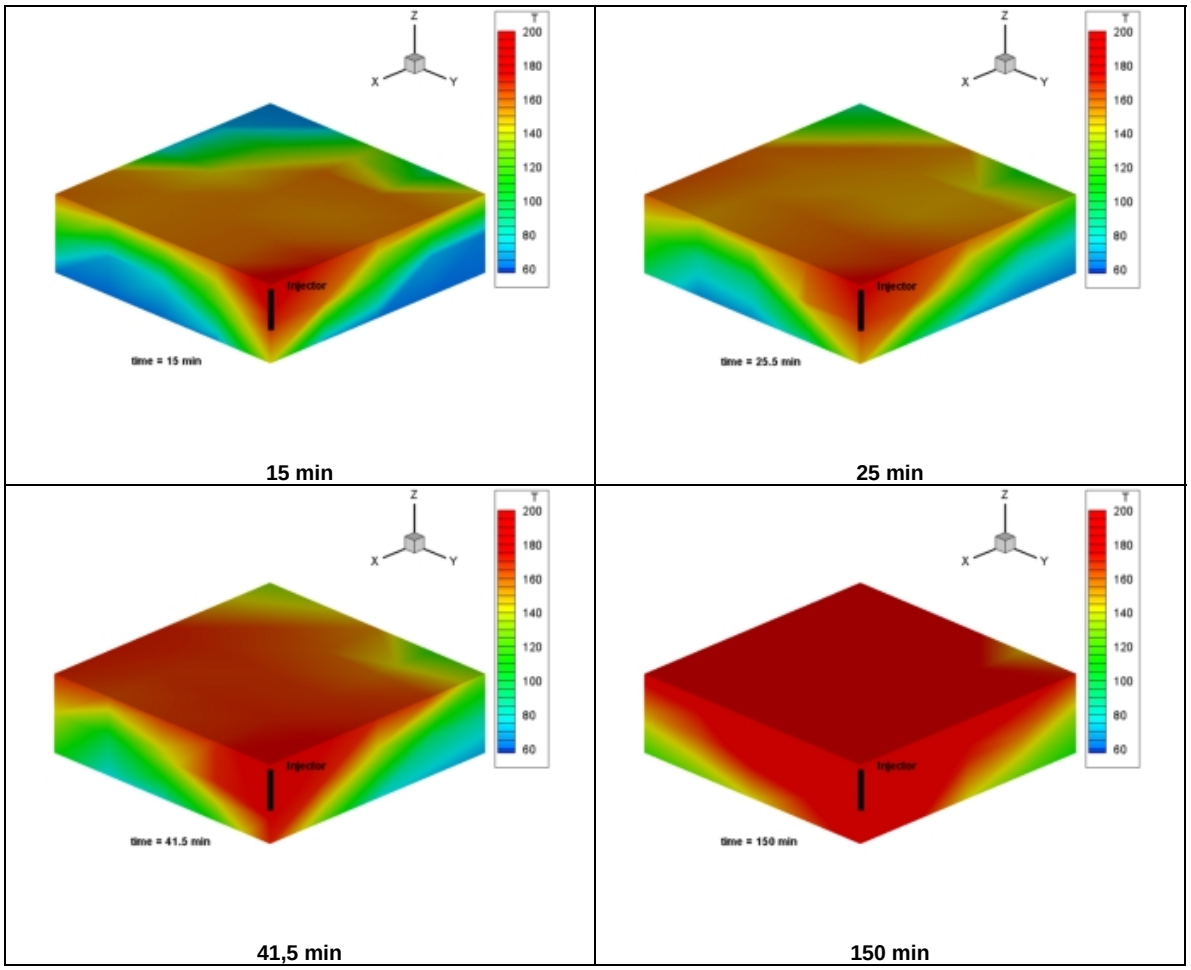

Fig. 6.50- Steam-propane injection in the vertical injector-smart horizontal well system (Run 5 – Configuration A): Temperature profiles in isometric view seen from the back of the cell.

A series of three-dimensional temperature profiled are shown in **Fig. 6.49**. At 30 and 41.5 minutes, the temperature profile shows evidence of hot fluid movement towards the area around the producing sections. The profiles at 100 and 150 minutes show that the size of the steam zone remains more or less the same, indicating steam recirculation from the injector to the producer in the model. Temperature profiles with an opposite orientation (seen from the injector's point of view) are shown in **Fig. 6.50**. Since injection occurs only in the top section of the injector, the steam front remains limited to the upper area of the cell at early times in the run. Since injection occurs only in the top section of the injector, the steam front remains limited to the upper area of the cell at early times in the run. As the run progresses, steam starts to occupy lower portions of the model.

6.5 Steam injection in the vertical injector–smart horizontal well system using configuration B (Run 6)

Two different configurations for the vertical injector-smart horizontal well system are tested in this research (see section 6). In configuration B (**see Fig. 6.1**), all horizontal sections are open to flow from the start of the experiment. Ninety seven minutes (approximately 11 years in field scale) after production starts, the producing section closer to the injector (section 3) is closed and 75 minutes later, section 2 is shut. In this experiment, production starts at 23 minutes, therefore, section 3 is closed at 120 minutes and section 2 is shut at 195 minutes. In this run, steam is injected exclusively in the top section of the vertical injector.

The steam injection temperature (shown in **Fig. 6.51**) remains more or less constant throughout the run at around 190ºC, which is approximately 10ºC superheated. Also shown in **Fig. 6.51**, is the injection flow rate, which averages 49.1 cm^3/min.

Fig. 6.52 depicts the steam injection pressure as well as the overburden pressure and the flowing pressures for each horizontal section open to flow. Injection pressure starts at 60 psig and then gradually increases to stabilize around 120 psig. The overburden pressure remains at 20-40 psig above the injection pressure.

During the first stage of the experiment all horizontal sections are open to flow, however, section 2 produced very little oil and/or water during this period. This may have been caused by a partial block in either the well, the production line or the backpressure regulator. After section 3 was closed, the temperature in the area around section 2 increased significantly and production started in that section.

In the first stage of the run, the flowing backpressures start around the set-point of 50 psig, however, they begin to increase after hot fluid production starts. The regulators are later re-adjusted and the set-point is maintained throughout the run. Due to the problem with the blockage explained before, the backpressure in section 2 remains erratic in the

first stage of the run, however, when production stabilizes, the flowing pressure stays around 50 psig.

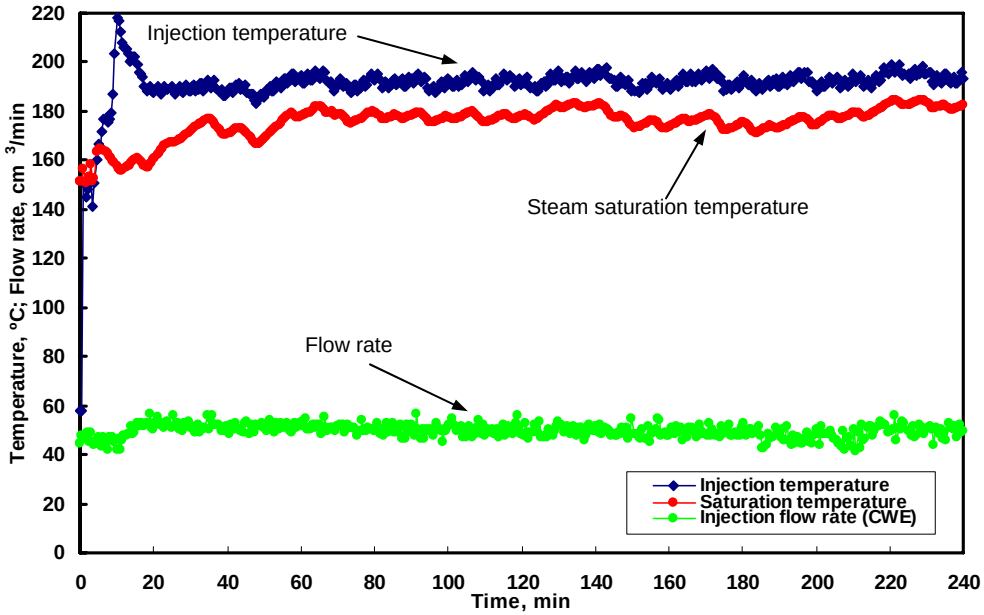

Fig. 6.51- Steam injection in the vertical injector-smart horizontal well system (Run 6 – Configuration B): Injection temperature and flow rate.

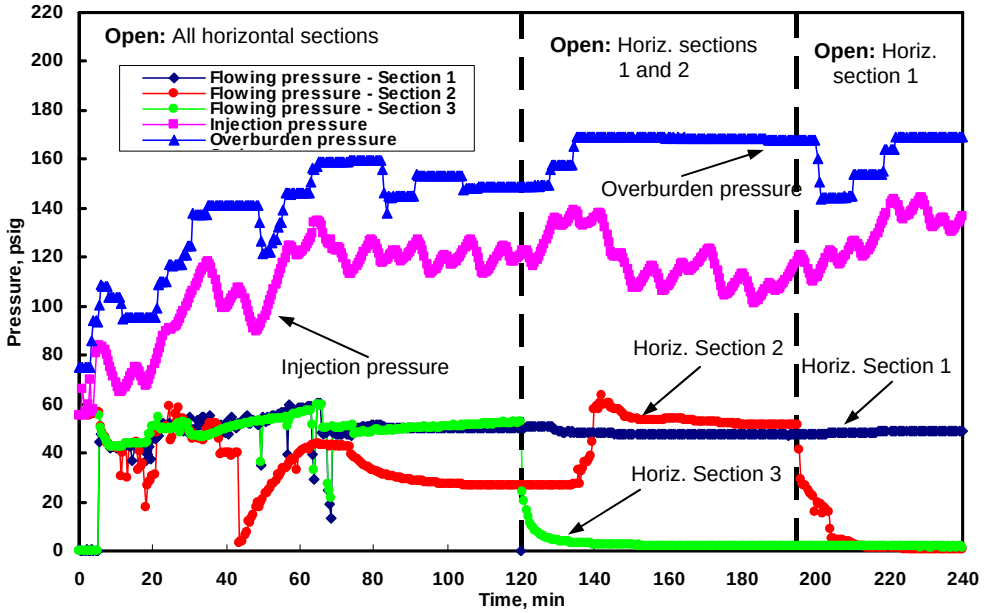

Fig. 6.52- Steam injection in the vertical injector-smart horizontal well system (Run 6 – Configuration B): Flowing pressure for the horizontal sections; injection pressure and overburden pressure.

Figs. 6.53, **6.54** and **6.55** present the water and oil rates for sections 1, 2 and 3 respectively. Section 1 produces throughout the entire experiment, while section 3 is open to flow only in the first 120 minutes. As explained before, although section 2 is open for the first 195 minutes of the run, it only begins significant fluid production at around 130 minutes, just after section 3 is closed.

The total oil production rate is depicted in **Fig. 6.56**. Oil production initially peaks at about 55 minutes with approximately 14 cm^3/min of oil. The rate begins to gradually decrease until 130 minutes when a surge occurs due to the contribution of section 2, in which steam had just broken into after a partial blockage prevented fluids from being produced in significant quantities.

A plot depicting the cumulative oil produced in this experiment is presented in **Fig. 6.57**. At the end of the run, the total amount of oil produced is 1772 cm^3, which corresponds to 49% of the original oil in place (according to **Fig. 6.58**).

Figs. 6.59 through **6.62** present a series of temperature profiles captured at different moments during the experiment. In early times (10 and 15 minutes) it can be observed how the temperature profile shows the advance of hot fluids towards the area around section 3. At 100 minutes (**Fig. 6.58**), the entire upper area of the cell is already at steam saturation temperature, which reflects that the steam zone occupies that portion on the physical model. At 120 minutes (the instant section 3 is closed), it can be observed that the areas around sections 1 and 3 at the bottom of the cell are hotter than the central area around section 2. This is explained by the lack of fluid production from section 2 due possibly to a partial blockage in that section. At 150 minutes, after significant production from section 2 is achieved, it can be noted that the temperature in the areas around sections 1 and 2 is higher than the temperature around section 1. This is explained by the shifting of fluid production from section 1 towards section 2. At 195 minutes (**Fig. 6.60**), when section 2 is closed, most of the middle portion of the cell is occupied by the steam zone. At 240 minutes, both the top and middle parts of the cell are completely occupied by steam as indicated by the steam saturation temperature.

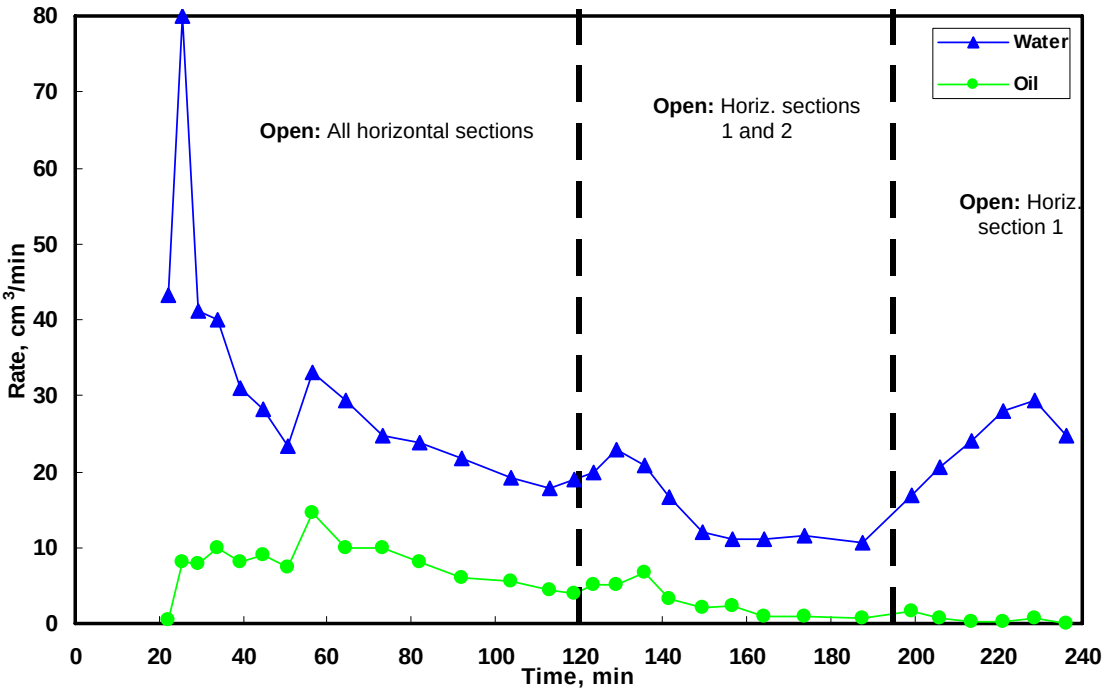

Fig. 6.53- Steam injection in the vertical injector-smart horizontal well system (Run 6 – Configuration B): Oil and water rates for horizontal section 1.

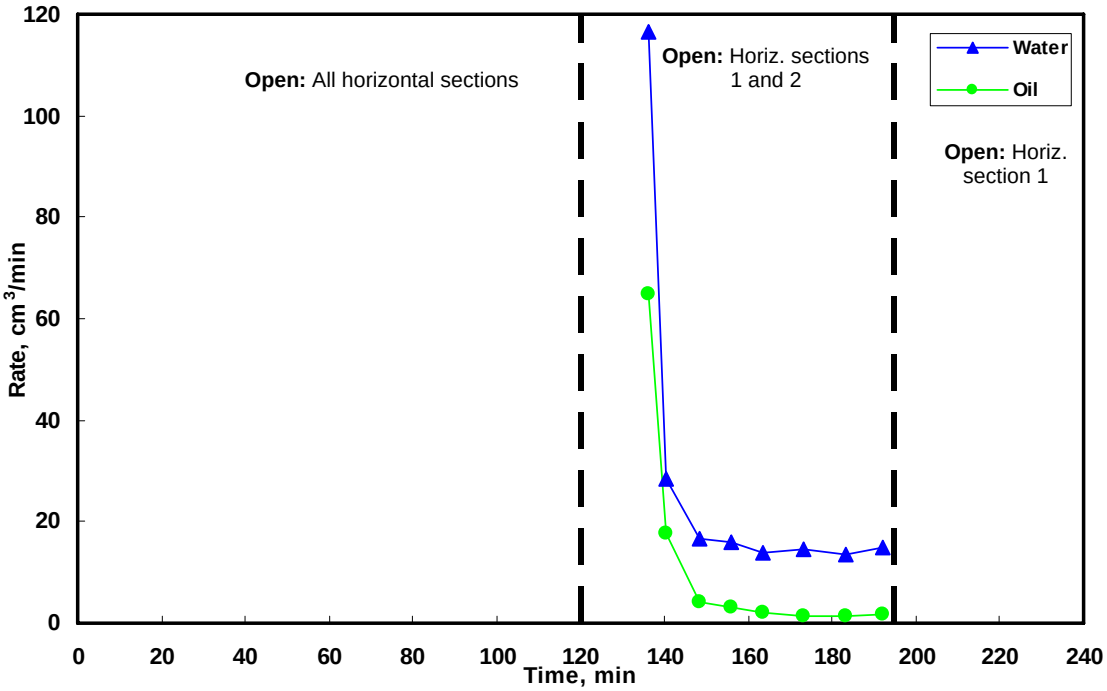

Fig. 6.54- Steam injection in the vertical injector-smart horizontal well system (Run 6 – Configuration B): Oil and water rates for horizontal section 2.

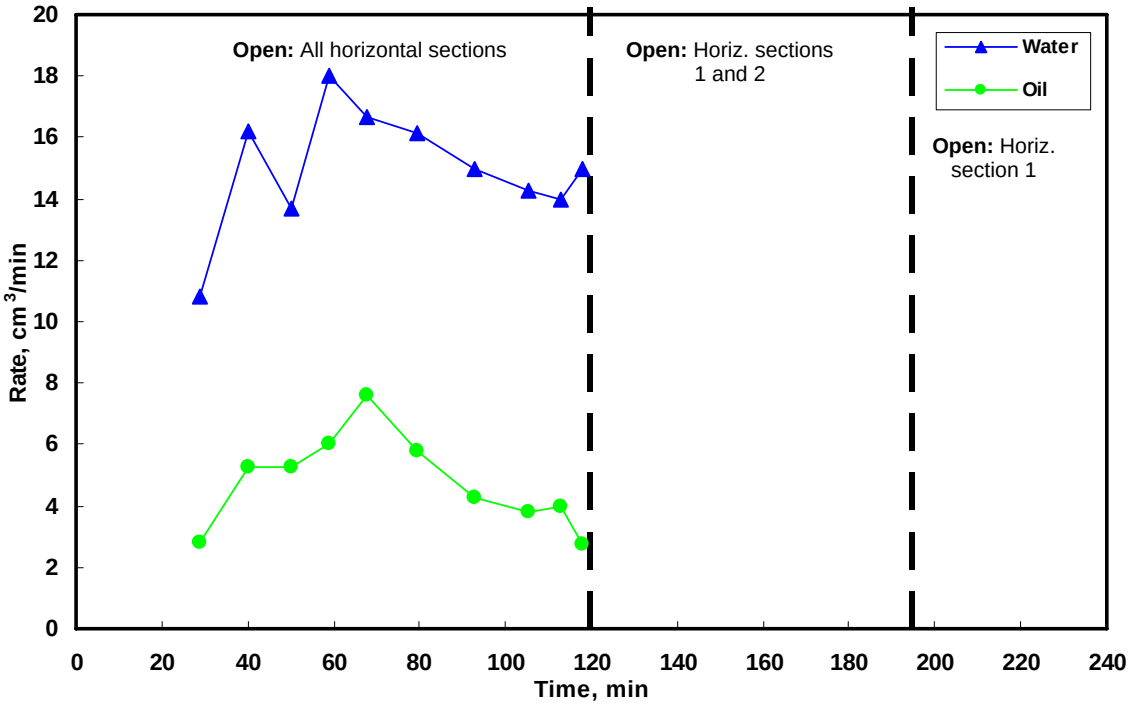

Fig. 6.55- Steam injection in the vertical injector-smart horizontal well system (Run 6 – Configuration B): Oil and water rates for horizontal section 3.

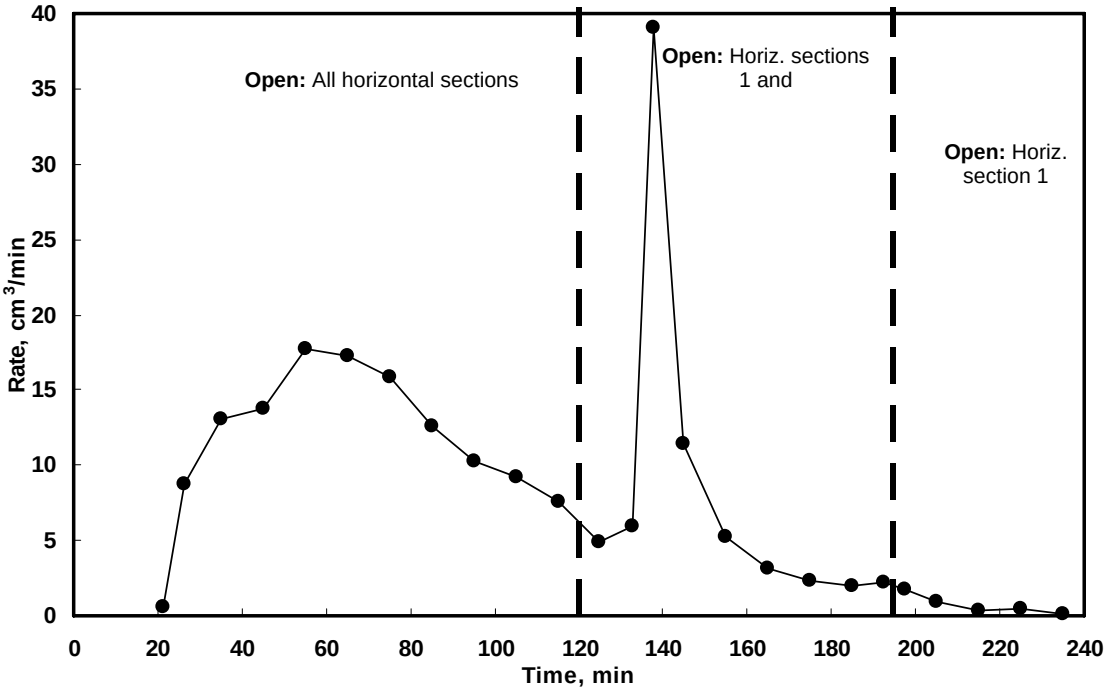

Fig. 6.56- Steam injection in the vertical injector-smart horizontal well system (Run 6 – Configuration B): Total oil rate.

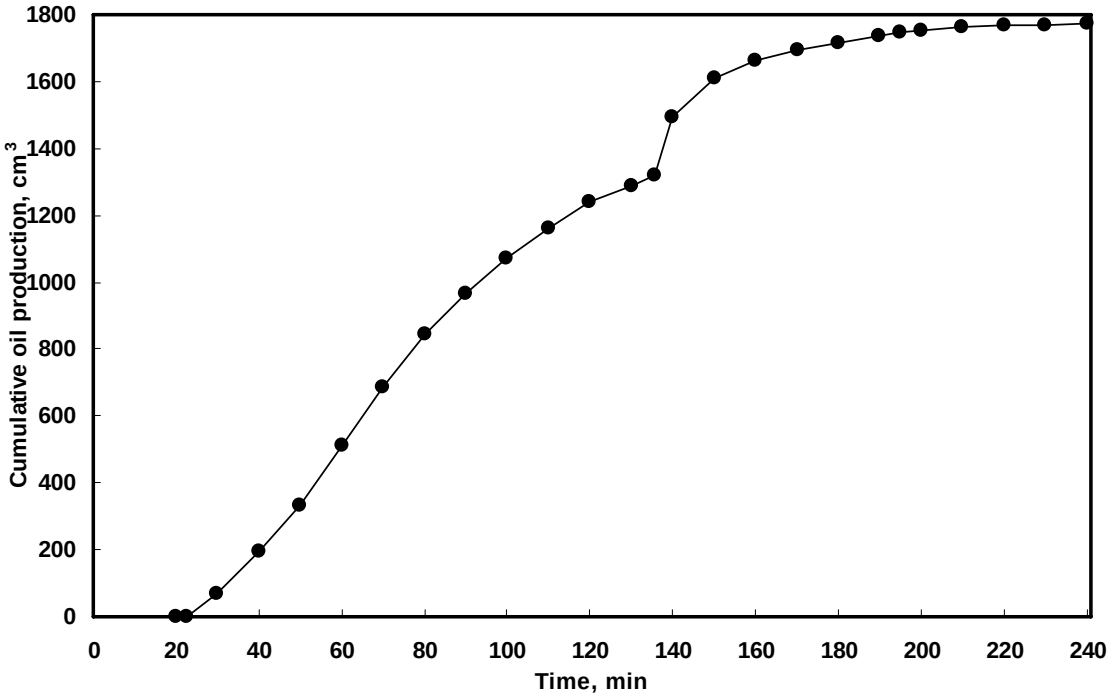

Fig. 6.57- Steam injection in the vertical injector-smart horizontal well system (Run 6 – Configuration B): Cumulative oil production.

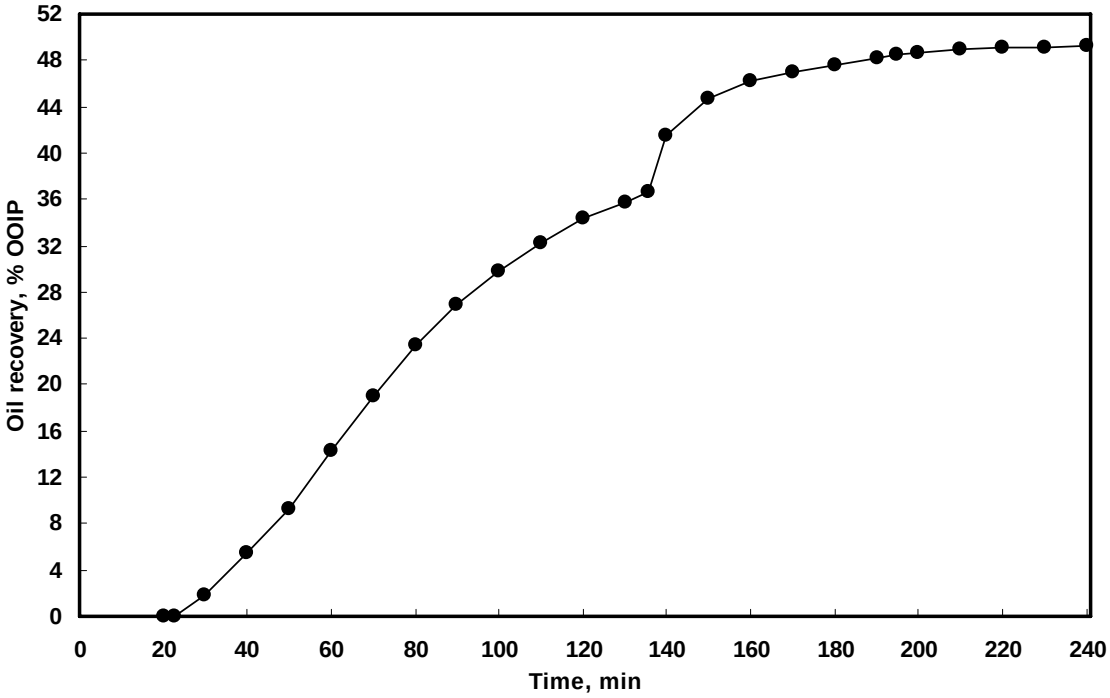

Fig. 6.58- Steam injection in the vertical injector-smart horizontal well system (Run 6 – Configuration B): Oil recovery.

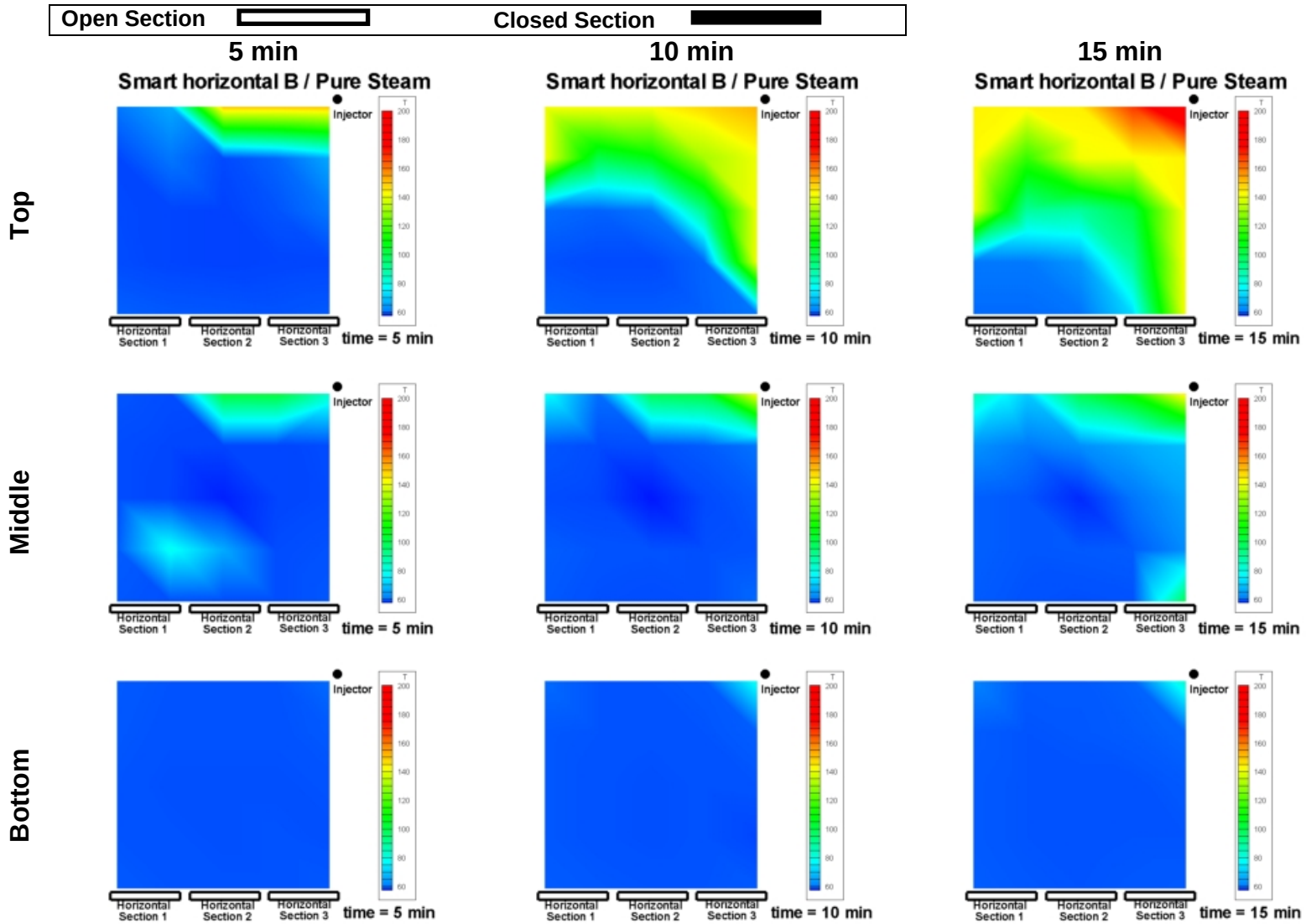

Fig. 6.59- Steam injection in the vertical injector-smart horizontal well system (Run 6 – Configuration B): Plan view of the temperature profiles in the physical model at 5, 10 and 15 minutes. The top, middle and bottom rows show the profile at the top, middle and bottom of the cell respectively.

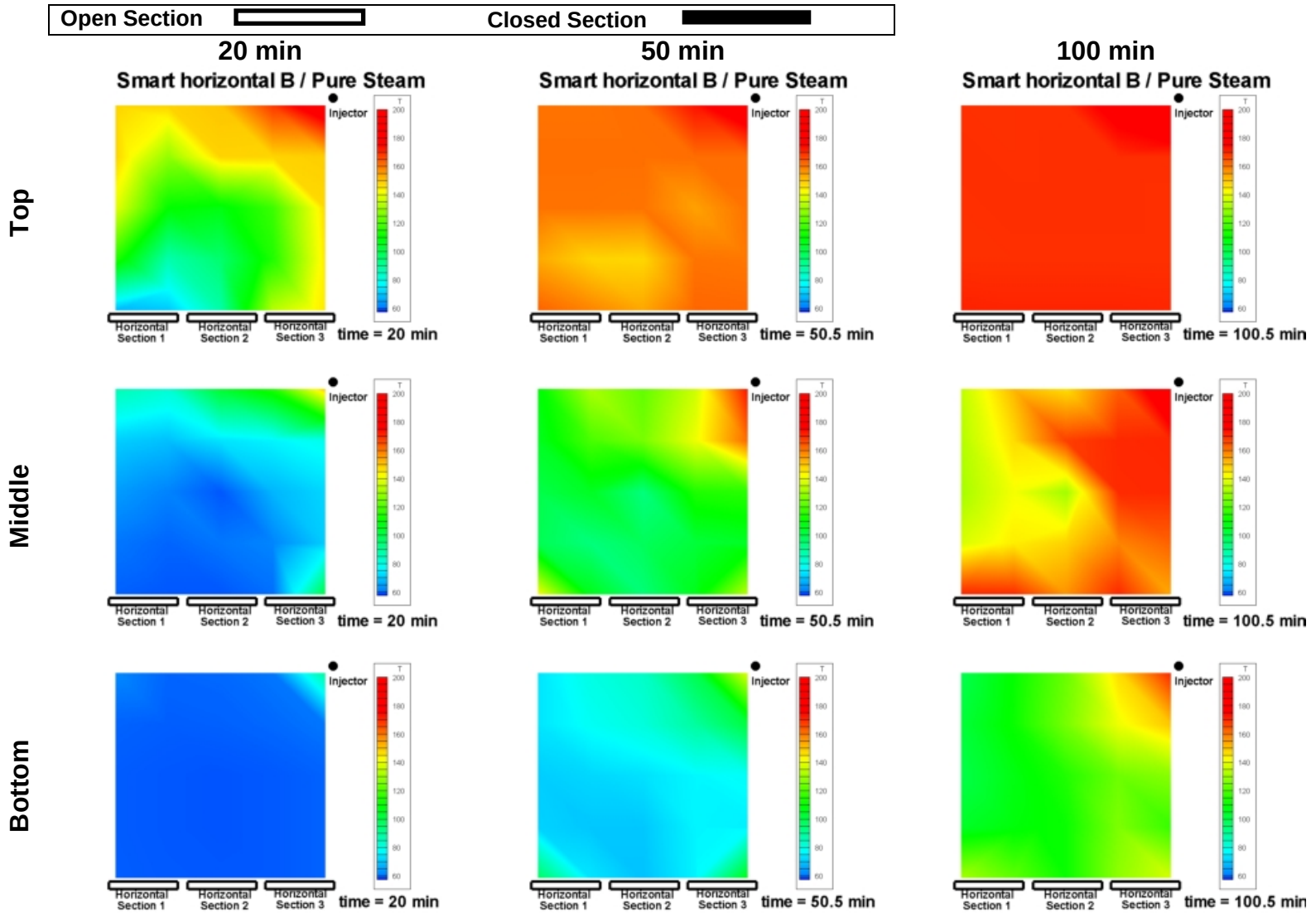

Fig. 6.60- Steam injection in the vertical injector-smart horizontal well system (Run 6 – Configuration B): Plan view of the temperature profiles in the physical model at 20, 50 and 100 minutes. The top, middle and bottom rows show the profile at the top, middle and bottom of the cell respectively.

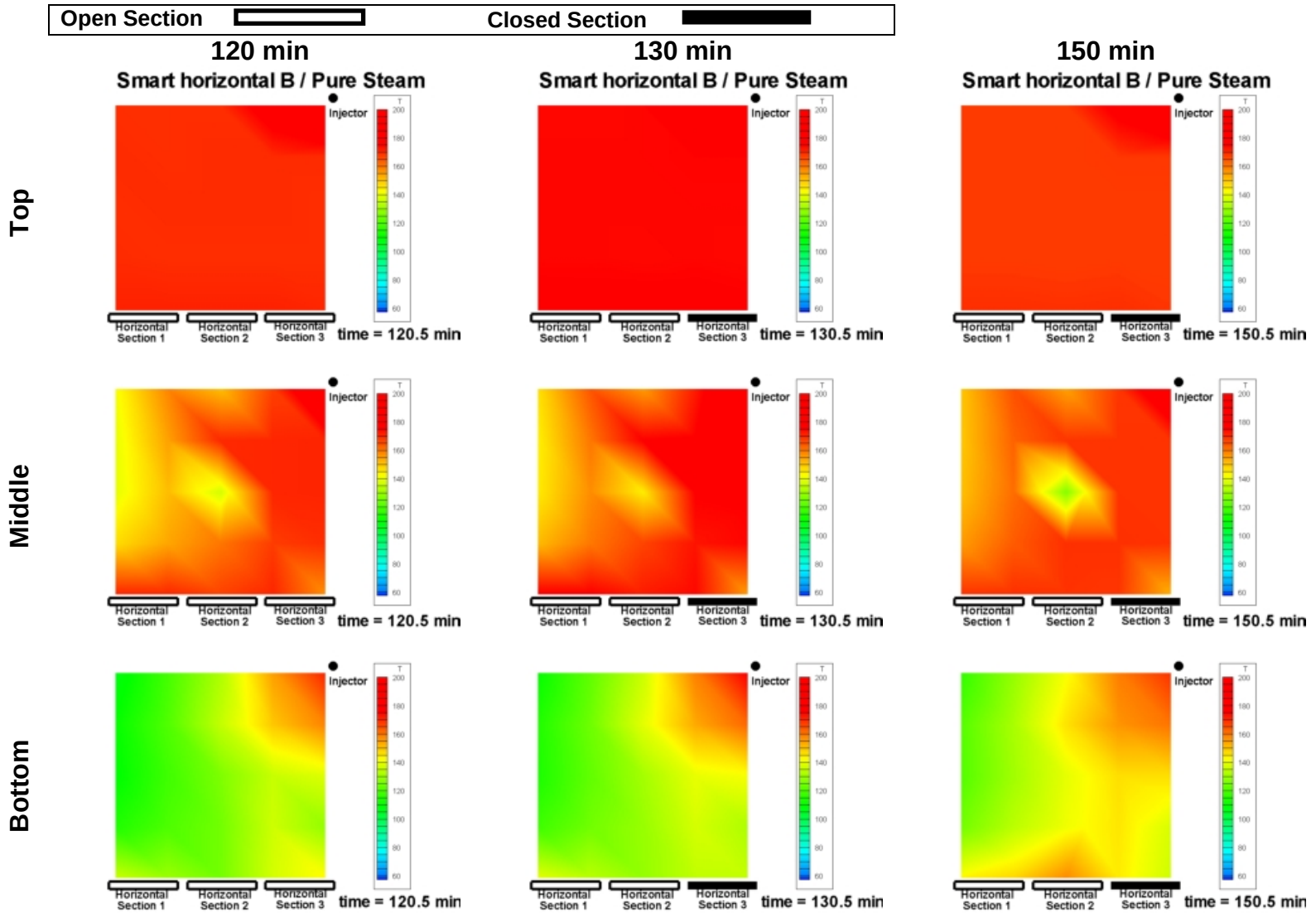

Fig. 6.61- Steam injection in the vertical injector-smart horizontal well system (Run 6 – Configuration B): Plan view of the temperature profiles in the physical model at 120, 130 and 150 minutes. The top, middle and bottom rows show the profile at the top, middle and bottom of the cell respectively.

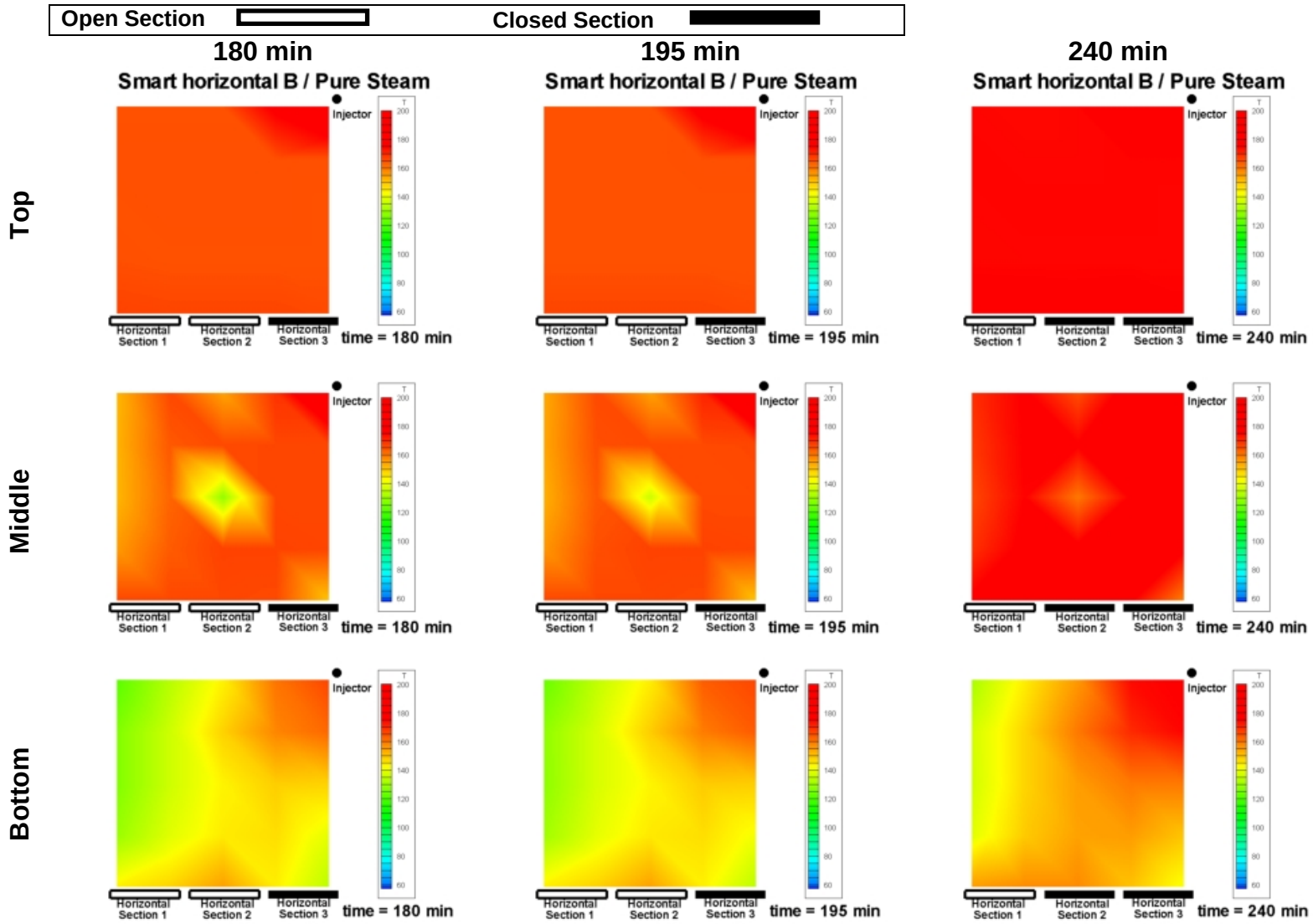

Fig. 6.62- Steam injection in the vertical injector-smart horizontal well system (Run 6 – Configuration B): Plan view of the temperature profiles in the physical model at 180, 195 and 240 minutes. The top, middle and bottom rows show the profile at the top, middle and bottom of the cell respectively.

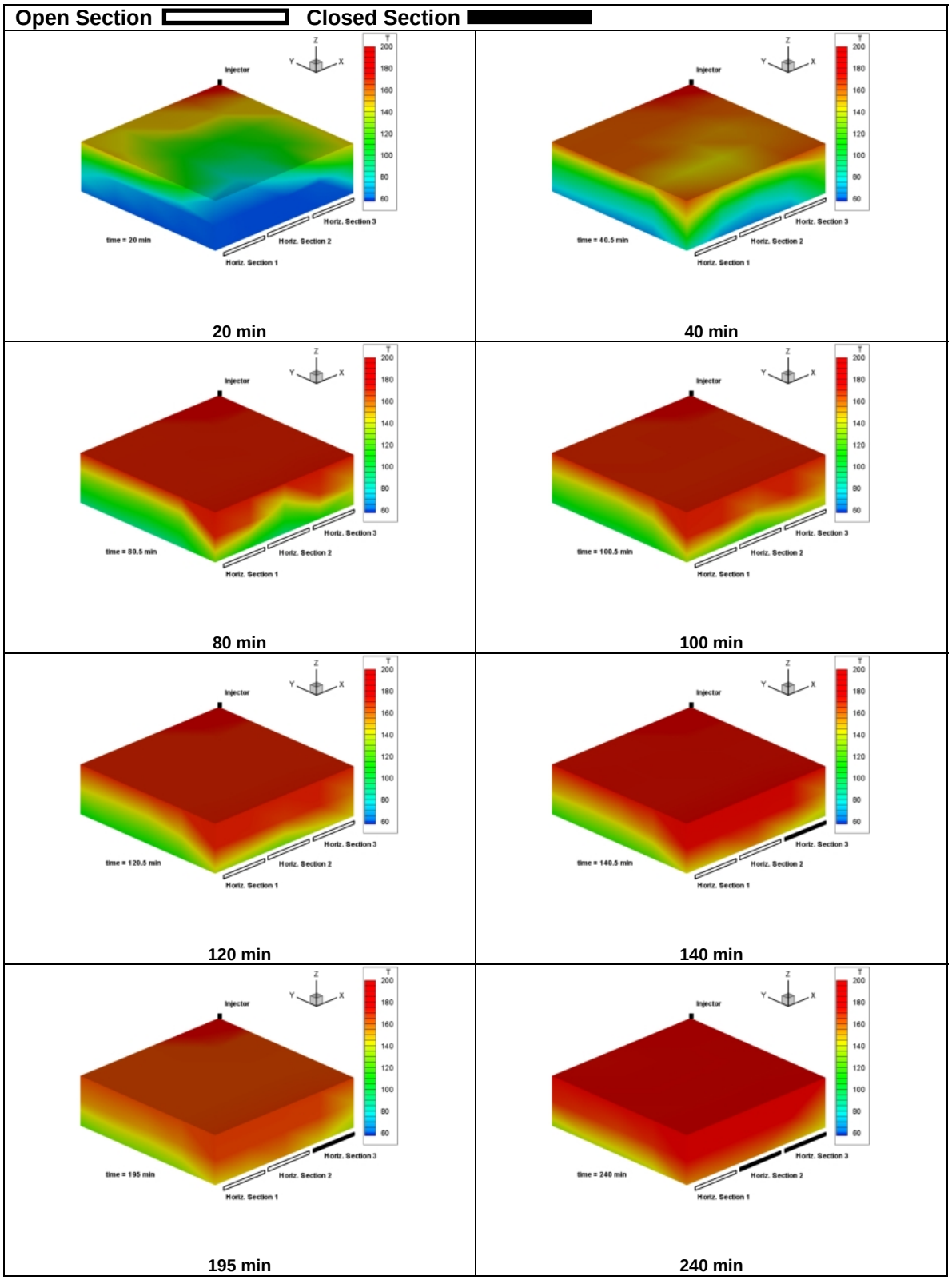

Fig. 6.63- Steam injection in the vertical injector-smart horizontal well system (Run 6 – Configuration B): Temperature profiles in isometric view seen from the front of the cell.

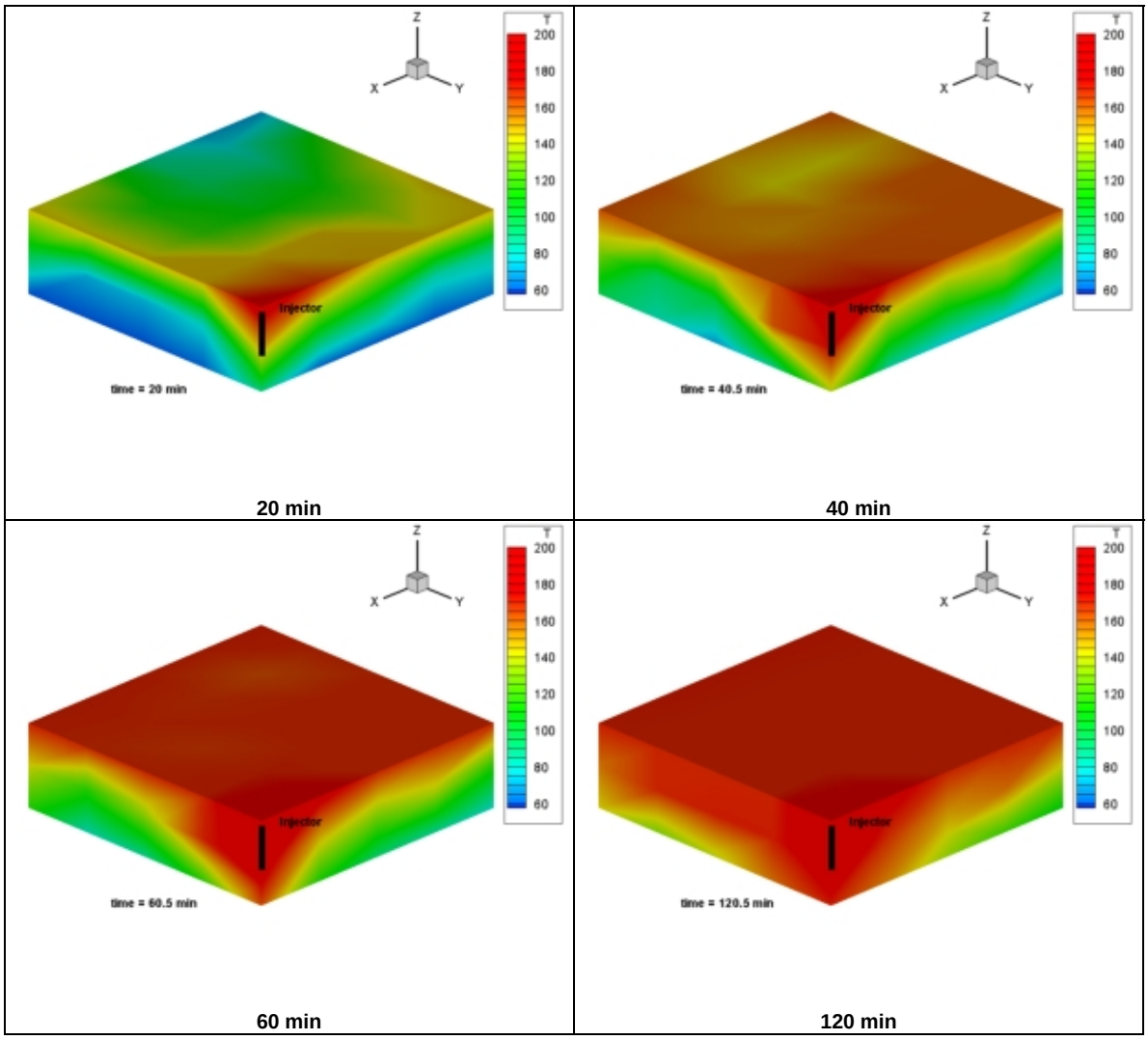

Fig. 6.64- Steam injection in the vertical injector-smart horizontal well system (Run 6 – Configuration B): Temperature profiles in isometric seen from the back of the cell.

Fig. 6.63 shows a series of temperature profiles in isometric view seen from the perspective of the horizontal producers. The plots at 40, 80, 100 and 120 minutes show that the temperature at the front face of the cell exhibits an arched profile, evidencing the movement of hot fluids towards sections 1 and 3, which are located towards the edges of the cell, leaving the central part (around section 2) at a lower temperature. As explained before, this is caused by the lack of substantial fluid production from section 2, probably caused by a partial block in this well. After section 3 is closed (120 minutes onwards), and section 2 begins to produce significant amounts of fluids, it can be noted that the arched profile disappears and the temperature around section 2 is as high as the temperature in section 1.

The temperature profile at the back side of the cell can be observed in **Fig. 6.64** which presents a series of isometric views seen from the perspective of the injector. As explained earlier, only the top section of the vertical injector is used in this experiment, therefore, the steam zone around the injection well, at early times, is concentrated mostly in the top of the cell. Later profiles (120 minutes) show that the steam zone boundaries have already advanced to occupy the majority of the cell's volume.

6.6 Comparative analysis on the use of steam and steam-propane injection in the vertical well system

In order to evaluate the performance of the steam propane injection process, two experimental runs using the vertical well system were carried out, runs 2 and 4. Run 2 serves as the base case since only steam was injected, while in run 4 propane is injected using a propane:steam mass ratio of 4:100.

A plot depicting the oil production rate for both runs is presented in **Fig. 6.65**. Oil rate for the pure steam run peaks at 110 minutes with a maximum of 13.5 cm^3/min. In contrast, maximum oil production rate is achieved at 50 minutes for the steam-propane run, reaching 18 cm^3/min.

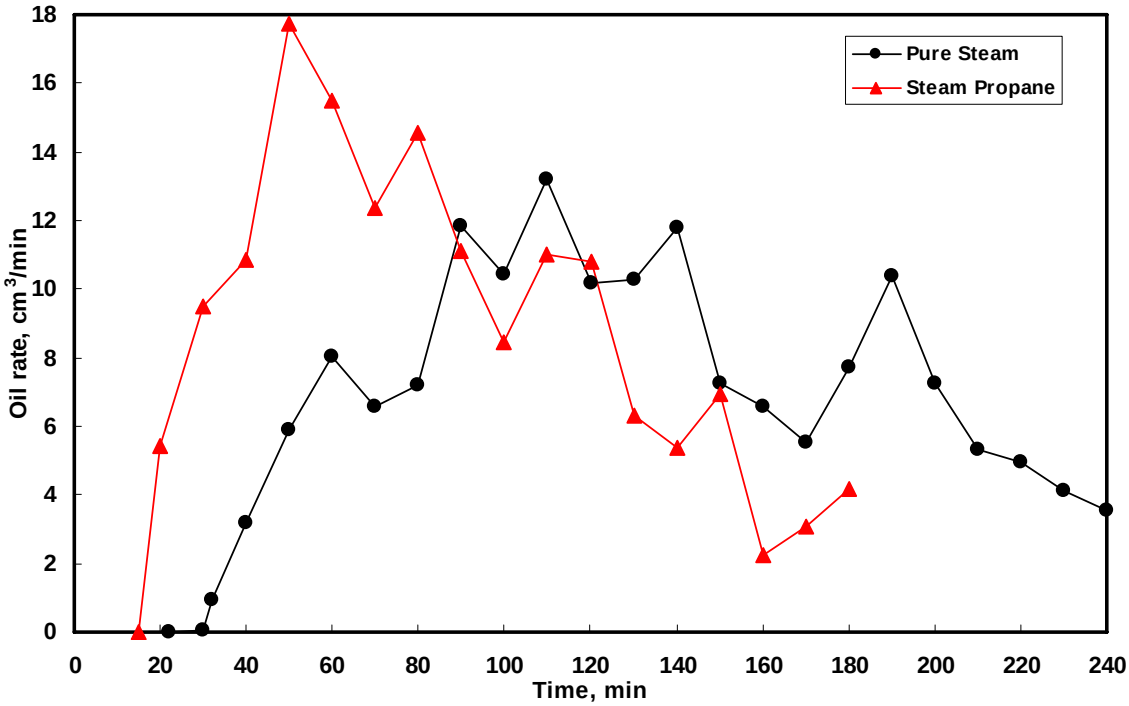

Fig. 6.65- Comparison of oil production rates under steam and steam-propane injection in the vertical well system.

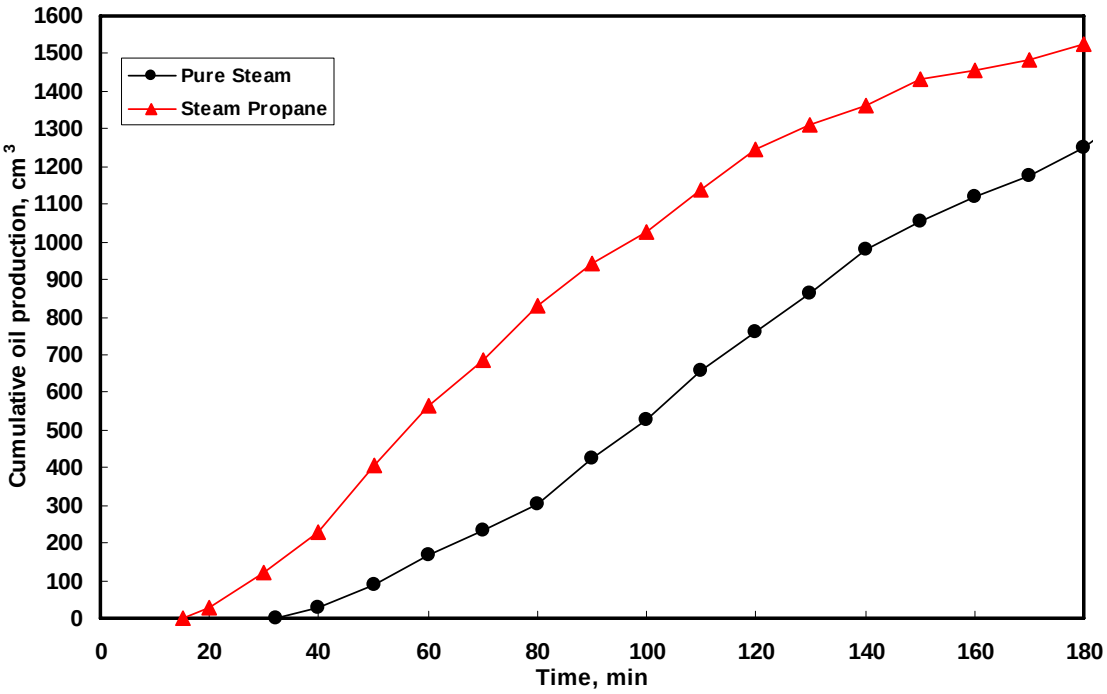

Fig. 6.66- Cumulative oil production under steam and steam-propane injection in the vertical well system.

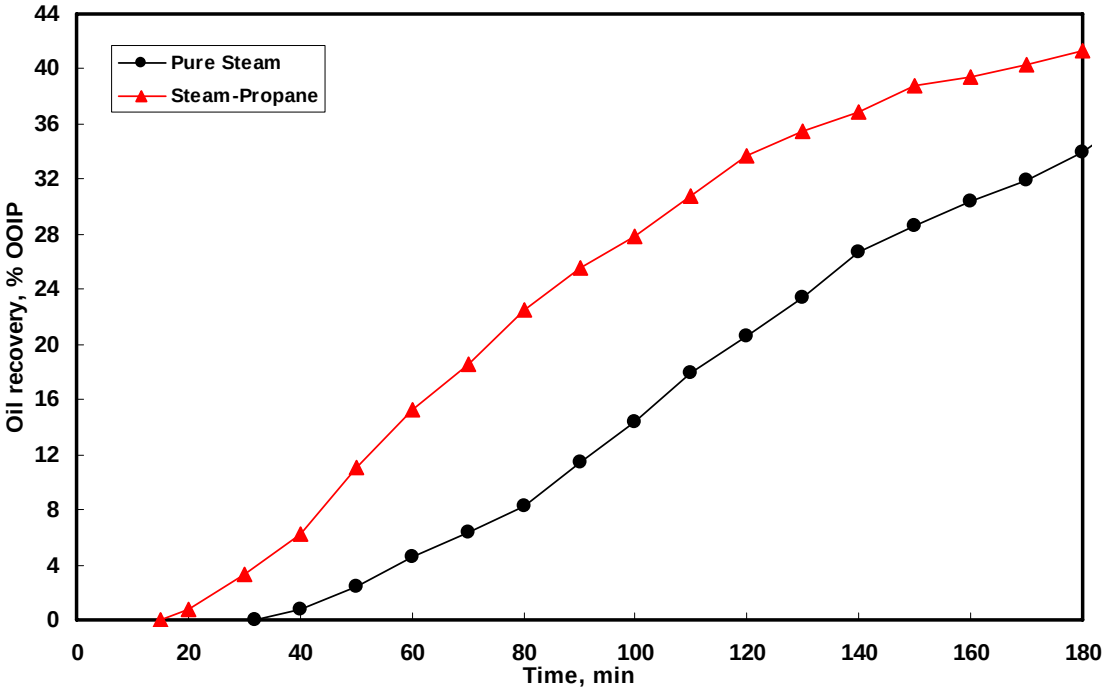

Fig. 6.67- Cumulative oil recovery under steam and steam-propane injection in the vertical well system.

Cumulative oil production for both runs is depicted in **Fig. 6.66**. At 180 minutes (the maximum run time attained for run 4), the total amount of oil produced in the pure steam run is 1250 cm^3, compared to 1526 cm^3 in the steam-propane run. These volumes correspond to 34.0 and 41.4% of the original oil in place (shown in **Fig. 6.67**), which represent an increase in oil recovery of more than 7% OOIP when propane is used as an additive.

One-dimensional experiments that have been conducted since 2001 in Texas A&M[11-17] with steam-propane injection did not show that oil recovery could be increased with the addition of propane. However, the results of this research, conducted using a three-dimensional model, indeed demonstrate that when propane is used as an additive, higher oil recovery is obtained. This discrepancy can be attributed to the fact that three-dimensional models can describe more accurately certain processes such as steam injection than one-dimensional models. One-dimensional models constitute a very valuable tool that allows for the preliminary evaluation of displacement processes in a simple and efficient manner. However, these models cannot accurately represent all the phenomena involved in processes such as steam injection plus additives (e.g. gravity segregation), which can be better modeled using a scaled three-dimensional cell such as the one employed in this research.

Oil production starts earlier when propane is used as an additive. In run 2 (pure steam), oil begins to be produced at 32 minutes, compared to 15 minutes in the steam-propane run, which represents an acceleration of 53% in time. These findings confirm the results obtained in previous experiments with steam-propane injection,[11-17] where production acceleration ranging from 12 to 30% was observed.

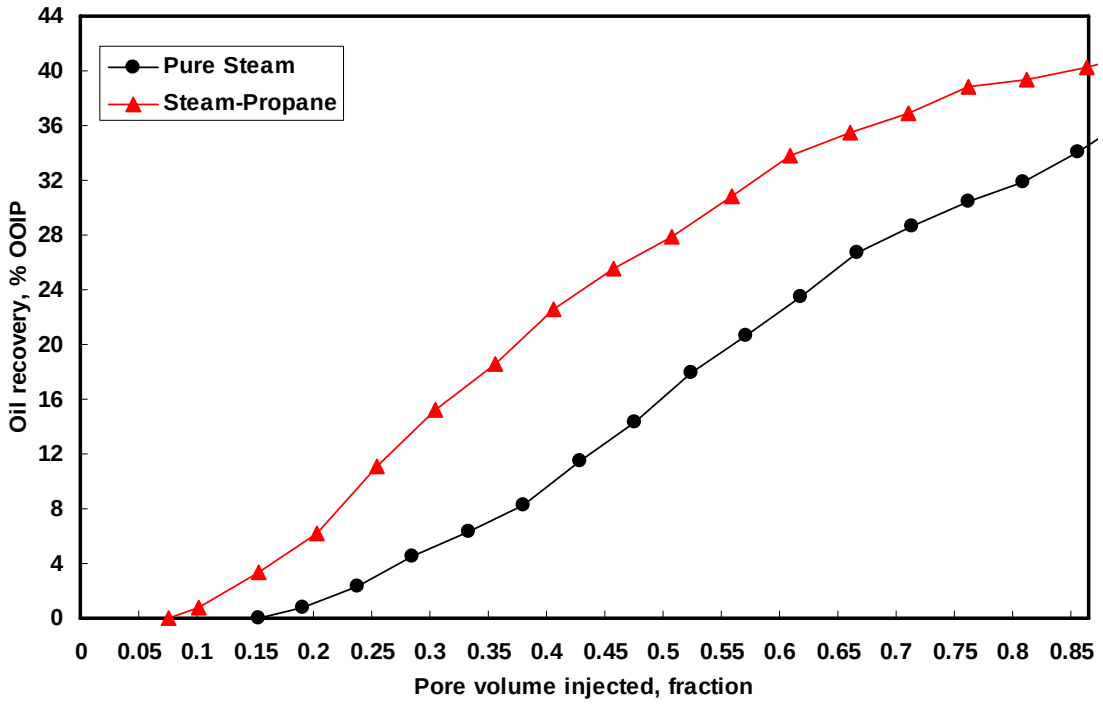

Fig. 6.68- Cumulative oil recovery as a function of pore volume injected under steam and steam-propane injection in the vertical well system.

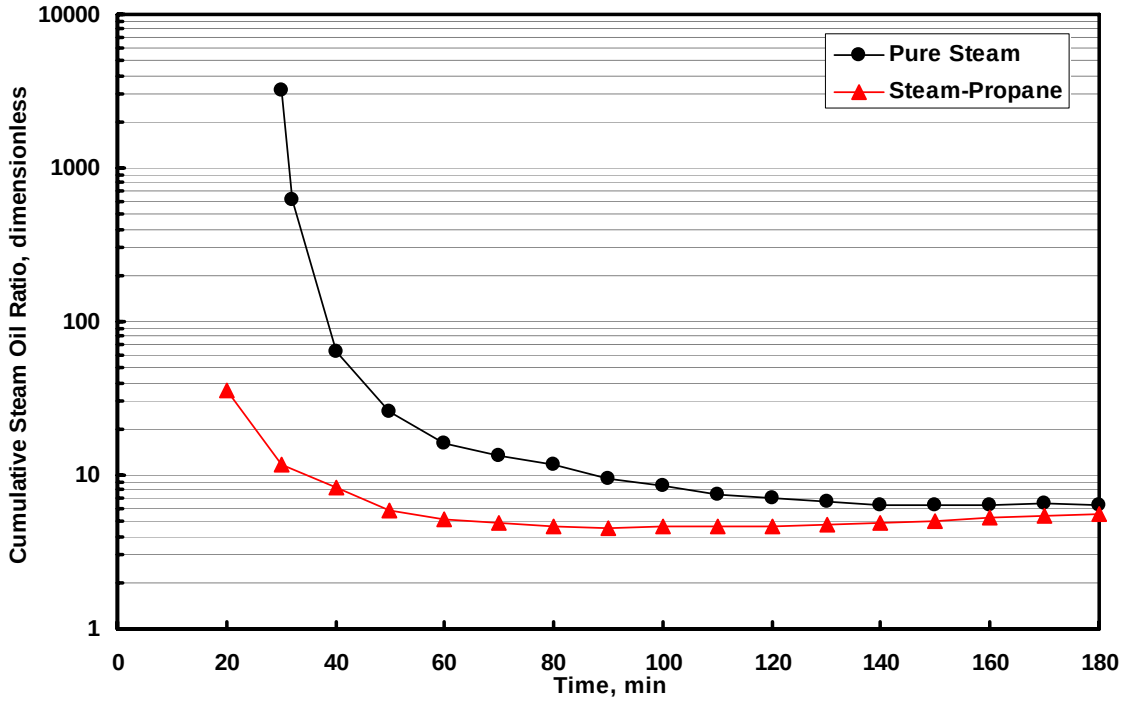

Fig. 6.69- Cumulative steam oil ratio under steam and steam-propane injection in the vertical well system.

Fig. 6.68 shows the cumulative oil recovery plotted against pore volume injected. Because of the small variations on the steam injection rates from run to run, there will be slight differences between the shape of the recovery curves in the time plots and the pore volume plots. To have an idea of the recovery acceleration provided by the addition of propane, it can be observed that to produce 25% of the OOIP, approximately 0.45 pore volumes must be injected, compared to the 0.65 pore volumes that have to be injected in the pure steam case.

The steam-oil ratio (SOR) is a parameter employed to quantify the efficiency of steam injection processes. It represents the volume of steam required to produce one unit-volume of oil, consequently, lower steam-oil ratios denote a more efficient utilization of the steam. Steam-oil ratios start at high values initially in the life of a steamflooding process. As time progresses, and the reservoir temperature increases, the process becomes more efficient and the values of SOR can decrease significantly. Later in the life of the project, the steam oil ratio can start to increase again as oil saturation decreases in the steam zone and it becomes more difficult to produce oil.

The cumulative steam-oil ratio (plotted in **Fig. 6.69**) is calculated using the cumulative steam injected and the cumulative oil produced at different times during the run. It can be observed that the SOR for the pure steam run starts around 2000, as opposed to the SOR for the steam-propane run that begins approximately at 30. Both SOR's start to decline rapidly as injection progresses, as it is evidenced by the curve representing the pure steam run, which decreases three orders of magnitude during the experiment. The SOR for the pure steam case stabilizes after 110 minutes at around 6, while the SOR for the steam-propane case stabilizes very early in the run at a value between 4 and 5. It can be noted that after approximately 100 minutes, the SOR for the steam-propane run starts to increase very slowly.

Figs. 6.70 through **6.74** show a series of comparisons between the temperature profiles of runs 2 and 4. These comparisons, which are presented for different times during the run, allow us to analyze and contrast the advance of the steam front in both the pure steam run and the steam-propane run.

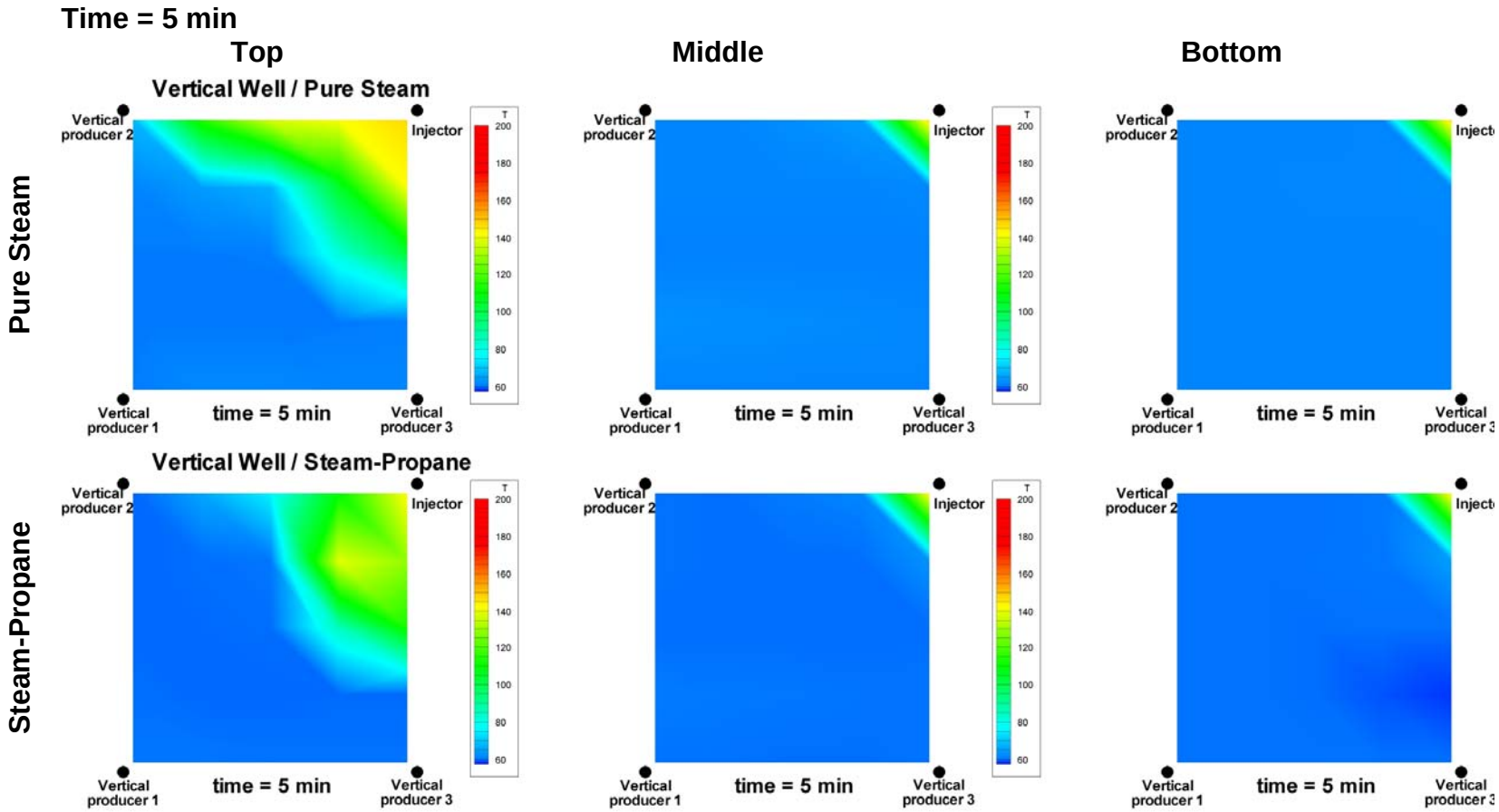

Fig. 6.70- Plan view of the top, middle and bottom temperature profiles in the physical model at 5 minutes. The top and bottom rows correspond to the pure steam run and the steam-propane run respectively.

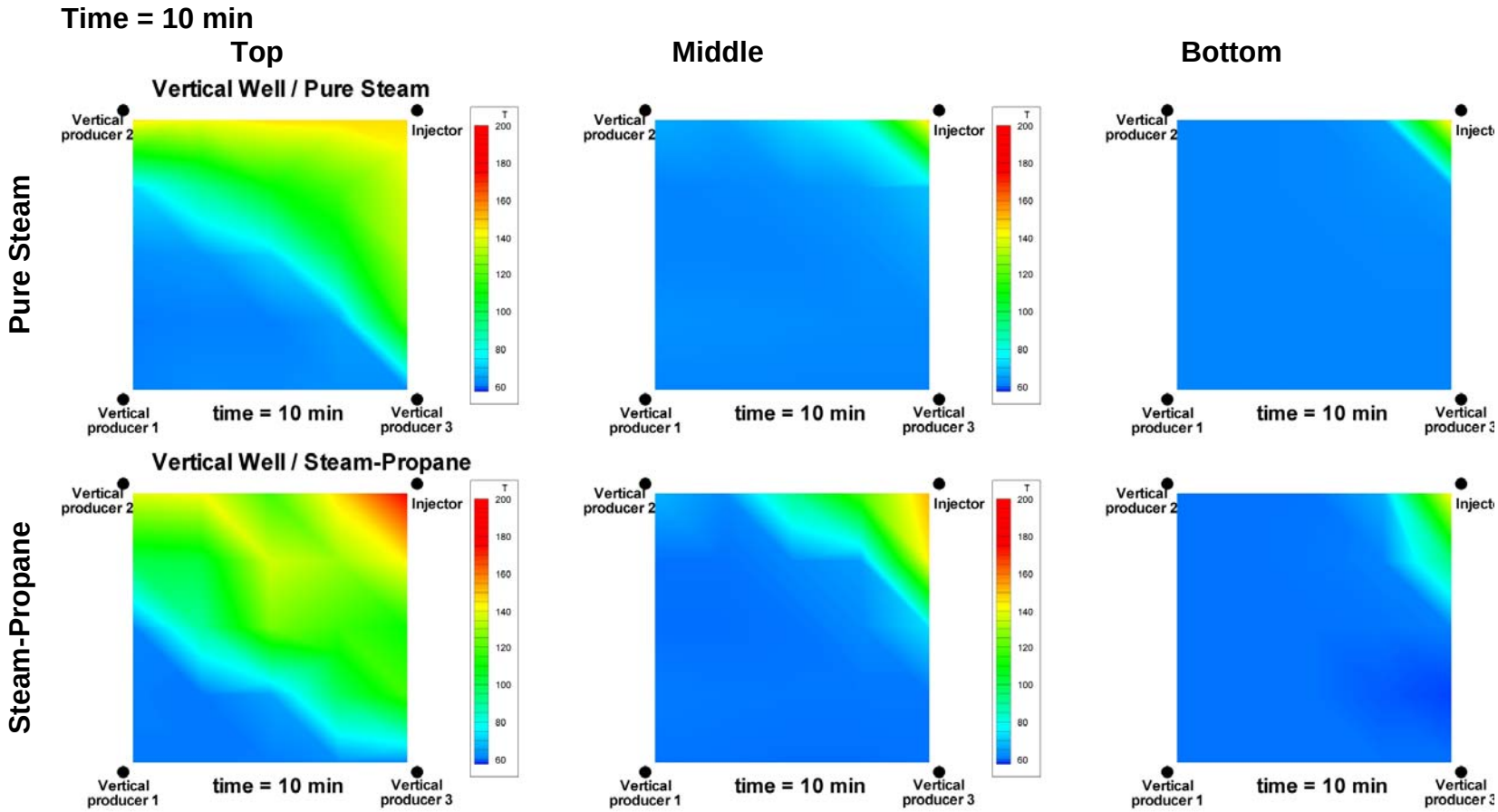

Fig. 6.71- Plan view of the top, middle and bottom temperature profiles in the physical model at 10 minutes. The top and bottom rows correspond to the pure steam run and the steam-propane run respectively.

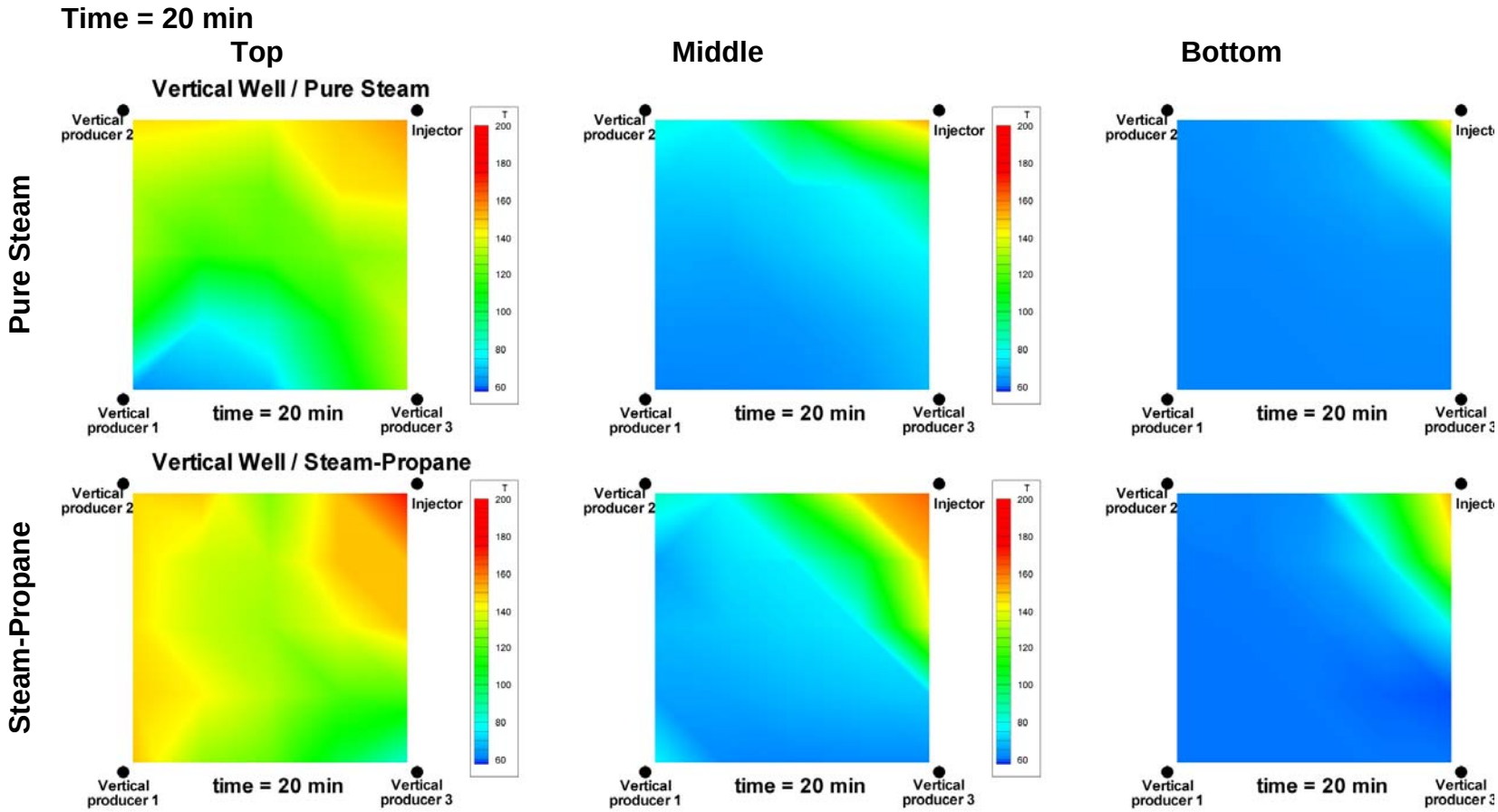

Fig. 6.72- Plan view of the top, middle and bottom temperature profiles in the physical model at 20 minutes. The top and bottom rows correspond to the pure steam run and the steam-propane run respectively.

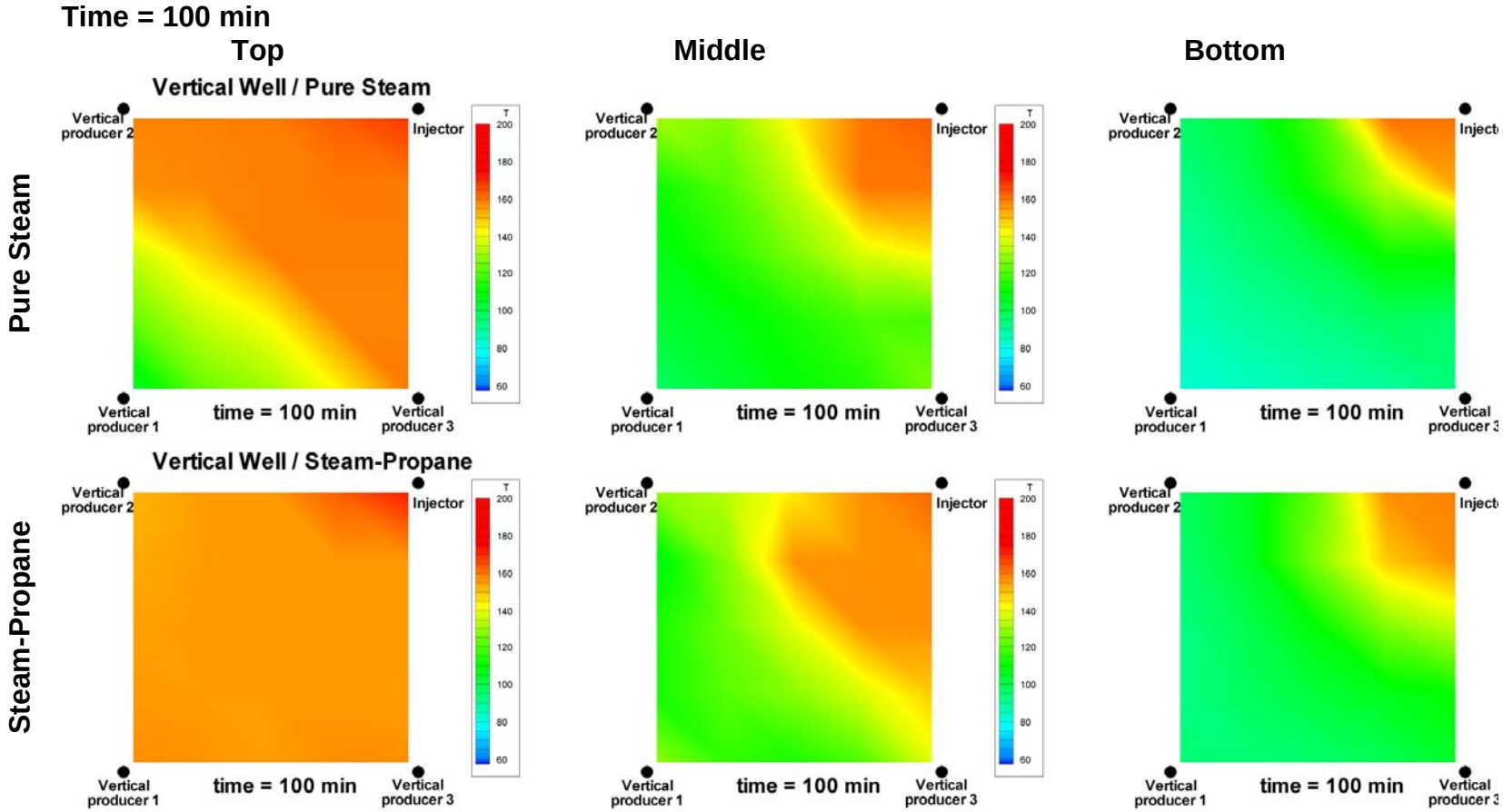

Fig. 6.73- Plan view of the top, middle and bottom temperature profiles in the physical model at 100 minutes. The top and bottom rows correspond to the pure steam run and the steam-propane run respectively.

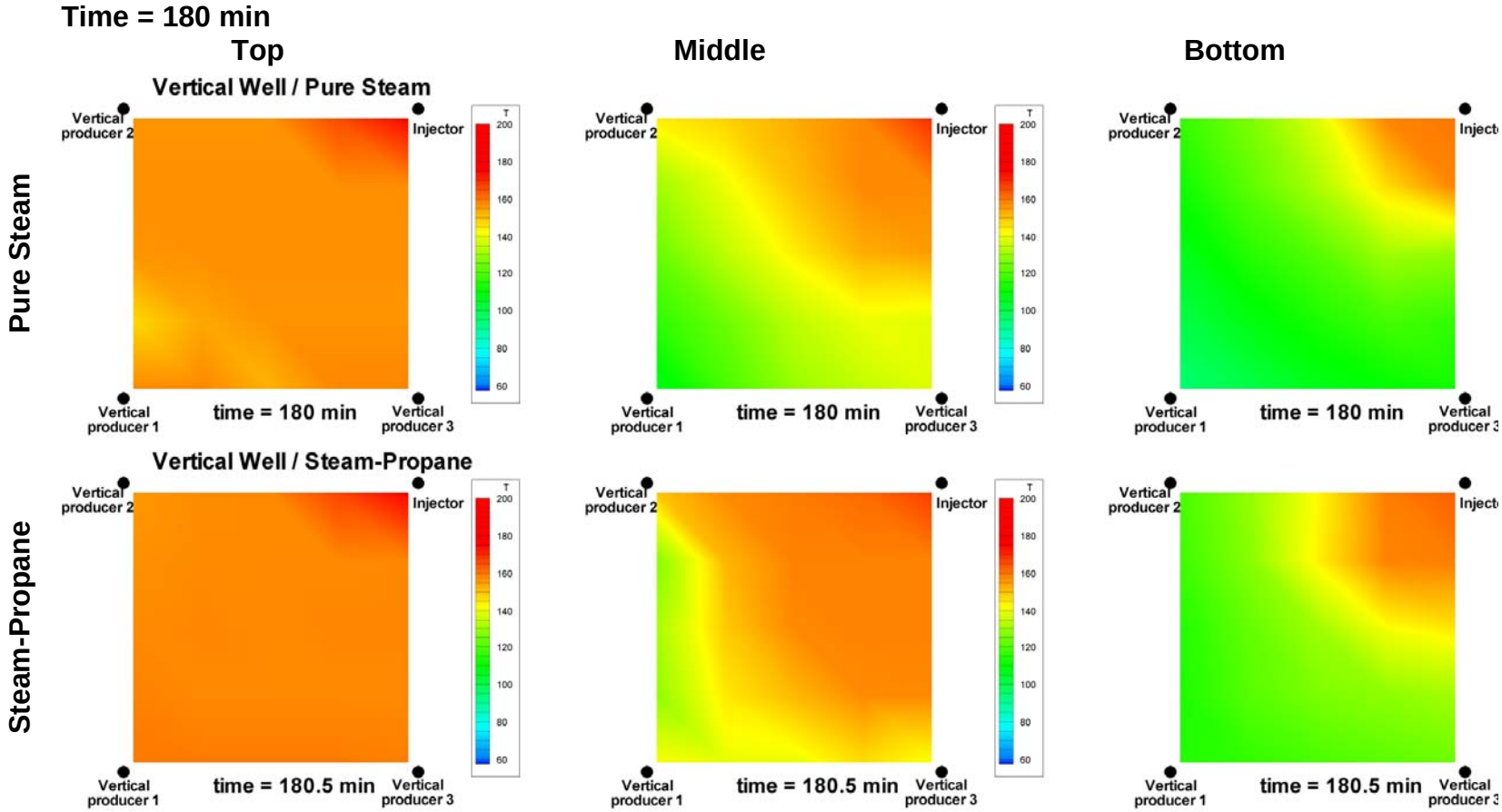

Fig. 6.74- Plan view of the top, middle and bottom temperature profiles in the physical model at 180 minutes. The top and bottom rows correspond to the pure steam run and the steam-propane run respectively.

The profile at 5 min (**Fig. 6.70**) shows that the temperature increase due to steam injection is limited only to the top section of the cell. At 10 minutes (**Fig. 6.71**), the middle and bottom sections of the cell, show a noticeable temperature increase for the steam-propane run, while the profile for the pure steam run remains almost unchanged. **Fig. 6.73** shows that at 100 minutes the steam front has not reached well 1 in the pure steam run, in contrast, the propane run shows that the entire area at the top of the cell is already at saturation temperature. This is evidence that the steam front has moved at faster rate when propane is used.

At the end of the run (180 minutes), all wells show steam breakthrough for both the steam and steam-propane experiments. Also, it can be noted that the middle and bottom sections of the cell are hotter in the steam-propane run. The size of the steam zone at any given time is bigger in the steam-propane experiment than in the pure steam run. Therefore, propane appears to be accelerating the movement of the steam front inside the cell, which is also corroborated by the earlier oil production observed in the experiment (**Fig. 6.66**).

More evidence of the effect of propane injection in the size of the steam zone can be seen in **Fig. 6.75**. Here, we can observe a time progression comparing the temperature profiles in a cross section between the injector and vertical producer 1.

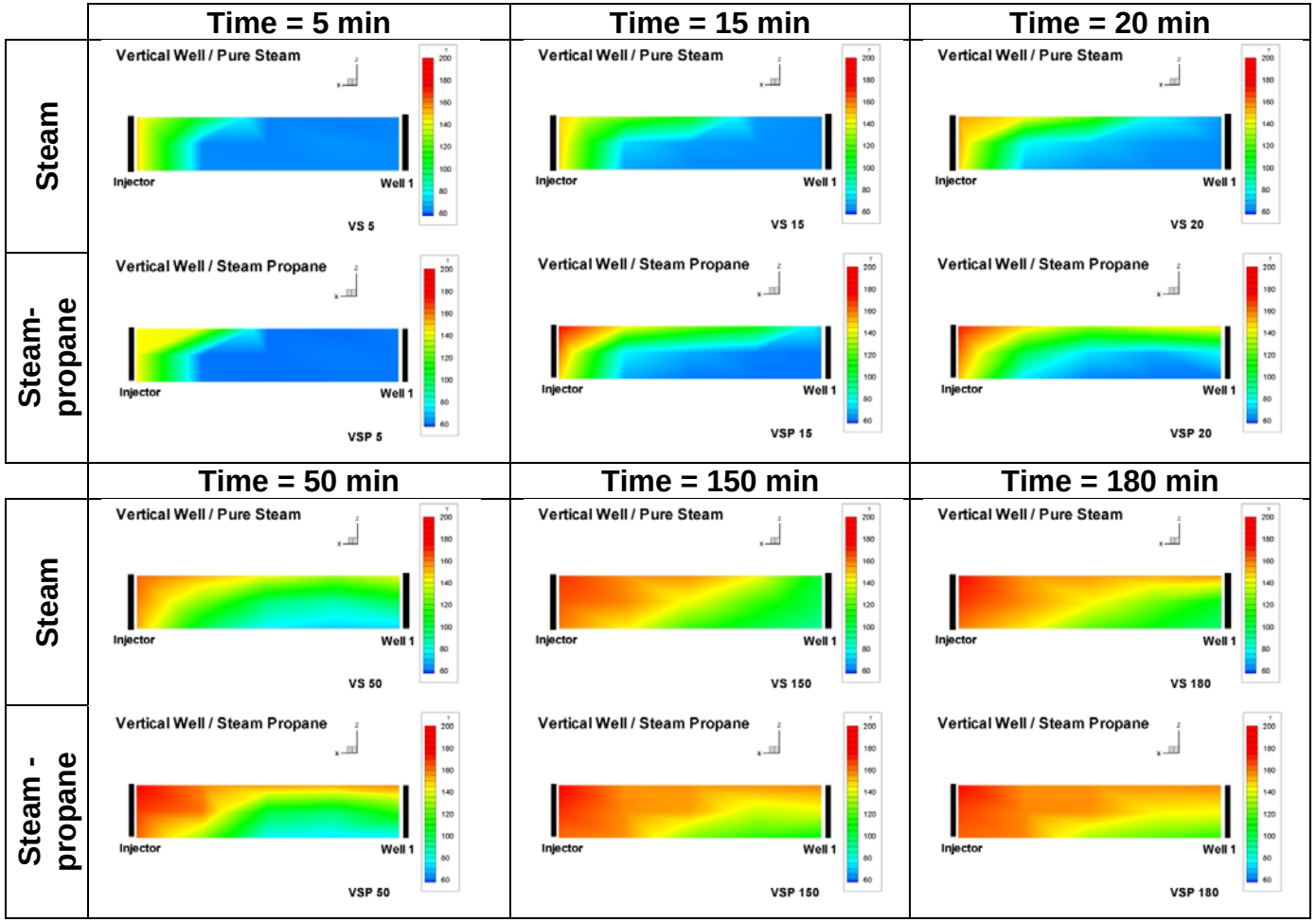

Fig. 6.75- Temperature profile of a cross section going through the injector and well 1. A comparison between steam injection (top) and steam-propane injection (bottom) is presented for each one of the times depicted.

The cross section shows the steam override phenomenon very clearly for both steam and steam-propane injection. In addition, it can be observed that the temperature tends to increase faster in the steam propane experiment; for instance, at 20 minutes, the area around the top section of well 1 already shows fluids at more than 120ºC, while the same zone in the pure steam run exhibits initial temperature. The same situation occurs at the end of the run (180 minutes), where we can observe that the temperature in the area around well 1 averages 120ºC in the steam experiment and 140 – 160ºC for the steam-propane run.

As explained before, the addition of propane causes the steam front to propagate faster in the cell and at the same time it helps the steam occupy a bigger volume inside the physical model. This produces acceleration in oil production and also increase in the ultimate oil recovery because more oil is being contacted by the steam zone.

The mechanism by which propane accelerates the steam front is probably due to additional viscosity reduction. This phenomenon is most likely explained by the fact that some of the propane injected dissolves in the hot oil, further decreasing its viscosity. The lower-viscosity oil moves faster towards the producing wells and it is also more easily displaced by the steam and condensed water.

6.7 Comparative analysis on the use of the vertical injector–smart horizontal well system

In this section, the performance of the vertical injector-smart horizontal and vertical well systems is compared. As mentioned earlier in this chapter, two different configurations were considered to test the smart horizontal system: configurations A and B (see sections 6.3 and 6.6).

The oil production rate for all three runs is shown in **Fig. 6.76**. Initially, the smart horizontal well (in both configurations) exhibit higher rates than the vertical well system, with configuration B showing a peak of 18 cm^3/min. As time progresses, oil rates for both configuration A and B start to decrease, and at some point, they become lower than the rates observed in the vertical well system. A second peak can be observed for configuration B at about 140 minutes. As explained in section 6.6, the closure of section 1 at 120 minutes brings a production surge in the oil rate for configuration B.

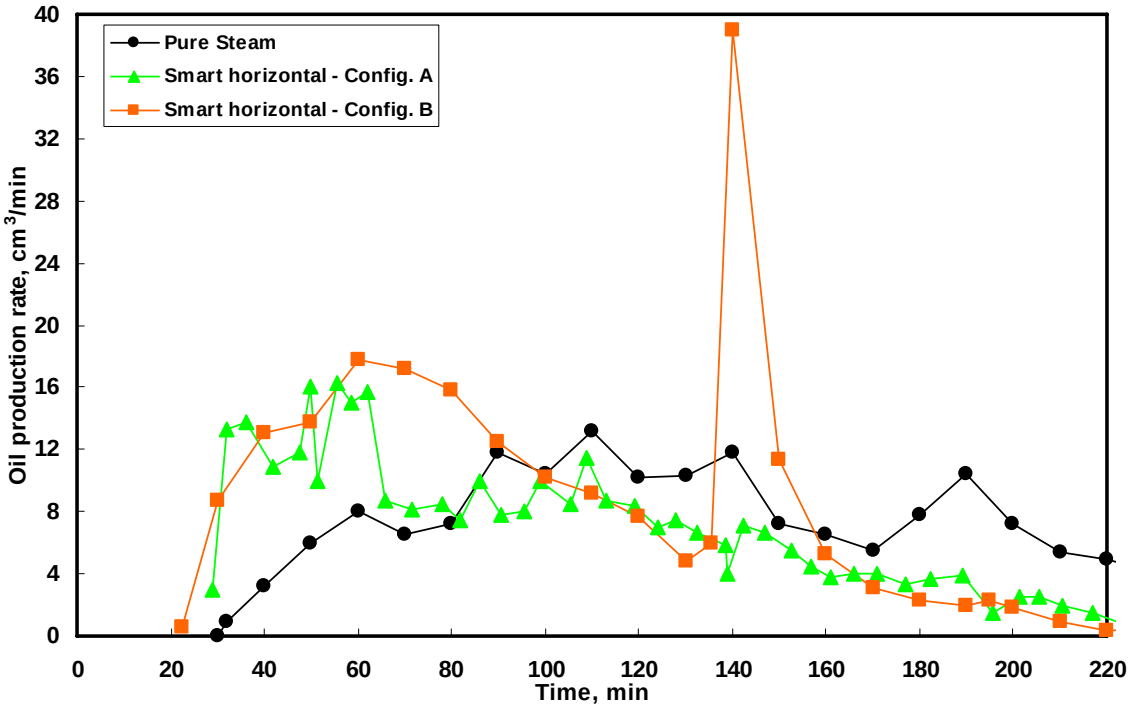

Fig. 6.76- Comparison of oil production rates for the vertical and smart horizontal well systems (configurations A and B).

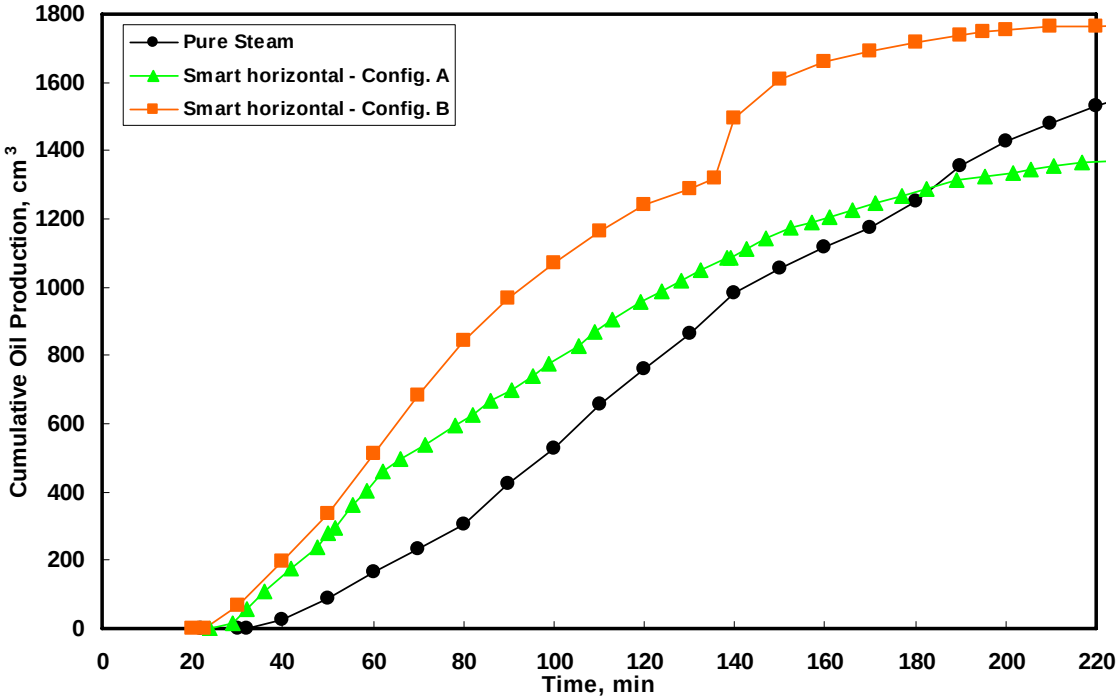

Fig. 6.77- Cumulative oil production for the vertical and smart horizontal well systems (configurations A and B).

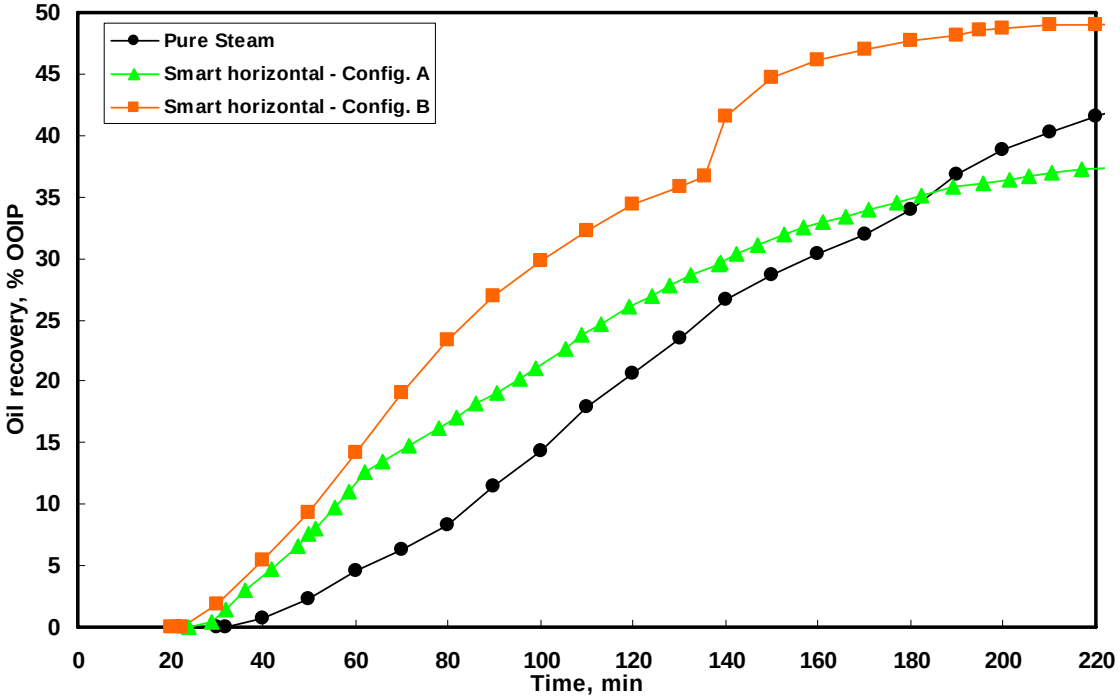

Fig. 6.78- Cumulative oil recovery for the vertical and smart horizontal well systems (configurations A and B).

Figs. 6.77 and **6.78** show plots of the cumulative oil production and cumulative oil recovery respectively. The smart horizontal configuration B yields the highest ultimate oil recovery (about 49% OOIP), compared with the 42% obtained with the vertical well system. The lowest ultimate recovery was obtained with configuration A of the smart horizontal well (37% OOIP), however, up to 180 minutes (or 0.8 pore volumes injected – **Fig. 6.79**), configuration A performed better than the vertical well system.

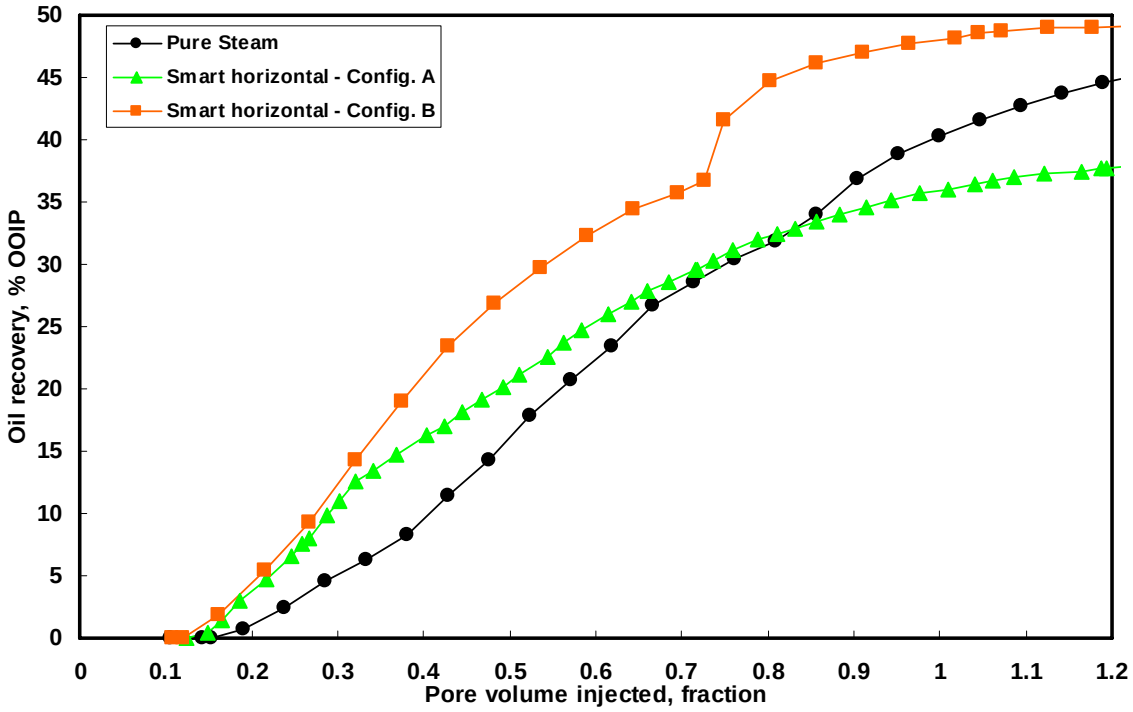

Fig. 6.79- Cumulative oil recovery as a function of pore volume injected for the vertical and smart horizontal well systems (configurations A and B).

The cumulative steam-oil ratio that is presented in **Fig. 6.80** shows that the most efficient utilization of steam is provided by configuration B. The least effective process is the vertical well system, at least until 180 minutes, when the SOR for configuration A increases above that of the vertical well system.

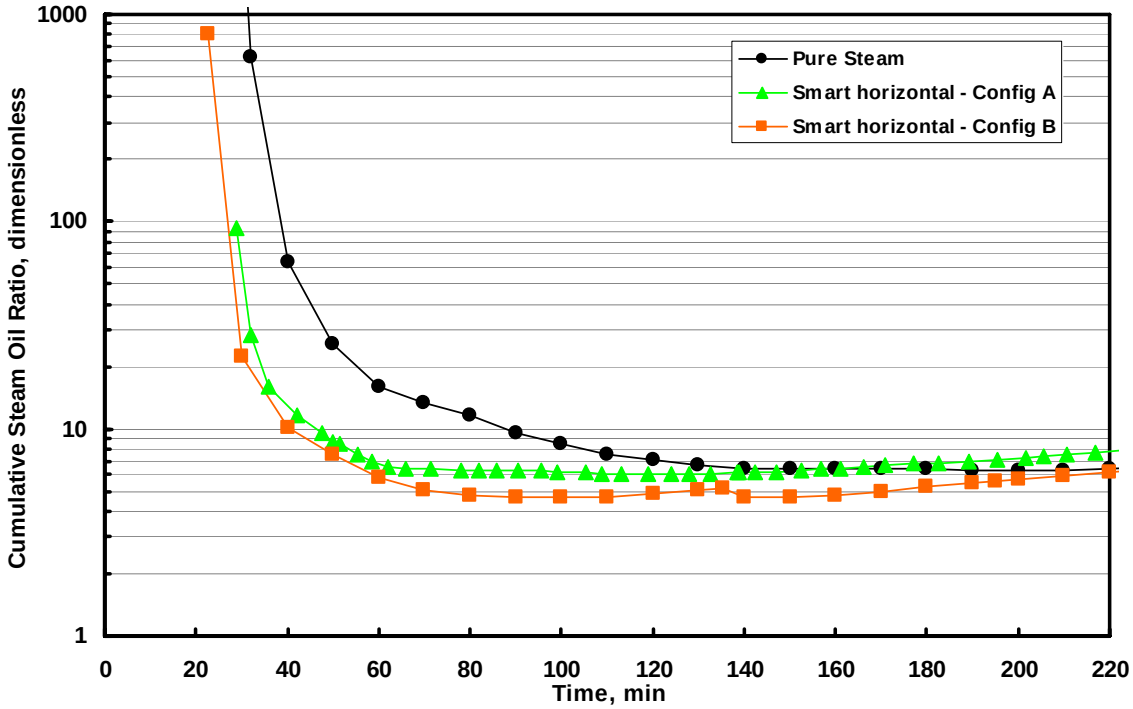

Fig. 6.80- Cumulative steam oil ratio for the vertical and smart horizontal well systems (configurations A and B).

A series of temperature profiles comparing all three runs at different times can be observed in **Figs. 6.81** through **6.86**. Early in the run (15 minutes – **Fig. 6.81**), the condensed steam bank (green color) covers most of the top of the cell in both; the vertical well system run and the configuration B experiment. However, the coverage for configuration A is more limited given the fact that only sections 2 and 3 of the horizontal well are open to flow, therefore, the steam tends to flow only towards that area. This behavior is also repeated at 50 minutes (**Fig. 6.82**), where it can be observed that the top temperature profile shows a cold area at the left of the physical model in configuration A; in contrast, in configuration B, the entire area at the top is already covered by the steam zone. The middle and bottom profiles show higher temperatures in the area around sections 2 and 3 in configuration A, demonstrating that the steam zone has already reached this area. In contrast, the same area in configuration B displays a much lower temperature, which can be explained by the fact that most of the steam is concentrated at the top of the cell.

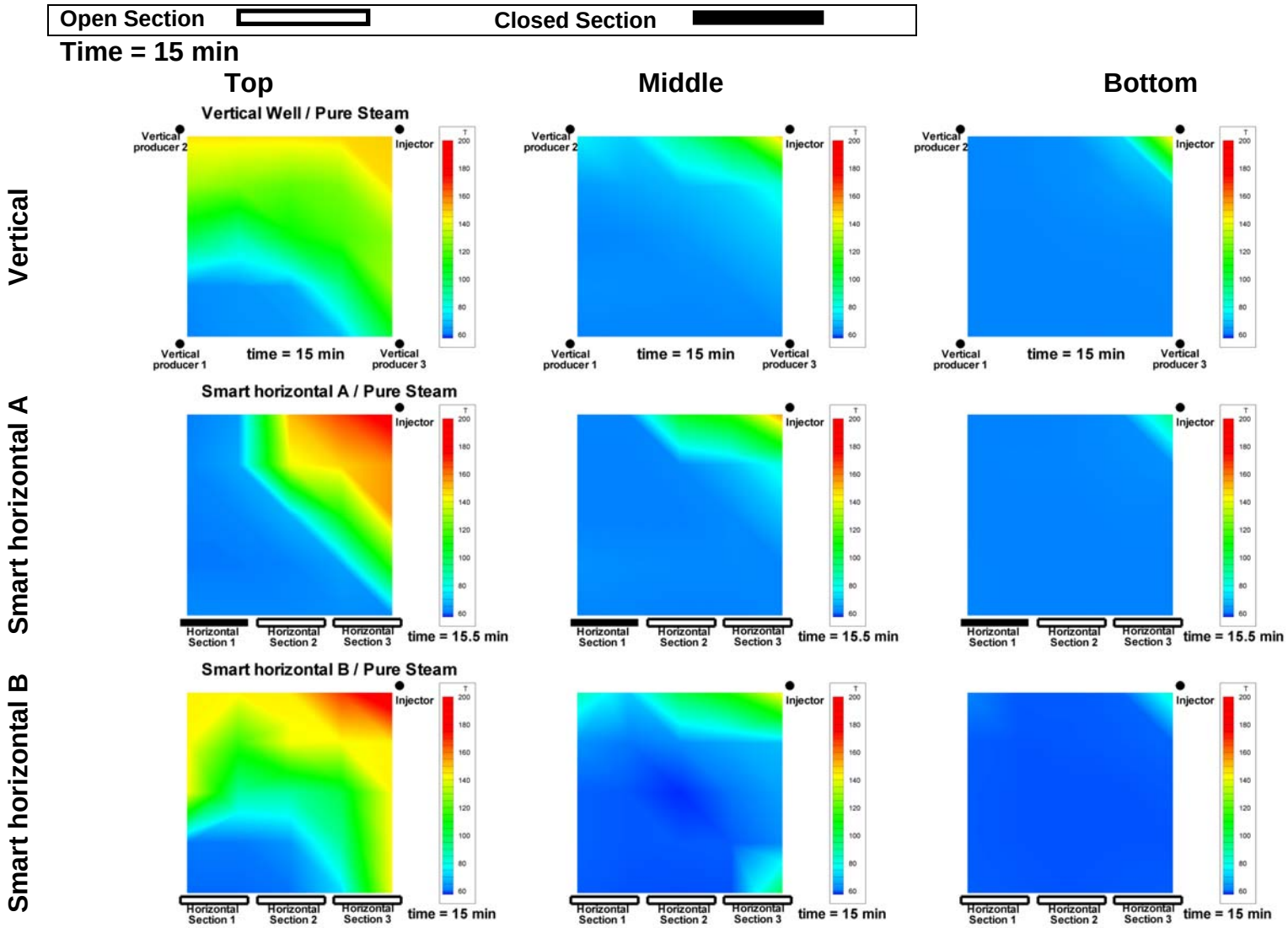

Fig. 6.81- Plan view of the top, middle and bottom temperature profiles in the physical model at 15 minutes. The top row shows the profile for the vertical well system. The middle and bottom rows depict the profiles for the smart horizontal well in configurations A and B respectively.

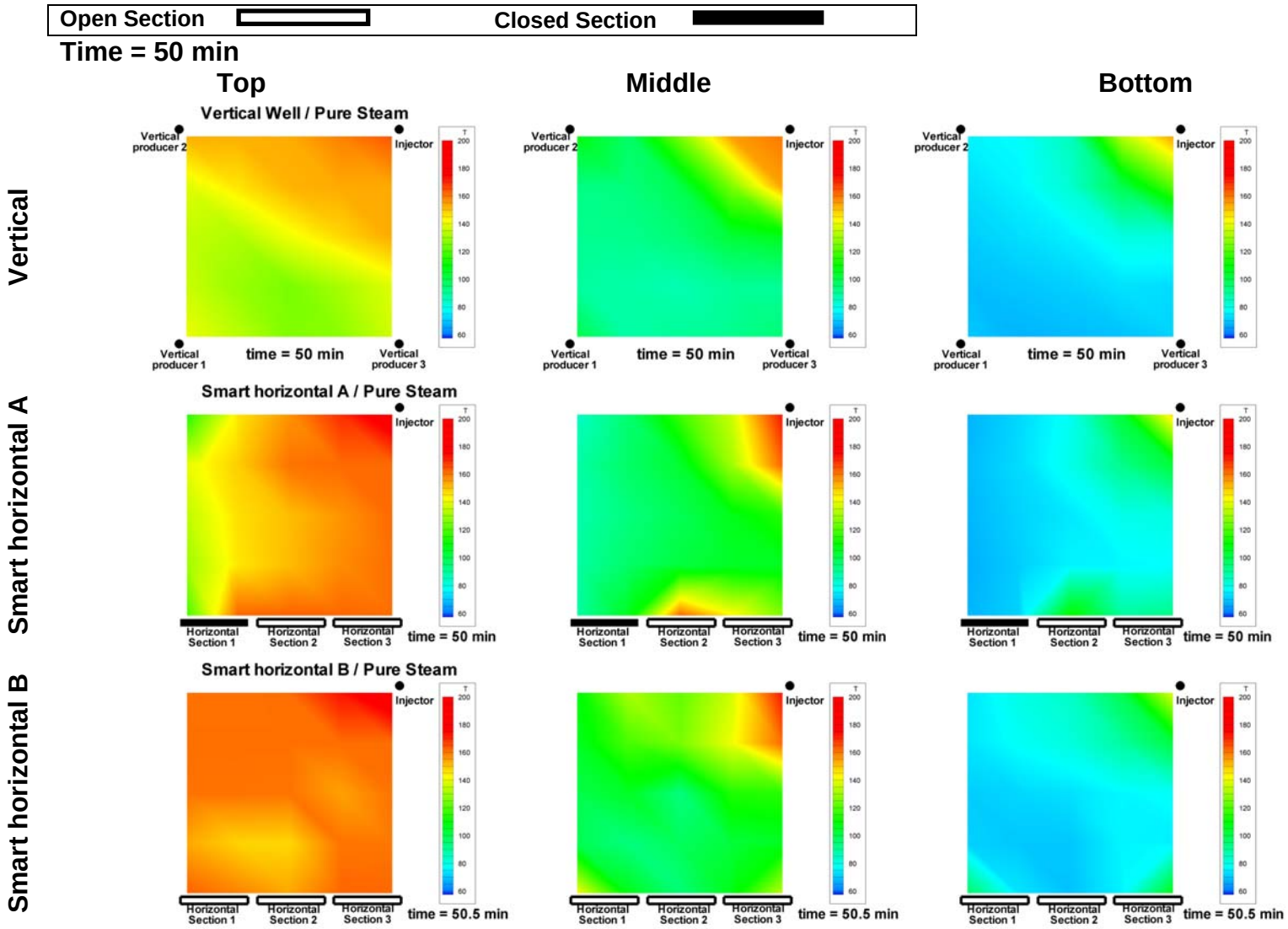

Fig. 6.82- Plan view of the top, middle and bottom temperature profiles in the physical model at 50 minutes. The top row shows the profile for the vertical well system. The middle and bottom rows depict the profiles for the smart horizontal well in configurations A and B respectively.

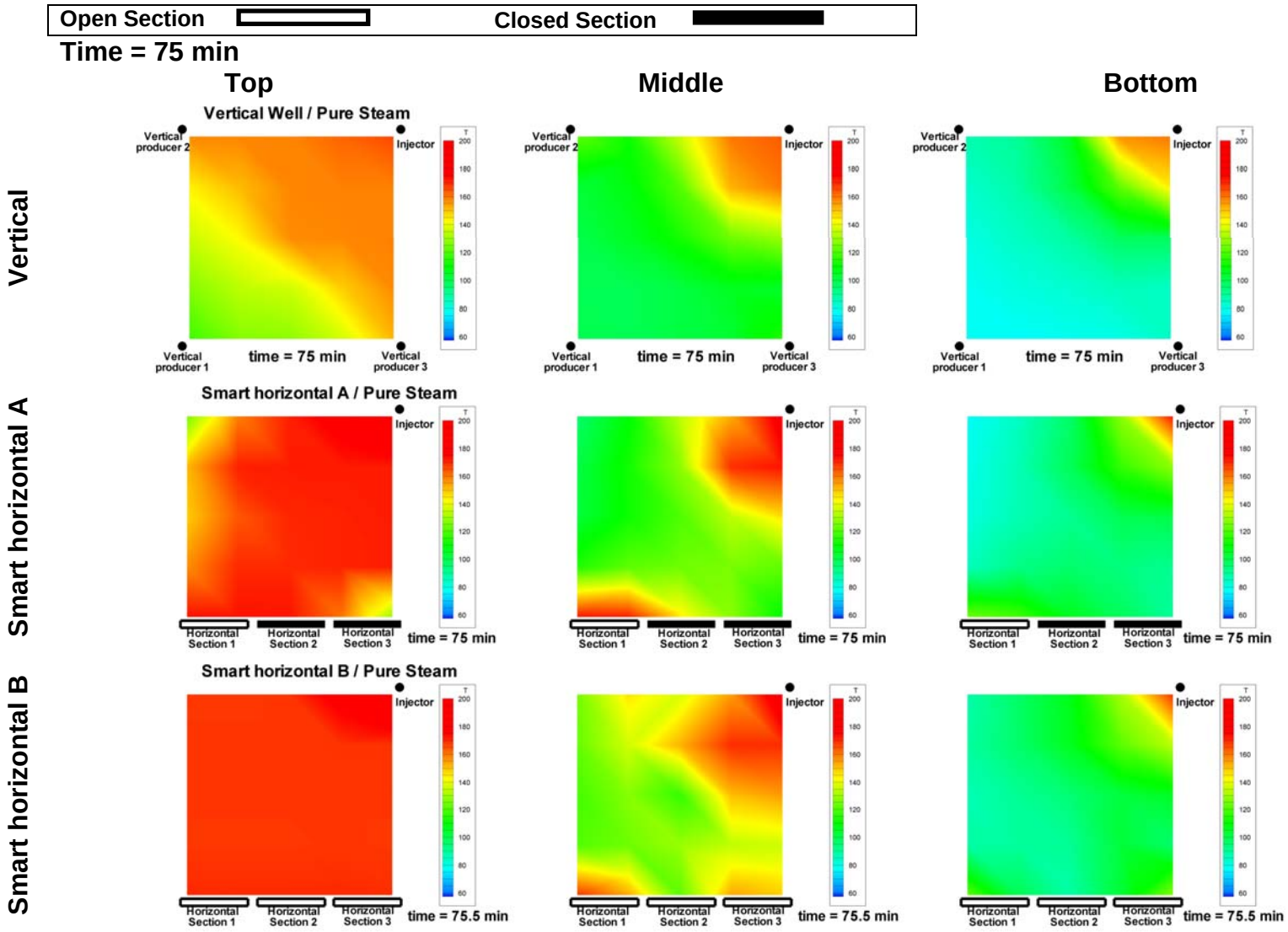

Fig. 6.83- Plan view of the top, middle and bottom temperature profiles in the physical model at 75 minutes. The top row shows the profile for the vertical well system. The middle and bottom rows depict the profiles for the smart horizontal well in configurations A and B respectively.

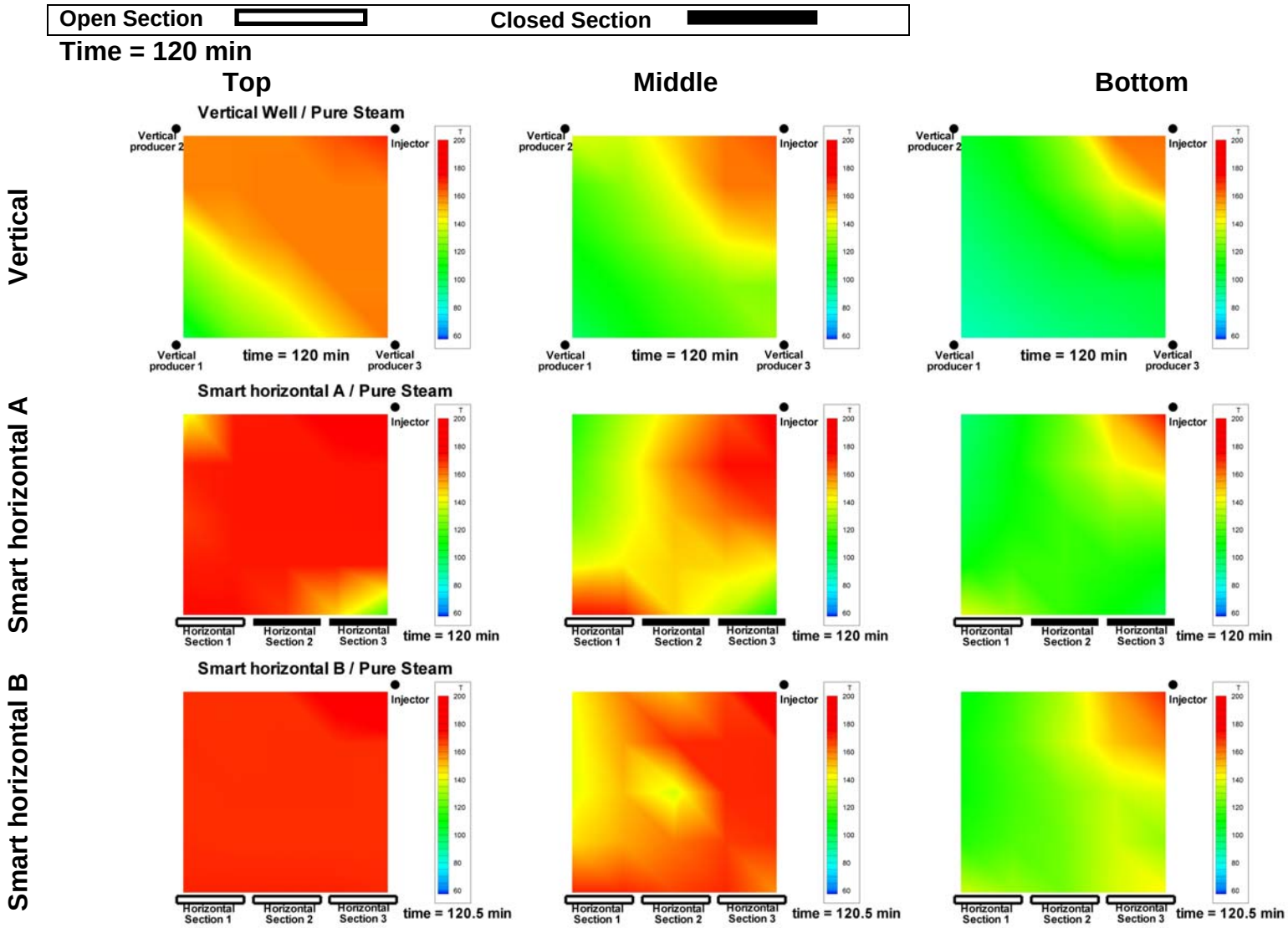

Fig. 6.84- Plan view of the top, middle and bottom temperature profiles in the physical model at 120 minutes. The top row shows the profile for the vertical well system. The middle and bottom rows depict the profiles for the smart horizontal well in configurations A and B respectively.

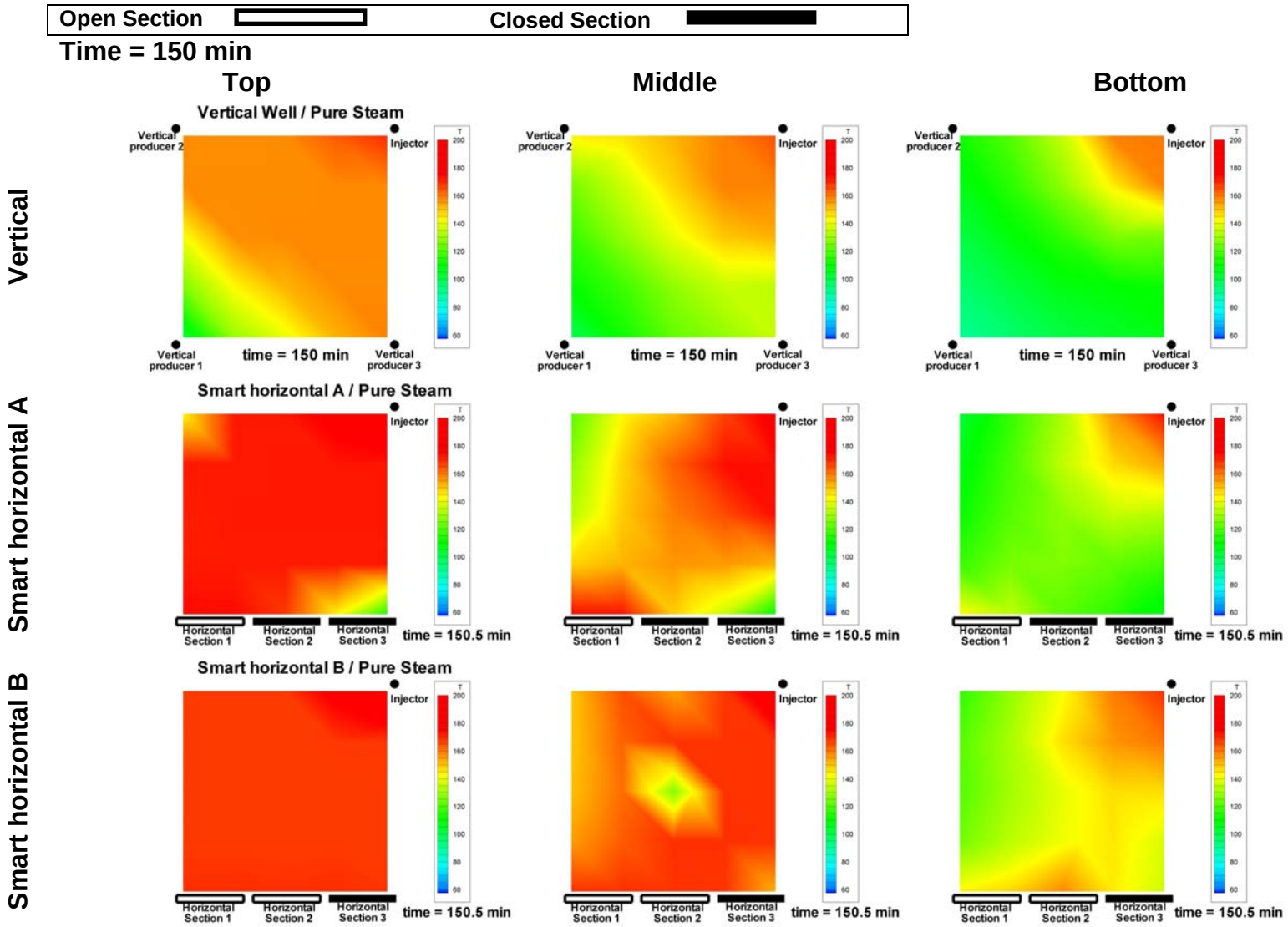

Fig. 6.85- Plan view of the top, middle and bottom temperature profiles in the physical model at 150 minutes. The top row shows the profile for the vertical well system. The middle and bottom rows depict the profiles for the smart horizontal well in configurations A and B respectively.

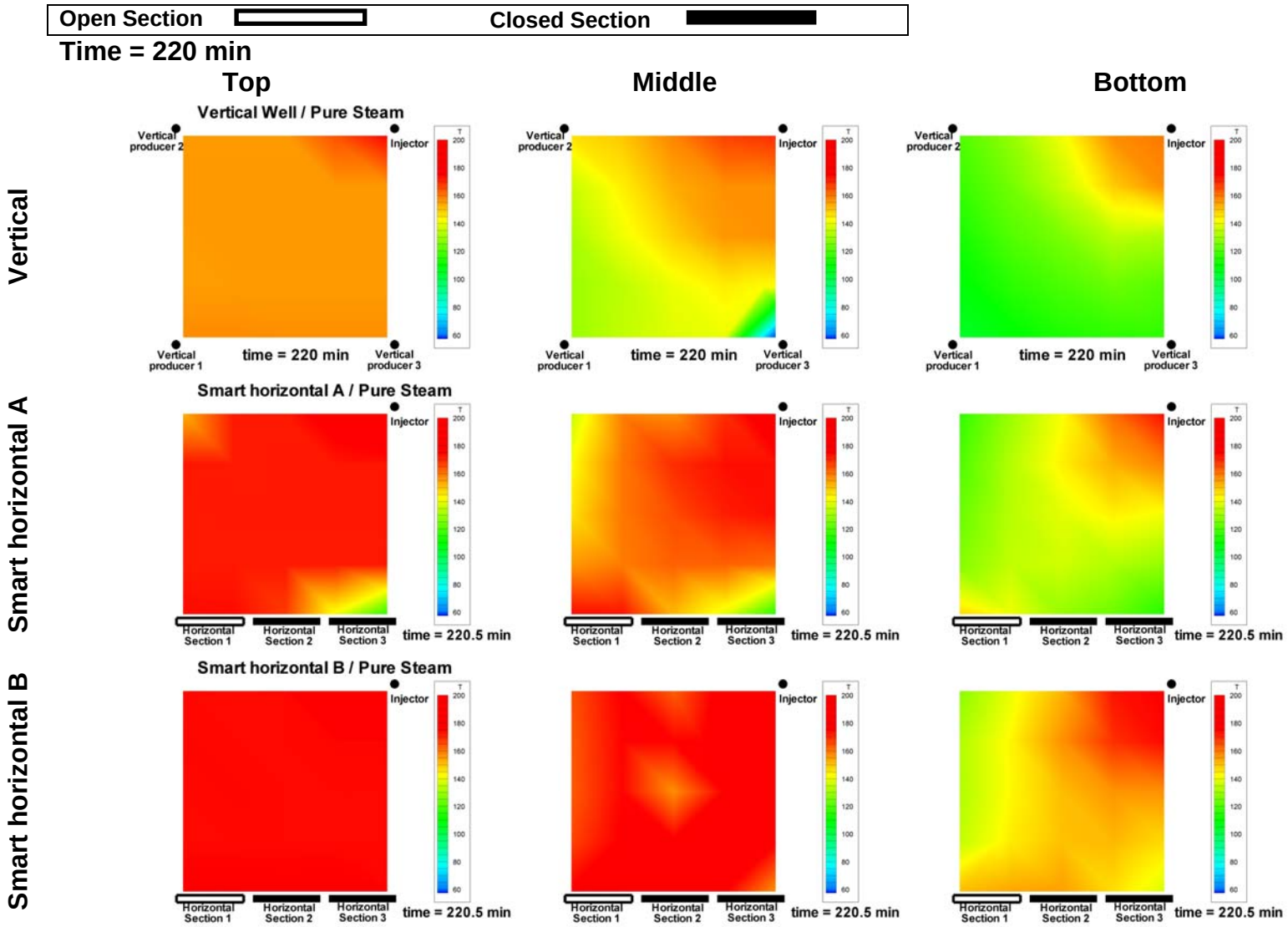

Fig. 6.86- Plan view of the top, middle and bottom temperature profiles in the physical model at 220 minutes. The top row shows the profile for the vertical well system. The middle and bottom rows depict the profiles for the smart horizontal well in configurations A and B respectively.

The profiles for both smart horizontal configurations at 75 minutes (**Fig. 6.83**), show very clearly the steam override phenomenon, which is evidenced by the accumulation of steam at the top of the cell and in the areas surrounding the injector and producers. In the configuration A experiment, the producing intervals of the horizontal well are changed at 50 minutes (shut sections 2 and 3 and open section 1), therefore, the steam front has now moved from the area around sections 2 and 3 to the vicinity of section 1.

A comparison of the temperature profiles for configurations A and B at 120 minutes (**Fig. 6.84**) reveals that the steam zone occupies a bigger volume in configuration B than in configuration A. The middle profile for configuration A shows that a preferential path for the steam to circulate from the injector towards section 1 has been created, leaving cold areas in the cell. In contrast, the same profile in configuration B shows a much more uniform temperature distribution. The same situation can be observed (albeit to a lesser degree) in the middle temperature profiles for 150 minutes (**Fig. 6.83**).

The results obtained show that the implementation of configuration A was more favorable than the vertical well system at the beginning of the run. However, towards the end of the experiment, it is evident that the performance of configuration A is worse than that of the vertical well system. The analysis of the temperature profiles presented earlier indicates that the problem was more likely caused by the premature closing of sections 2 and 3. At 50 minutes, when the closing occurred, the steam zone was barely forming around the vicinity of the producing sections and most of the oil around that area was not produced. Changing to section 1 prematurely left a big section of the cell unswept by the steam; in contrast, in configuration B, those sections were left open for a much longer period of time ensuring a higher recovery.

Based in the results obtained in this research, it can be concluded that the use of the smart horizontal well will not solve completely the problem of steam override, however, it will mitigate its effects and improve the sweep efficiency by increasing the amount of oil contacted by the steam and consequently enhance oil recovery.

6.8 Comparative analysis on the use of steam-propane injection in the vertical injector–smart horizontal well system

Run 5 (section 6.4) was carried out to test the feasibility of combining the implementation of the vertical injector-smart horizontal well system with steam-propane injection. Run 3 (pure steam injection in configuration A) will be used as a base case.

Fig. 6.87 shows a plot comparing the oil production rate for the steam propane run and the pure steam experiment. The oil production rate for the steam propane run is always lower than that of the pure steam run, except for the early moments of the experiment.

Figs. 6.88 and **6.89** show the cumulative oil recovery plotted as a function of time and pore volume injected respectively. Oil production starts at 15.5 minutes for the steam propane run, while the pure steam run shows a production starting time of 24 minutes, which translates into an acceleration of 19% in time. At 200 minutes, oil recovery for the pure steam run is 36% OOIP compared to 30% OOIP obtained in the steam-propane run.

The cumulative steam oil ratio is presented in **Fig. 6.90**. In the early stages of the experiment, the SOR for the steam-propane run is lower than that of the pure steam run, demonstrating a more efficient process that uses less steam to produce the same amount of oil. After 80 minutes, the trend is reversed and the SOR for the pure steam run becomes smaller.

An analysis of the temperature profiles presented in **Figs. 6.91** through **6.94** reveals that the addition of propane accelerates the advance of the steam front in the experiment. This translates into a bigger steam zone in the steam-propane experiment at any given time during the run when compared to the size of the steam zone for the pure steam run.

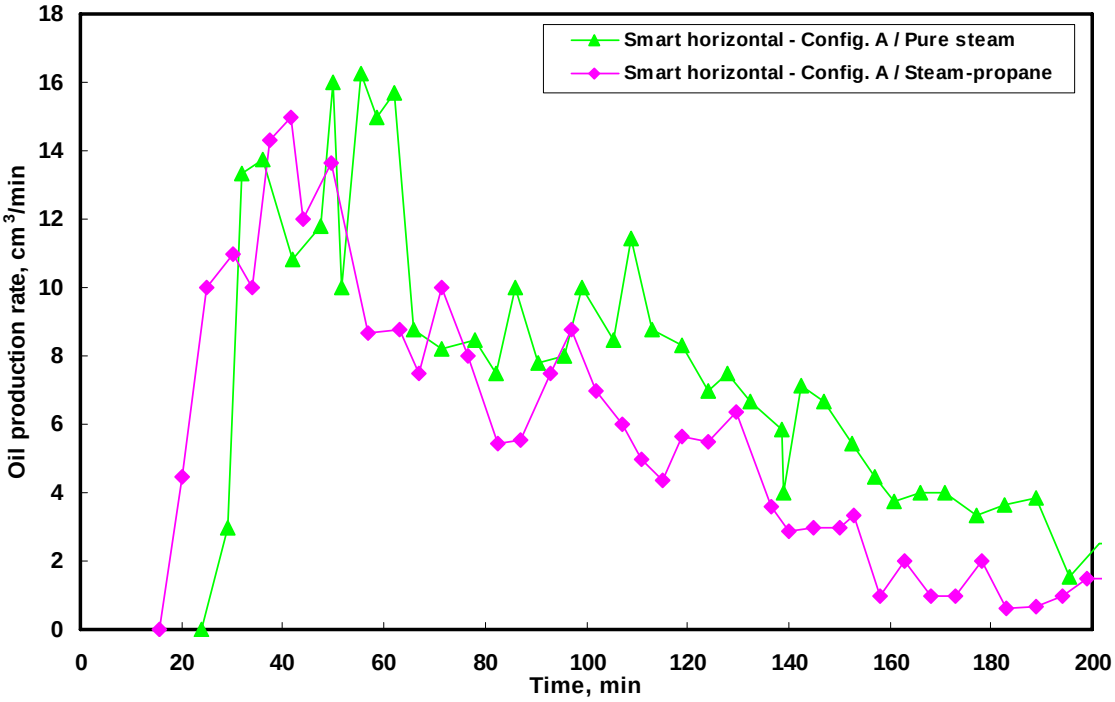

Fig. 6.87- Oil production rates for the smart horizontal well system (configuration A) under steam and steam-propane injection.

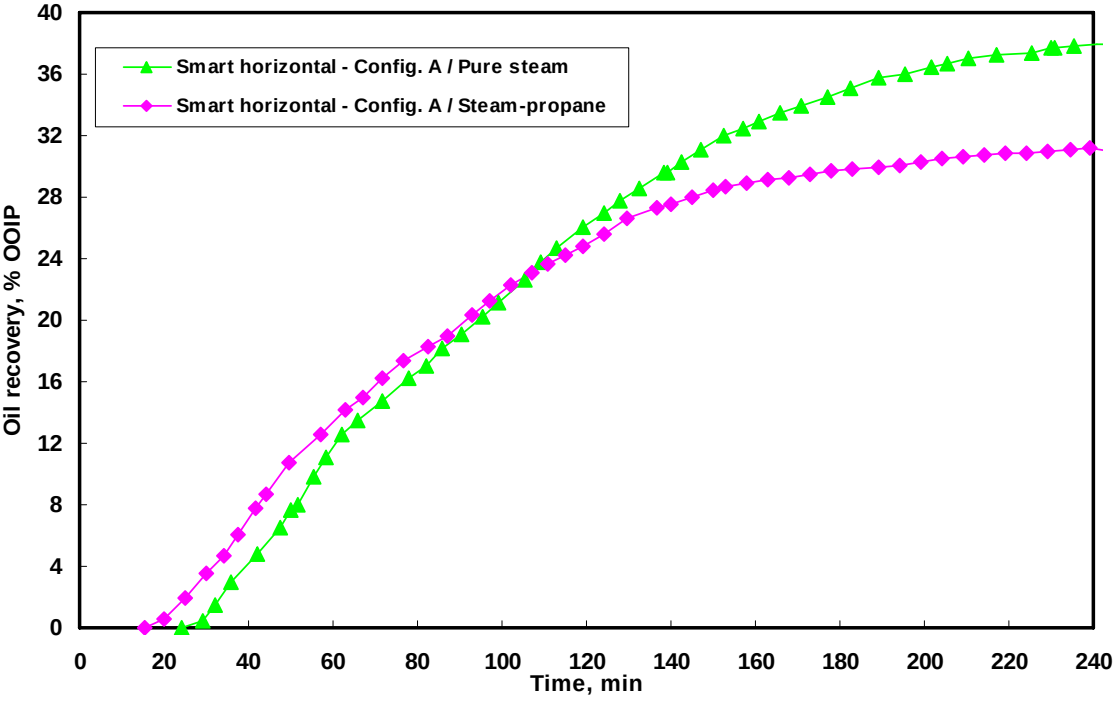

Fig. 6.88- Cumulative oil recovery for the smart horizontal well system (configuration A) under steam and steam-propane injection.

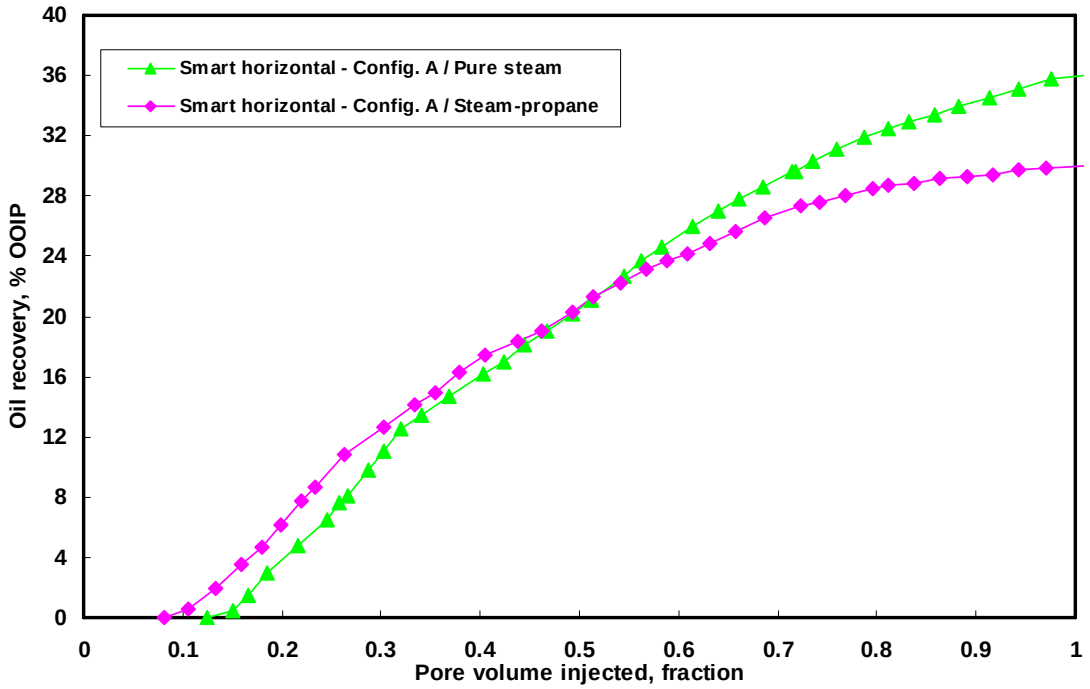

Fig. 6.89- Cumulative oil recovery as a function of pore volume injected for the smart horizontal well system (configuration A) under steam and steam-propane injection.

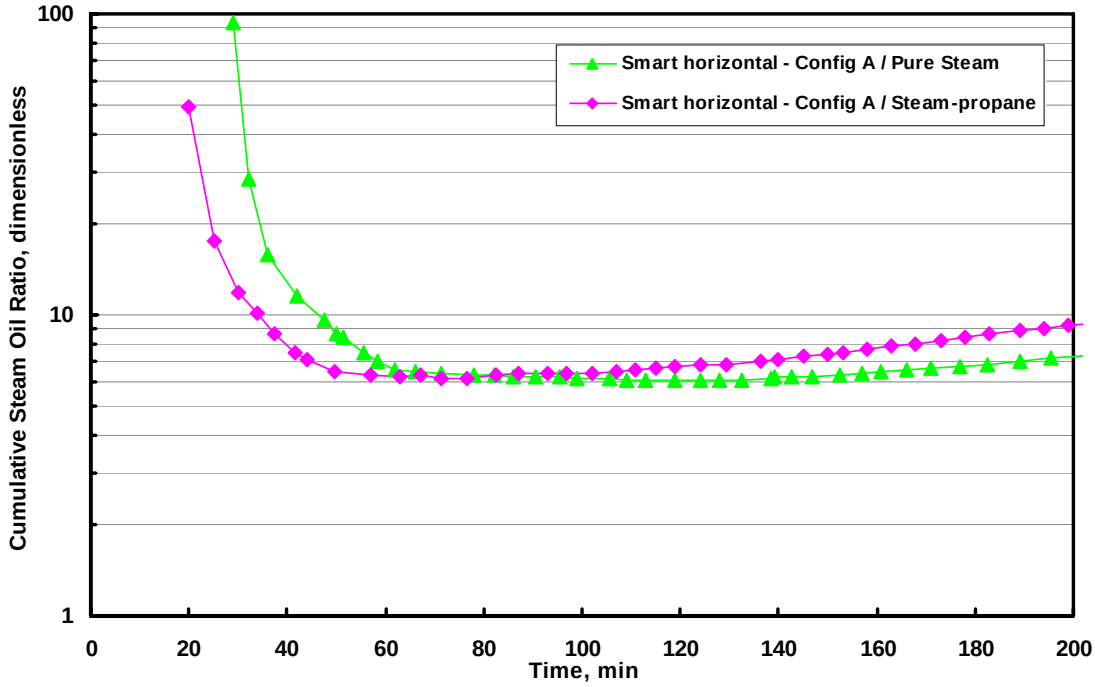

Fig. 6.90- Cumulative steam oil ratio for the smart horizontal well system (configuration A) under steam and steam-propane injection.

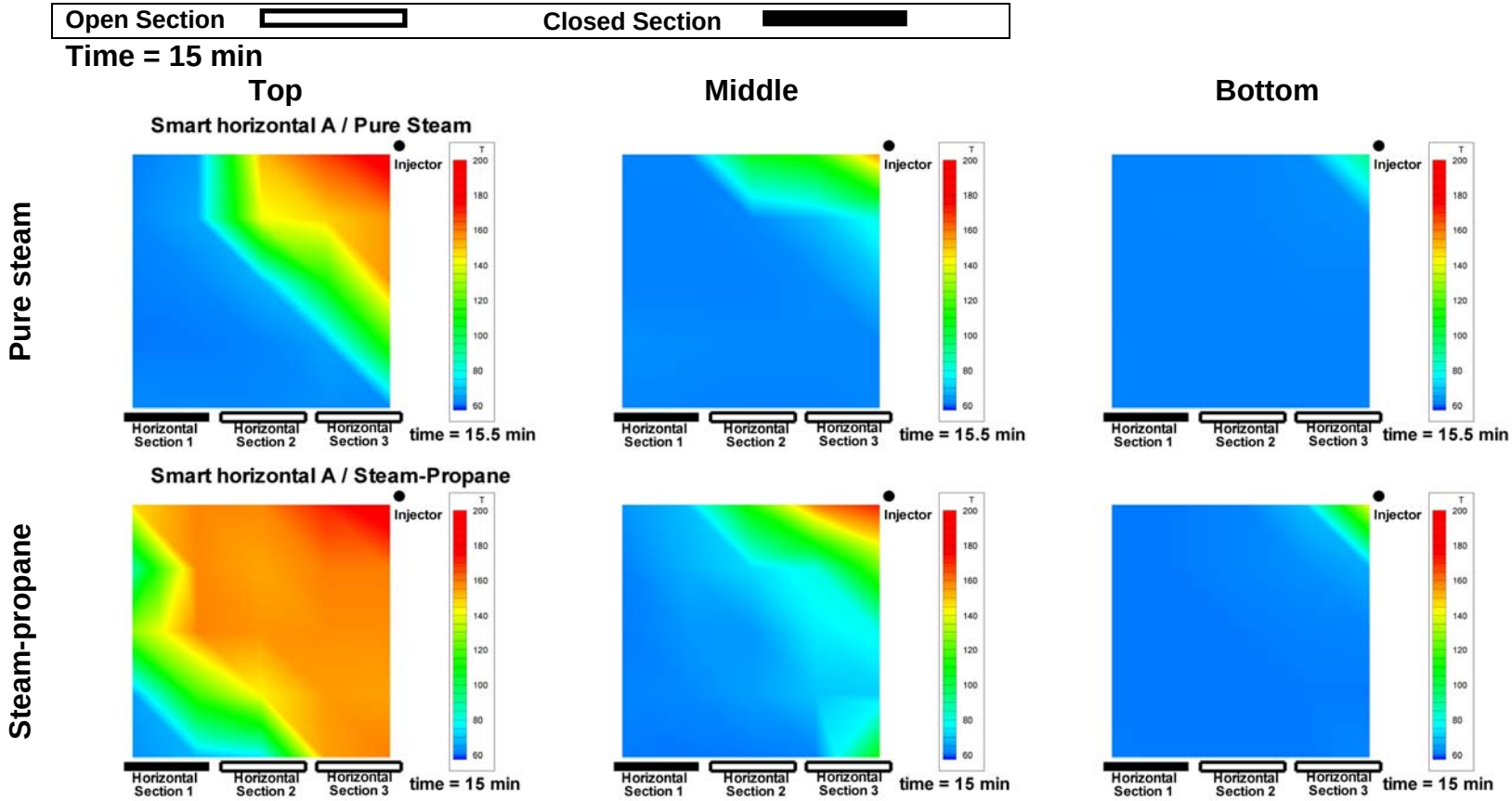

Fig. 6.91- Plan view of the top, middle and bottom temperature profiles in the physical model at 15 minutes for configuration A of the smart horizontal well system. The top and bottom rows correspond to pure steam and steam-propane injection respectively.

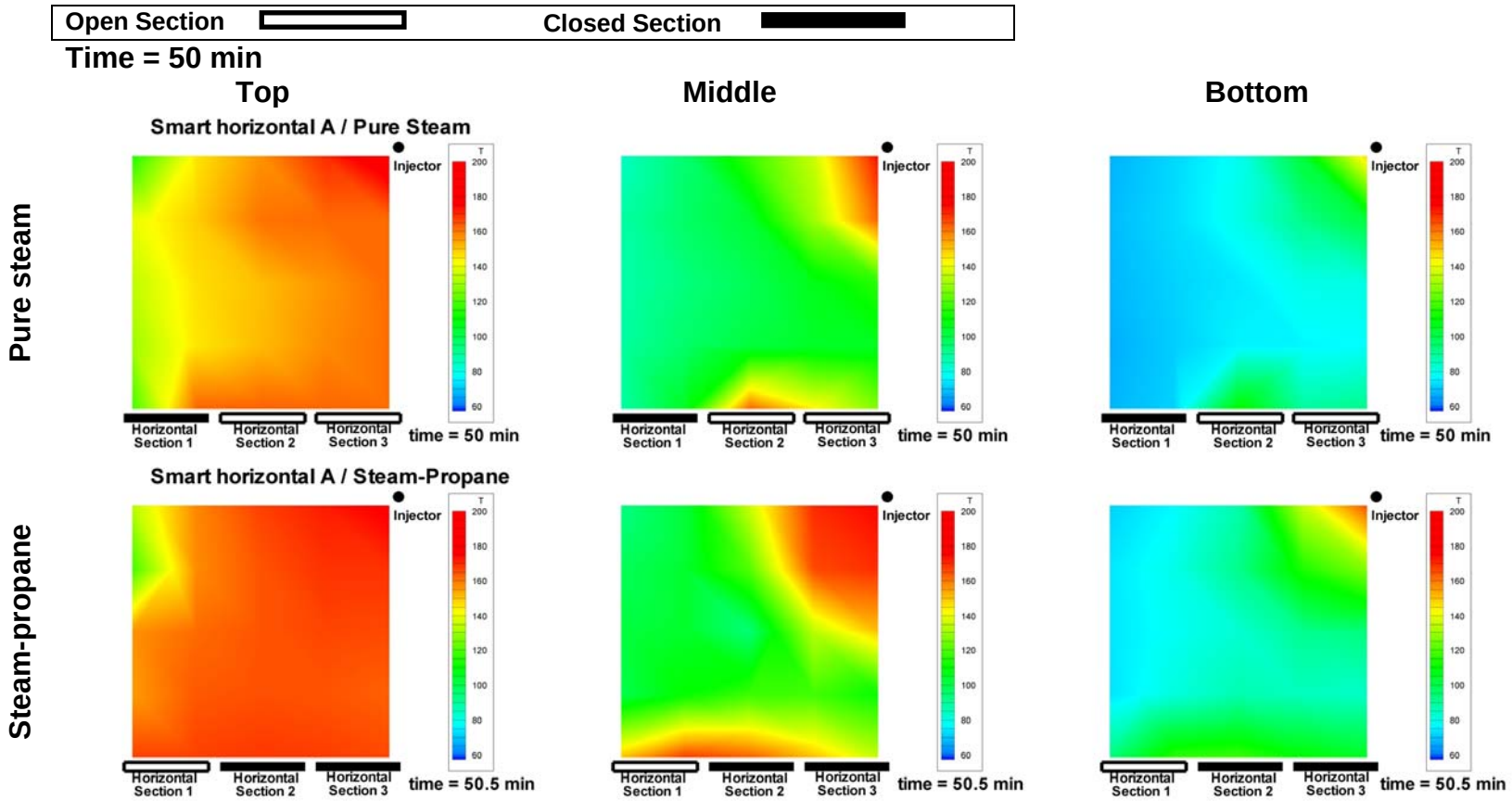

Fig. 6.92- Plan view of the top, middle and bottom temperature profiles in the physical model at 50 minutes for configuration A of the smart horizontal well system. The top and bottom rows correspond to pure steam and steam-propane injection respectively.

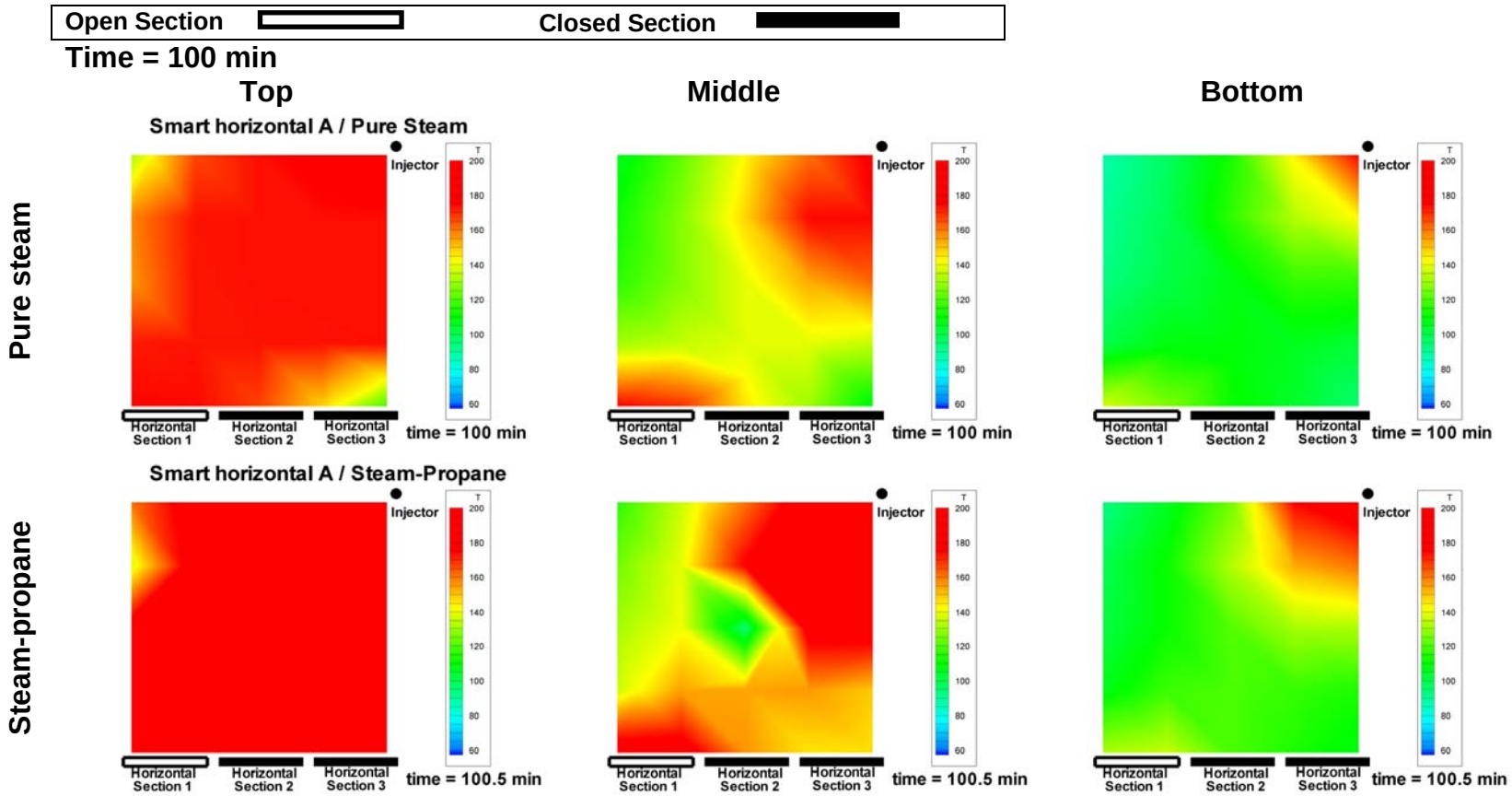

Fig. 6.93- Plan view of the top, middle and bottom temperature profiles in the physical model at 100 minutes for configuration A of the smart horizontal well system. The top and bottom rows correspond to pure steam and steam-propane injection respectively.

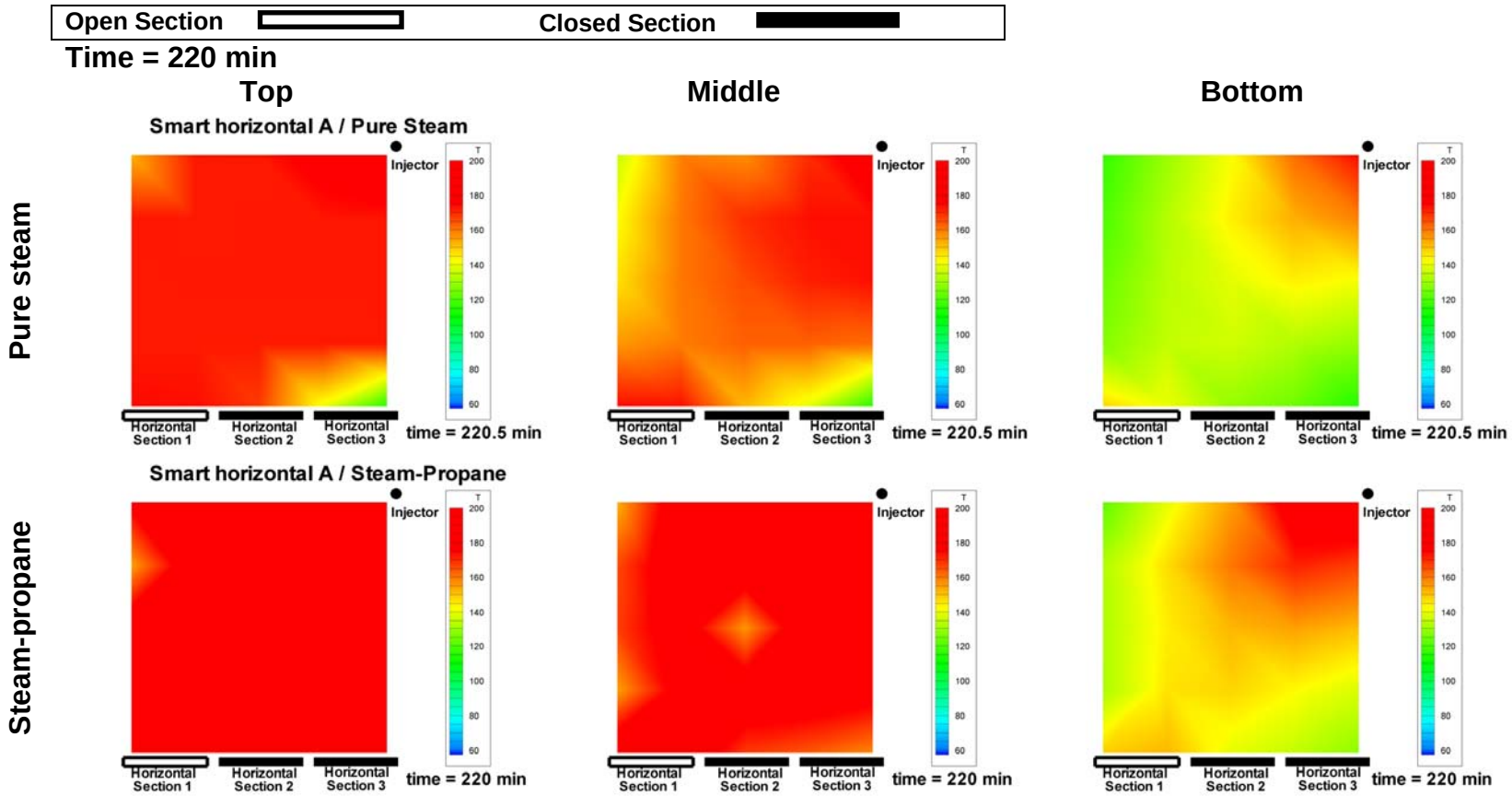

Fig. 6.94- Plan view of the top, middle and bottom temperature profiles in the physical model at 220 minutes for configuration A of the smart horizontal well system. The top and bottom rows correspond to pure steam and steam-propane injection respectively.

The use of propane in run 5 causes oil production acceleration, which confirms the results of previous research,[13-21] however, ultimate oil recovery is reduced 6% OOIP when propane is used. This finding contradicts the results obtained in this research with the vertical well system (see section 6.6), where the addition of propane increased ultimate oil recovery.

Sandoval's[10] simulation study indicated that oil recovery for the smart horizontal well is dependent on the steam injection rate. As can be seen in **Fig. 6.95**, steam injection rates greater than 150 bbl/day (CWE) yield lower recovery with steam-propane injection. Similarly, it appears that the steam injection rate used in the experiments, 48 cm^3/min, results in a lower oil recovery with steam-propane injection. A possible explanation for this phenomenon is that at high injection rates, the propane does not have sufficient time to contact the oil. Instead, it bypasses the oil, resulting in lower recovery.

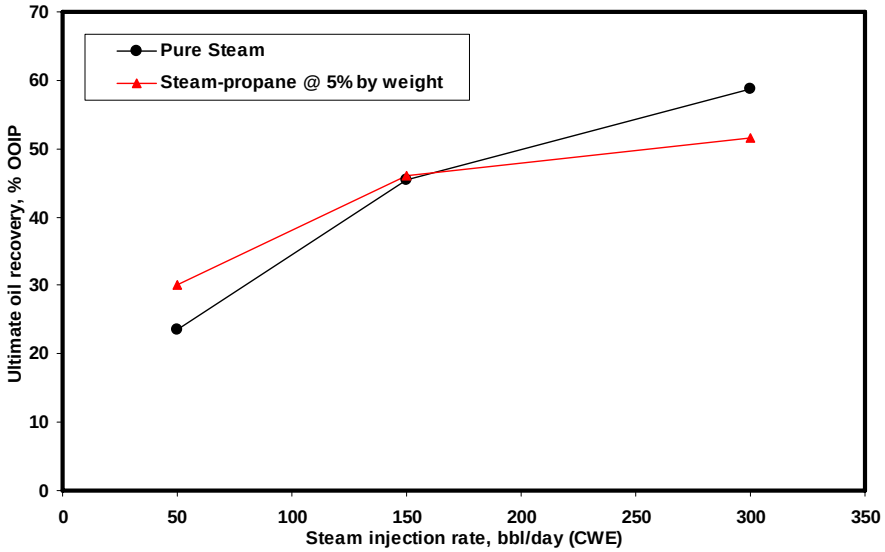

Fig. 6.95- Oil recovery as a function of steam injection rate for the smart horizontal well system – Results from numerical simulation. (after Sandoval[10]).

CHAPTER VII

SUMMARY, CONCLUSIONS AND RECOMMENDATIONS

7.1 Summary

A 16'' x 16'' x 5.6'' scaled three-dimensional physical model was constructed to represent a quarter of a 9-spot pattern in the San Ardo field. The main objectives of this study were to evaluate the effect on oil rate and recovery of steam-propane injection and a novel production configuration involving a smart horizontal well.

A propane:steam mass ratio of 4:100 was used in the study, while the model outlet pressure was kept constant at 50 psig. Superheated steam was injected at 48 cm^3/min at 190 – 210ºC. Produced oil and water were collected, treated, separated and their volumes measured.

Based on these experimental runs, the following conclusions may be drawn:

7.2 Conclusions

1. The use of propane as a steam additive was found to accelerate the start of oil production. For the vertical well system, oil production begins at 32 minutes (3.7 years in field scale); in contrast, production starts at 15 minutes for steam-propane injection. Acceleration was also observed when propane was added to the smart horizontal experiments. In this case, the start of oil production is 24 minutes for pure steam injection and is reduced to 15.5 minutes when propane is used.

2. In the vertical well system, the use of propane increases oil recovery from 34% OOIP to 41.4% OOIP. This finding contrasts with the results obtained in previous

one-dimensional steam-propane injection experiments conducted in Texas A&M, where the addition of propane caused production acceleration only but oil recovery remained the same.

3. The advance of the steam front is accelerated with the injection of propane. Additionally, at any given time during the experiment, the steam zone occupies a larger volume inside the physical model when steam-propane is used.

4. The primary mechanism by which propane causes acceleration in oil production and increase in ultimate recovery appears to be caused by the fact that some of the propane dissolves in the hot oil generating a further reduction in its viscosity. Additional mechanisms, such as improved oil distillation by the reduction of the boiling point of some hydrocarbon fractions could also be taking place during the steam-propane experiments.

5. The implementation of the vertical injector-smart horizontal well system increases the ultimate oil recovery when compared to that obtained with the conventional 9-spot vertical well system. Configuration B of the smart horizontal well yielded an ultimate oil recovery of 49% OOIP; in contrast the conventional vertical well system produced a total of 42% OOIP.

6. The performance of the smart horizontal well system is heavily influenced by its configuration (number of sections and closing times). The performance of configuration A of the smart horizontal well was initially better than that of the conventional vertical system; however, due to the premature closing of one section, the performance decreased drastically resulting in a lower ultimate recovery when compared to that of the vertical well system.

7. The steam override phenomenon is not completely eradicated with the use of the vertical injector-smart horizontal well system; however its effects are mitigated by an improved steam sweep efficiency. The volume occupied by the steam zone is larger when the smart horizontal system is used; thus increasing the amount of oil contacted by the steam, which in turn enhances oil recovery.

8. If the technology is developed to effectively and reliably close and open sections in a horizontal well, the substitution of vertical wells in injection patterns by smart horizontal wells will bring improved oil recovery and reduced capital expenses, given that 4 smart horizontals will be used instead of the 8 vertical producers employed in a 9-spot pattern.

9. A comparison of the results obtained in previous one-dimensional experiments and the findings of this research demonstrate that a thorough evaluation of a complex process such as steam injection plus additives requires the use of a three-dimensional scaled model. Given its simplicity and ease of operation, 1D experiments are invaluable at providing fast, preliminary results on the merits on certain processes. However, if a more complete representation of the mechanisms operating in displacement processes is required, then a 3D model is recommended.

7.3 Recommendations

1. Test the steam propane injection process at lower propane concentrations. Previous experiments indicated that the favorable effects of propane were still experienced with propane:steam mass ratios as low as 1.25:100. This will improve the economics of the process.

2. Investigate the influence of pressure in oil recovery with the steam-propane process. Propane solubility in the oil should increase with pressure; therefore, ultimate recovery will vary according to the pressure conditions. This will also help understand if propane is acting as a solvent in the process.

3. Study different configurations of the smart horizontal well, varying closing times and the number of sections open at any given time during the experiment. Also, test the possibility of injecting the steam along the entire length of the vertical

injector and not just on the top half. This will probably improve sweep efficiency by forcing some of the steam towards the lower sections of the cell.

4. In order to avoid heterogeneities caused by non-uniform tamping of the sandmix, attempt to change the methodology for preparing the physical model. The methodology initially considered for this research involved filling the cell with sand and imbibe water into the porous medium while evacuating air with a vacuum pump and a water trap. Once 100% water saturation is reached, inject the oil displacing several pore volumes, to ensure connate water saturation. This technique was successfully applied to saturate the model in this research, however it had to be discarded because the initial steam injection pressure was too high and the overburden pressure could not be controlled. This can be avoided by initially injecting steam at lower rates and then increase the rate later (this is even more representative of the field conditions).

5. Change the design of the physical model. Instead of using ¾" thick Teflon sheets for the cell walls, build instead a new cell using aluminum and line its interior with ¼" or ½" Teflon. This will prevent leaks and will also allow for the application of higher overburden pressures that will help to better handle the high injection pressures observed when steam is initially injected. The Teflon lining will still serve the purpose of minimizing heat losses to the sides of the model.

NOMENCLATURE

Latin

A_{iw}	Area open to flow in a producer or injector well, [L^2]
a	Geometric scaling factor, dimensionless
C	Heat capacity, [$L^2/(M^2t)$]
d_w	Diameter of a producer or injector well, [L]
h	Thickness, [L]
K	Absolute permeability, [L^2]
L	Length, [L]
m	Mass, [M]
Q	Cumulative heat losses, [ML^2/t^2]
t	Time, [t]
V	Volume, [L^3]
w	Width, [L]
W	Injection rate, [L^3/t]

Greek

α	Thermal diffusivity, [L^2/t]
κ	Thermal conductivity, [$ML/(t^3\ T)$]
Δp	Pressure differential, [$M/(t^2\ L)$]
ΔT	Temperature differential, [T]
μ	Viscosity, [M/(L t)]
ρ	Density, [M/L^3]

Subscript

c	Pertaining to surrounding formations (caprock)
$cell$	Pertaining to the cell used in the physical model
f	Finite case

M	Model
o	Oil
P	Prototype
pore	Pertaining to pore volume
sand	Pertaining to the sand in the physical model
st	Steam
w	Water
∞	Infinite case

REFERENCES

1. Alboudwarej, H. *et al*.: "Higlighting Heavy Oil," *Oilfield Review* (2006) **18**, No. 2, 34.

2. Christianson, B. A. and Berger, E. L.: "San Ardo Field Production Testing System Upgrade," paper SPE 21533 presented at the 1991 Int. Thermal Ops. Symposium, Bakersfield, California, 7-8 February.

3. Lolley, C. S. and Richardson, W. C.: "Compositional Input for Thermal Simulation of Heavy Oils with Application to the San Ardo Field," paper SPE 37538 presented at 1997 SPE International. Thermal Operations and Heavy Oil Symposium, Bakersfield, California, 10-12 February.

4. Piper, E. M., Riddell, A. W., and Trent, R. H.: "An Evaluation of Heavy Oil Mining," final report, Contract No. DOE/PC/30259-1, U.S. DOE, Washington, DC (March 1983).

5. Hong, K. C., *Steamflood Reservoir Management: Thermal Enhanced Oil Recovery*, PennWell Books, Tulsa, Oklahoma (1994).

6. Chiang, J.C. *et al*.: "Foam as a Mobility Control Agent in Steam Injection Processes," paper SPE 8912 presented at the 1980 SPE California Regional Meeting, Los Angeles, California, 9-11 April.

7. Sander, P.R.: "Steam-Foam Diversion Process Developed to Overcome Steam Override in Athabasca," paper SPE 22630 presented at the 1991 SPE Annual Technical Conference and Exhibition, Dallas, Texas, 6-9 October.

8. Turta, A.T.: "Field Foam Applications in Enhanced Oil Recovery Projects: Screening and Design Aspects," paper SPE 48895 presented at the 1998 SPE International Oil and Gas Conference and Exhibition, Beijing, China, 2-6 November.

9. Mamora, D.D., "2004 Ramey Laboratory Research Program," (Report), Texas A&M University, College Station (November 2003).

10. Sandoval, J.E.: "A Simulation Study of Steam and Steam-Propane Injection Using a Novel Smart Horizontal Producer to Enhance Oil Production," MS Thesis, Texas A&M University, College Station (2004).

11. Goite, J.G. and Mamora, D.D.: "Experimental Study of Morichal Heavy Oil Recovery Using Combined Steam and Propane Injection," paper SPE 69566

presented at the 2001 SPE Latin American and Caribbean Petroleum Engineering Conference, Buenos Aires, Argentina, 25-28 March.

12. Ferguson, M. A., Mamora, D. D., and Goite, J. G.: "Steam-Propane Injection for Production Enhancement of Heavy Morichal Oil," paper SPE 69689 presented at the 2001 SPE International Thermal Operations and Heavy Oil Symposium, Margarita Island, Venezuela, 12-14 March.

13. Tinss, J.C.: "Experimental Studies of Steam-Propane Injection to Enhance Recovery of an Intermediate Crude Oil," MS Thesis, Texas A&M University, College Station (2001).

14. Rivero, J.A.: "Experimental Study of Enhancement of Injectivity and in situ Oil Upgrading by Steam-Propane Injection for the Hamaca Heavy Oil Field," MS Thesis, Texas A&M University, College Station (2002).

15. Rivero, J.A. and Mamora, D.D.: "Production Acceleration and Injectivity Enhancement Using Steam-Propane Injection for Hamaca Extra-Heavy Oil," paper SPE 75129 presented at the 2002 SPE/DOE Symposium on Improved Oil Recovery, Tulsa, Oklahoma, 13-17 April.

16. Venturini, G.J.: "Simulation Studies of Steam-Propane Injection for the Hamaca Heavy Oil Field," MS Thesis, Texas A&M University, College Station (2002).

17. Mamora, D.D., Rivero, J.A., Hendroyono, A., and Venturini, G.J.: "Experimental and Simulation Studies of Steam-Propane Injection for the Hamaca and Duri Fields," paper SPE 84201 presented at the 2003 SPE Annual Technical Conference and Exhibition, Denver, Colorado, 5-8 October.

18. Plazas, J.: "Experimental Study of Oil Yields and Properties of Light and Medium Venezuelan Crude Oils Under Steam and Steam-Propane Distillation," MS Thesis, Texas A&M University, College Station (2002).

19. Ramirez, M.: "Experimental and Analytical Studies of Hydrocarbon Yields Under Dry-, Steam-, and Steam with Propane-Distillation," PhD Dissertation, Texas A&M University, College Station (2004).

20. Nesse, T.: "Experimental Comparison of Hot Water/Propane Injection to Steam/Propane Injection for Recovery of Heavy Oil," MS Thesis, Texas A&M University, College Station (2004).

21. Simangunsong, R.: "Experimental and Analytical Modeling Studies of Steam Injection with Hydrocarbon Additives to Enhance Recovery of San Ardo Heavy Oil," MS Thesis, Texas A&M University, College Station (2005).

22. Redford, D.A.: "The Use of Solvents and Gasses with Steam in the Recovery of Bitumen from Oil Sands," *J. Can. Pet. Tech.* (1982) **21**, No. 1, 45.

23. Harding, T.G., Farouq Ali, S.M. and Flock, D.L.: "Steam Performance in the Presence of Carbon Dioxide and Nitrogen," *J. Can. Pet. Tech.* (1983) **22**, No. 6, 30.

24. Stone, T. and Malcolm, J.D.: "Simulation of a Large Steam-CO_2 Coinjection Experiment," *J. Can. Pet. Tech.* (1985) **24**, No. 7, 51.

25. Stone, T. and Ivory, J.: "An Examination of Steam-CO_2 Processes," *J. Can. Pet. Tech.* (1987) **26**, No. 3, 54.

26. Nasr, T.N., Prowse, D.R. and Frauenfeld. T.W.J.: "The Use of Flue Gas with Steam in Bitumen Recovery from Oil Sands," *J. Can. Pet. Tech.* (1987) **26**, No. 3, 62.

27. Fraunfeld, T.W.J., Ridley, R.K. and Nguyen, D.M.: "Effect of an Initial Gas Content on Thermal EOR as Applied to Oil Sands," *J. Can. Pet. Tech.* (1988) **27**, No. 2, 333.

28. Metwally, M.: "Effect of Gaseous Additives on Steam Processes for Lindbergh Field, Alberta", *J. Can. Pet. Tech.* (1990) **29**, No. 6, 26.

29. Gumrah, F. and Okandan, E.: "Steam-CO_2 Flooding: An Experimental Study," *In Situ* (1992) **16**, No.2, 89.

30. Bagci, S. and Gumrah, F.: "Steam-Gas Drive Laboratory Tests for Heavy-Oil Recovery," *In Situ* (1998) **22**, No.3, 263.

31. Butler, R.M. and Mokrys, I.J.: "A New Process (VAPEX) for Recovering Heavy Oils Using Hot Water and Hydrocarbon Vapour," *J. Can. Pet. Tech.* (1991) **30**, No. 1, 97.

32. Butler, R.M. and Mokrys, I.J.: "In-Situ Upgrading of Heavy Oils and Bitumen by Propane Deasphalting: The Vapex Process," paper SPE 25452 presented at the 1993 Production and Operations Symposium, Oklahoma City, Oklahoma, 21-23 March.

33. Butler, R.M. and Mokrys, I.J.: "Recovery of Heavy Oils Using Vapourized Hydrocarbon Solvents: Further Development of the Vapex Process," *J. Can. Pet. Tech.* (1993) **32**, No. 6, 56.

34. Butler, R.M. and Mokrys, I.J.: "Closed Loop Extraction Method for the Recovery of Heavy Oils and Bitumens Underlain by Aquifers: The Vapex Process," *J. Can. Pet. Tech.* (1993) **32**, No. 4, 56.

35. Deng, X: "Recovery Performance and Economics of Steam/Propane Hybrid Process," paper SPE 97760 presented at the 2005 International Thermal Operations and Heavy Oil Symposium, Calgary, Alberta, 1-3 November.

36. Leaute, R.P.: "Liquid Addition to Steam for Enhancing Recovery (LASER) of Bitumen with CSS: Evolution of Technology from Research Concept to a Field Pilot at Cold Lake," paper SPE 79011 presented at the 2002 SPE International Thermal Operations and Heavy Oil Symposium and International Horizontal Well Technology Conference, Calgary, Alberta, 4-7 November.

37. Leaute, R.P. and Carey, B.S.: "Liquid Addition to Steam for Enhancing Recovery (LASER) of Bitumen with CSS: Results from the First Pilot Cycle," paper 2005-161 presented at the 2005 Annual Petroleum Society CIM Technical Meeting, Calgary, Alberta, 7-9 June.

38. Stegemeier, G.L. *et al*.: "Representing Steam Processes with Vacuum Models," *SPEJ* (June 1980) 171.

39. Pujol, L. and Boberg, T.C.: "Scaling Accuracy of Laboratory Steam Flooding Models," paper SPE 4191 presented at the 1972 California Regional Meeting of the SPE of AIME, Bakersfield, California, 8-10 November.

40. Kimber, K.D., Farouq Ali, S.M. and Puttagunta, V.R.: "New Scaling Criteria and Their Relative Merits for Steam Recovery Experiments," *J. Can. Pet. Tech.* (1988) **27**, No. 4, 86.

41. Kimber, K.D. and Farouq Ali, S.M.: "Verification of Scaling Approaches for Steam Injection Experiments," *J. Can. Pet. Tech.* (1989) **28**, No. 1, 40.

42. Kimber, K.D. and Farouq Ali, S.M.: "Scaled Physical Modeling of Steam-Injection Experiments," *SPERE* (Nov. 1991) 467.

43. Kimber, K.D.: "High Pressure Scaled Model Design Techniques for Thermal Recovery Processes," PhD Dissertation, The University of Alberta, Edmonton, Alberta, Canada (1989).

APPENDIX

CALCULATION OF PORE VOLUME AND MIXTURE PREPARATION

The experiments were carried out by packing the cell with 20/40 mesh white Ottawa sand, with a density of 2.65 g/cm^3. To calculate the porosity in the physical model, the cell was completely packed with clean sand.

Mass of sand inside cell, m_{sand} = 38289 g

The volume of sand grains inside the cell can be calculated using the sand density:

$$V_{sand} = \frac{m_{sand}}{\rho_{sand}} = \frac{38289\ \text{g}}{2.65\ \text{g/cm}^3} = 14449\ \text{cm}^3 \quad \text{(A1)}$$

The internal cell dimensions are 16×16×5.6 in., which results in a total volume of:

V_{cell} = 23409 cm^3

The pore volume is the difference between the total cell volume and the sand volume:

$$V_{pore} = V_{cell} - V_{sand} = 23409\ \text{cm}^3 - 14449\ \text{cm}^3 = 8960\ \text{cm}^3 \quad \text{(A2)}$$

Porosity can be calculated using:

$$\phi = \frac{V_{pore}}{V_{cell}} = \frac{8960\ \text{cm}^3}{23409\ \text{cm}^3} 100 = 38.28\% \quad \text{(A3)}$$

The amount of oil and water in the mixture can be calculated using the pore volume and the fluid saturations:

$$V_o = V_{pore} S_o \quad \text{(A4)}$$

$$V_w = V_{pore} S_w \quad \text{(A5)}$$

Using the density of water and oil, the mass of each fluid can be calculated using:

$$m_o = V_o \rho_o \tag{A4}$$

$$m_w = V_w \rho_w \tag{A5}$$

For each run, an excess of mixture is prepared to account for the differences in tamping that may occur during the process of packing the cell. The amount of mixture left after packing is carefully weighed to determine the mass of mixture inside the cell.

Using the effective amount of mixture inside the cell and the mass proportions used to initially prepare the mixture, the mass of sand, oil and water in the physical model is calculated. Using these values, the pore volume is recalculated to account for deviations produced by differences in tamping for each run.

VITA

Name:	Jose A. Rivero Diaz
Contact Information:	Department of Petroleum Engineering Texas A&M University 3116 TAMU Richardson Building College Station, TX 77843-3116
Email Address:	joserivero@hotmail.com
Education:	Ph.D., Petroleum Engineering, Texas A&M University, 2007 M.S., Petroleum Engineering, Texas A&M University, 2002 B.S., Petroleum Engineering, Universidad Central de Venezuela, 1999
Professional Affiliations:	Society of Petroleum Engineers, Member